

The *Arabidopsis thaliana* GATA factors *GNC* and *GNL* repress
the growth of starch granules, coordinating the interplay
between gravitropism and phototropism

Jan Sala Vila

Vollständiger Abdruck der von der TUM School of Life Sciences der Technischen Universität
München zur Erlangung eines

Doktors der Naturwissenschaften

genehmigten Dissertation.

Vorsitz: Prof. Dr. Corinna Dawid

Prüfer*innen der Dissertation:

1. Prof. Dr. Claus Schwechheimer
2. Prof. Dr. Ralph Hückelhoven

Die Dissertation wurde am 17.02.2023 bei der Technischen Universität München
eingereicht und durch die TUM School of Life Sciences am 09.05.2023 angenommen.

Thank you

Gràcies

I would like to thank Prof. Dr. **Claus Schwechheimer** for providing me with this opportunity, assistance and supervision throughout my Ph.D.

I would also like to thank Prof. Dr. **Miguel A. Blázquez** for his guidance as a mentor; Prof. Dr. **Erika Isono**, Dr. **John Lunn**, **Yao Xiao**, **Niccolò Mosesso**, **Nico Rossi** and **Cecilia Manjón** for collaborating in this project; Ing. **Dominik Fielder** for his expertise in scanning electron microscopy; **Andreas Arnold** for his expertise in Adobe Illustrator and InDesign; and Prof. Dr. **Corinna Dawid** and Prof. Dr. **Ralph Hückelhoven** for taking part in the examining committee.

Finally, I would also like to thank all members of **Lehrstuhl für Systembiologie der Pflanzen**.

Alina, Carlos, Dario, Lana and Peter

Thank you for your support and for your friendship. Scientific discussions in the kitchen, fruitful protocol optimizations and climbing glaciers made this project more sharp, and a real adventure.

Família Sala Vilà

Moltes gràcies de tot cor pel vostre suport i amor incondicional. Per creure en mi en tot moment. Aquest projecte, i aquesta etapa de vida, no haurien estat possible sense vosaltres. Gràcies.

10 Abstract

13 Introduction

- 13 State of the art
- 14 GATA Transcription factors
 - *GNC* and *GNL*
- 17 Plant tropisms
 - Gravitropism
 - Gravitropism and phototropism
- 19 Starch metabolism
 - Starch synthesis
 - Starch granule initiation
 - Starch degradation
- 23 Plastid development

24 Objectives

27 Materials and methods

- 27 Biological material
- 28 Transcriptomics
 - RNA-sequencing
- 29 Metabolomics
 - Purification of starch granules
 - Starch quantification
 - Liquid Chromatography tandem Mass Spectrometry
- 30 Phenomics
 - Tropism assays
 - Physiological assays
 - Iodine staining
- 31 Microscopy
 - Confocal laser scanning microscopy
 - Scanning electron microscopy
 - Transmission electron microscopy

34 Chapter 1

- 34** *GNC* and *GNL* repress gravitropism
- Sucrose treatment rescues disrupted gravitropism in *GNL*ox seedlings, but not in *pifq* seedlings
- 38** *GATA* factors regulate the expression of genes involved in starch metabolism
- Starch metabolism genes are upregulated in *gnc gnl* seedlings
 - Sucrose does not impact the expression profile of starch metabolism genes
 - Comparative transcriptomics reveals a significant conservation in the differential regulation of starch metabolism genes between *Arabidopsis thaliana* and *Marchantia polymorpha*
- 45** The number and size of starch granules are altered in *gnc gnl* and *GNL*ox seedlings
- Starch granule morphology undergoes alterations in the dark
 - *GNC* and *GNL* independently repress starch granule growth, regardless of *PIF* factors
 - *GNC* and *GNL* repress starch granule growth in a manner dependent on *SEX1* and *SS4*
- 49** Starch granule initiation is repressed by *GNC* and *GNL*
- *GNC* and *GNL* repress starch granule initiation in a manner dependent on *SS4*
- 52** Ectopic expression of *GNL* represses transitory starch degradation
- Transitory starch degradation is repressed by *GNC* and *GNL* at the whole-plant level, partially independent of chlorophyll accumulation
 - *GNL* independently represses starch synthesis, regardless of *PGM1*
- 58** Ectopic expression of *GNL* induces the differentiation of amyloplasts to etioplasts
- The growth of starch granules remains unaffected despite impaired amyloplast differentiation in *GNL*ox seedlings

- 60 The regulation of *GNC* and *GNL* on starch granule growth affect gravitropism
- The perception of gravity in the root is modulated by the repression exerted by *GATA* factors on starch granule growth
 - The perception of gravity in the shoot is modulated by the repression exerted by *GNC* and *GNL* on starch granule growth
 - *GNC* and *GNL* balance between gravitropism and phototropism

67 Chapter 2

- 67 *GNC* and *GNL* regulate the expression of genes involved in photosynthesis and stomata development

- 69 Cell wall biogenesis might be regulated by *GATA* factors

- 71 Sugar transport and allocation might be regulated by *GATA* factors
- The flux of carbon into starch is tightly regulated in *gnc gnl* and *GNLox*

74 Discussion

- 76 *GNC* and *GNL* play a multifaceted role in the regulation of starch metabolism
- Starch granule initiation, and consequently, starch granule number and size, are regulated by *GNC* and *GNL*
 - *GNC* and *GNL* repress transitory starch degradation

- 80 Overexpression of *GNL* induces plastid differentiation, potentially downstream of *PIF* factors and cytokinin

- 81 The perception of gravity is modulated by the repression of *GNC* and *GNL* on starch granule initiation

- 82 *GNC* and *GNL* balance between gravitropism and phototropism

86 References

96 Appendix

SUMMARY

This dissertation presents new findings on the role of the GATA factors *GNC* (*GATA*, *NITRATE-INDUCIBLE*, *CARBON METABOLISM-INVOLVED*) and *GNL/CGA1* (*GNC-LIKE/CYTOKININ-RESPONSIVE GATA1*) in the regulation of starch metabolism in *Arabidopsis thaliana*. The research explores the multifaceted regulation of *GNC* and *GNL*, from their impact on starch granule initiation in non-photosynthetic cells to their involvement in transitory starch synthesis and degradation at the whole-plant level, influencing gravitropic responses.

Previous studies have shown that *GATA* factors impact starch accumulation in photosynthetic cells. However, this research goes further by demonstrating the involvement of *GNC* and *GNL* in starch metabolism, employing RNA sequencing experiments with dark-grown seedlings. The use of seedlings grown in the dark allowed to decouple starch metabolism from impaired chlorophyll accumulation and chloroplast differentiation, two responses that have been well studied in relation to *GATA* factors. The transcriptomic data reveals that *GNC* and *GNL* play a regulatory role in genes associated with a wide range of functions, including starch anabolism, starch catabolism, starch granule development, and sugar transport.

Moreover, this dissertation uncovers a novel role of *GNC* and *GNL* in starch granule initiation, revealing that they act either upstream or in parallel with genes involved in this process, such as *SS4* and *PTST2*. Ectopic expression of *GNL* leads to an increase in starch granule initiation, while simultaneously repressing starch degradation, resulting in the formation of aberrantly sized starch granules. Additionally, the research identifies the formation of compound starch granules in *GATA* factor mutants, representing a new and previously unobserved phenomenon in *Arabidopsis thaliana*.

Additionally, compelling information is provided that changes in starch granule size, number, and morphology have a significant impact on gravity perception and the modulation of gravitropic responses in plants. The larger starch granules observed in *gnc gnl* mutants may result in an increased sedimentation speed, affecting the compression of the cytoskeleton and peripheral endoplasmic reticulum, both of which play crucial roles in gravity perception. These effects are also evident in various genetic backgrounds, including *ss4 gnc gnl* and *ss4 GNLox*.


Overall, this dissertation integrates novel knowledge about the functions of *GNC* and *GNL* with previous studies on chlorophyll accumulation, chloroplast development, and stomata formation, establishing *GATA* factors as key regulators of carbon assimilation and storage. The research indicates that *GNC* and *GNL* play a critical role in maintaining a balance between gravitropic and

phototropic growth through their influence on starch granule accumulation. Upon illumination, seedlings overexpressing *GNL* can rapidly transition to photosynthetically active stages, surpassing the performance of wild-type plants, and accumulating transitory starch rapidly. This finding highlights the significant role of *GNC* and *GNL* in coordinating the transition from dark conditions to photosynthetic activity, offering new insights into plant adaptation to the environment.

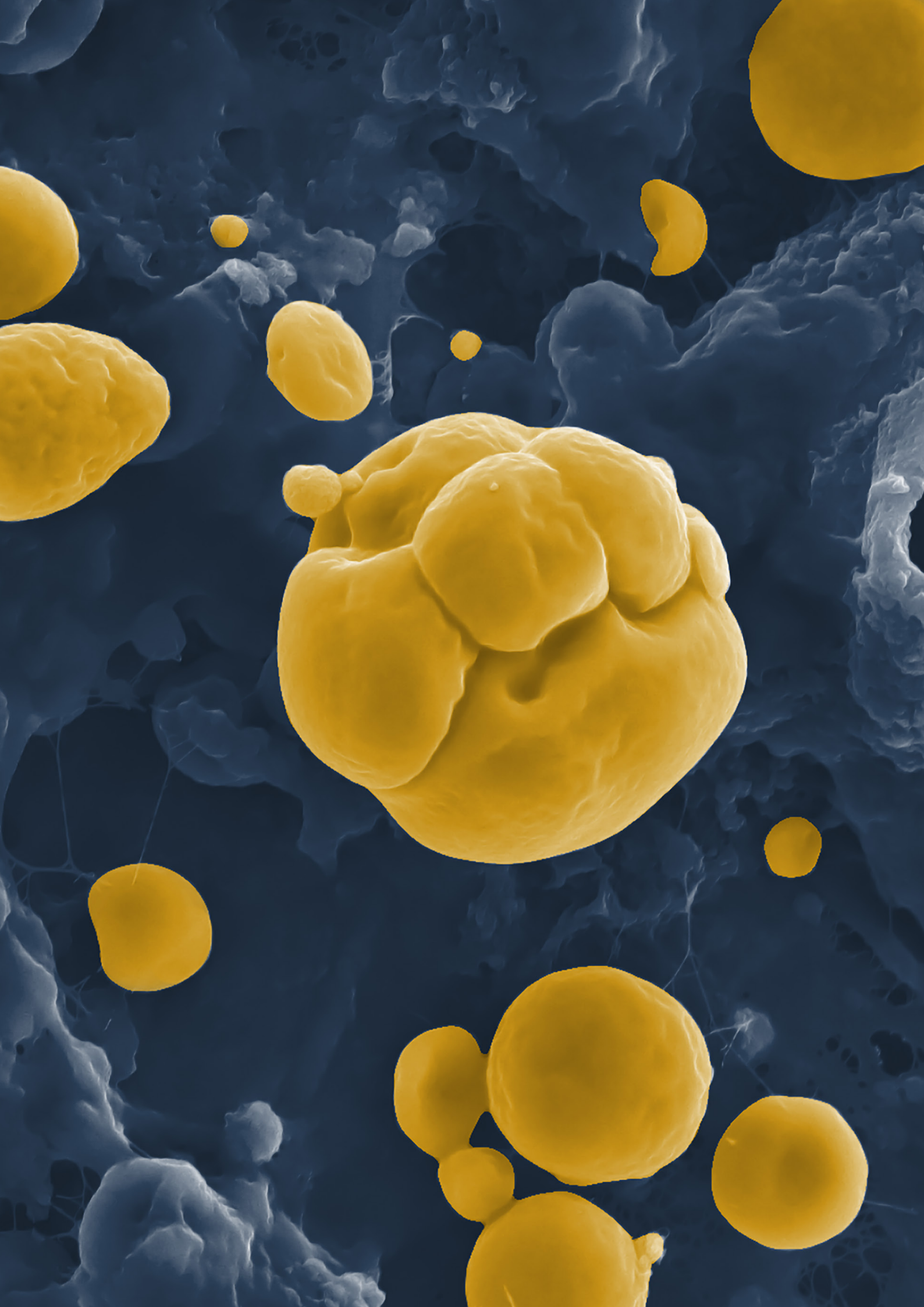
01

ABSTRACT

Plants integrate a wide range of signals that allow them to adapt to their environment. In the dark, plants sense the direction of gravity through the sedimentation of starch-filled amyloplasts. This dissertation elucidates a new role of the *Arabidopsis thaliana* GATA factors GNC (GATA, NITRATE-INDUCIBLE, CARBON METABOLISM-INVOLVED) and GNL/CGA1 (GNC-LIKE/CYTOKININ-RESPONSIVE GATA1) in the regulation of starch metabolism. In the dark, I found that GNC and GNL repress starch granule growth and amyloplast development. In the GATA genotypes analysed, the differential accumulation of starch granules in hypocotyl endodermal and root columella cells explains their altered gravitropic responses. At the whole-plant level GNC and GNL play a multifaceted role in the regulation of starch granule initiation and growth, and transitory starch synthesis and degradation. This dissertation provides evidence that GNC and GNL help balance between gravitropic and phototropic growth, through the differential accumulation of starch granules.

The background of the page is a scanning electron micrograph (SEM) of plant cells, likely from Arabidopsis thaliana. The image shows a complex network of cell walls and membranes in shades of blue and grey. Scattered throughout the field are numerous bright yellow, rounded granules of varying sizes, which are starch granules. Some granules are large and spherical, while others are smaller and more irregular. The overall appearance is that of a cellular structure with internal storage organelles.

Pflanzen weisen eine Vielzahl an Signalen auf, die es ihnen ermöglichen, sich an ihre Umwelt anzupassen. Im Dunkeln reagieren Pflanzen auf die Schwerkraft durch die Sedimentation von stärkegefüllten Amyloplasten. Diese Dissertation zeigt eine neue Rolle der GATA-Faktoren *GNC* (*GATA*, *nitrate-inducible*, *carbon metabolism-involved*) und *GNL/CGA1* (*GNC-LIKE/cytokinin-responsive GATA1*) von *Arabidopsis thaliana* bei der Regulierung des Stärkestoffwechsels. Im Dunkeln unterdrücken *GNC* und *GNL* das Wachstum der Stärke-Granula und die Entwicklung von Amyloplasten. Bei den untersuchten *GATA*-Genotypen ist die unterschiedliche Anhäufung von Stärke-Granula, die in den Endodermiszellen des Hypokotyls und in den Kolumella-Zellen der Wurzel zu finden sind, Ursache für ihre veränderte gravitropische Reaktionen. Auf der Ebene der gesamten Pflanze spielen *GNC* und *GNL* eine vielschichtige Rolle bei der Regulierung der Initiierung und des Wachstums von Stärke-Granula sowie der transienten Stärkesynthese und des Stärkeabbaus. Diese Dissertation liefert Beweise dafür, dass *GNC* und *GNL* durch die unterschiedliche Akkumulation von Stärke-Granula zum Gleichgewicht zwischen gravitropem und phototropem Wachstum beitragen.



02

INTRODUCTION

STATE OF THE ART

The European starch industry produces yearly over 11 million tons of starch, extracted from 25 million tons of EU-grown wheat, maize and potatoes (Starch Europe, 2022). In Bavaria more than 150.000 tons of potato starch are produced every year (Südstärke GmbH, 2021), and more than half of the starch produced is consumed in food in the form of native and modified starch.

Starch is the most abundant carbohydrate in the Western diet (Cordain et al, 2005), and national Food-based dietary guidelines (FBDG) recommend a daily intake of up to 10 starch-rich servings per day. Most of the starch consumed is soluble starch, which can be easily digested in the small intestine. However, 2-20% of dietary starch, referred to as resistant starch, is only processed in the colon by specialized gut microbiota (Cerqueira et al, 2020). The ratio between the 2 glucose polymers that constitute starch; amylose and amylopectin, determine the digestibility of resistant starch. In the recent years, attention has

shifted towards resistant starch due to its beneficial implications in gut microbiome and health (DeMartino & Cockburn, 2020; Cesbron-Lavau et al, 2021).

The use of starch in the food industry is widespread among a variety of products and purposes. Nevertheless, the abundance, biodegradability and non-toxicity of starch is also valued in non-food applications such as paper, adhesives, textiles or in pharmaceuticals.

Plant biology has the potential to face challenges related to food and health by improving the quality of starch in crops.

GATA TRANSCRIPTION FACTORS

GATA factors are evolutionarily conserved transcription factors (Schwechheimer et al, 2022) that bind the consensus sequence W-GATA-R (W, thymidine (T) or adenosine (A); R, guanidine (G) or adenosine (A)) (Lowry & Atchley, 2000; Reyes et al, 2004). The DNA-binding domain, in the form of a type-IV zinc finger, is characterized by 2 cysteines (Cys) at the beginning of the motif, an intermediate loop containing 17 to 20 residues, and 2 further cysteines at the end of the motif (C-X₂-C-X₁₇₋₂₀-C-X₂-C) (Reyes et al, 2004). The type-IV zinc finger is highly conserved among eukaryotes and plays a critical role in the development, differentiation and proliferation of cells (Bi et al, 2005). In vertebrates, GATA factors are responsible for the differentiation of the haematopoietic system and cardiovascular embryogenesis (Bresnick et al, 2012; Lentjes et al, 2016), whereas in fungi they mediate carbon metabolism and siderophore biosynthesis (Arst & Cove, 1973; Voisard et al, 1993; Chudzicka-Ormaniec et al, 2019). In plants, the interest for studying GATA factors raised from the observation that GATA motifs are enriched in promoters of light-regulated genes (Arguello-Astorga & Herrera-Estrella, 1998).

Arabidopsis thaliana encodes 30 GATA factors that divide in 4 distinct families based on their zinc finger motif (Schwechheimer et al, 2022). The class B GATA (B-GATA) encompasses

11 factors with a single zinc finger, and are subdivided into HAN- or LLM-domain B-GATA factors. The HAN-domain B-GATA factors encode 3 redundantly acting proteins: HAN, HAN-LIKE1 (HANL1) and HAN-LIKE2 (HANL2); which contain the HAN-domain located N-terminally to the zinc finger motif (Zhao et al, 2004). On the other hand, LLM-domain B-GATA factors contain a leucine-leucine-methionine repeat at the C-terminal region of the protein (Richter et al, 2010; Schwechheimer et al, 2022). According to the length of the N-termini, the LLM-domain factors can be further subdivided into long family members, such as GATA, NITRATE-INDUCIBLE CARBON METABOLISM INVOLVED (GNC) and CYTOKININ-RESPONSIVE GATA FACTOR 1 / GNC-LIKE (GNL), which differ from shorter members like GATA15, GATA16, GATA17, GATA17-LIKE (GATA17L) and GATA23 (Behringer & Schwechheimer, 2015; Schwechheimer et al, 2022). Notably, whether B-GATA factors in *Arabidopsis* contain only the HAN- or the LLM-domain, analysis from vascular plants revealed that mosses like *Physcomitrium patens* and liverworts like *Marchantia polymorpha* contain both the HAN- and the LLM-domains (Schwechheimer et al, 2022).

GNC and GNL

GNC and GNL are to date the most prominent B-GATA factors in *Arabidopsis thaliana* and are known to regulate plant development downstream of the hormones auxin, cy-

tokinin (CK) and gibberellin (GA); nitrogen and light (**Illustration 1**) (Wang et al, 2003; Bi et al, 2005; Naito et al, 2007; Richter et al, 2010; Richter et al, 2013b). The expression of *GNC* and *GNL* is strongly induced by blue, red and far-red light, but repressed by GA through PHYTOCHROME INTERACTING FACTORS (PIFs) (Richter et al, 2010; Ranftl et al, 2016). PIFs are a set of basic helix-loop-helix transcription factors that negatively regulate photomorphogenesis. Upon illumination, photoactivated phytochromes (Pfr) translocate into the nucleus and interact with PIF proteins (Klose et al, 2015), which are phosphorylated and degraded, resulting in photomorphogenesis (Leivar & Quail, 2011; Leivar & Monte, 2014). At the same time, GA-binding triggers the degradation of DELLA proteins, suppressing their repressive interaction with the PIFs (Li et al, 2016).

The presence of GA also modulates the abundance of AUXIN RESPONSIVE FACTOR2 (ARF2) (Richter et al, 2013b). Members of the ARF family, such as ARF5 – ARF8, are known to dimerize with Auxin/Indole-3-Acetic acid (Aux/IAA), regulating the expression of auxin responsive genes (Vernoux et al, 2011). In the presence of auxin, Aux/IAA proteins are ubiquitinated and degraded by the 26S proteasome, releasing the ARFs (Vernoux et al, 2011). Other ARF members like ARF2, do not engage in Aux/IAA repressive interactions, thus their abundance is not modulated by auxin (Vernoux et al, 2011). ARF2 and

ARF7 are known to bind the promoter regions of *GNC* and *GNL*. The loss-of-function mutants *arf2* and *arf7* share similar phenotypes with *GNC* and *GNL* overexpression lines (Richter et al, 2013b), indicating that the expression of GATA factors is modulated by the cross-talk between auxin and GA (Richter et al, 2013b; Behringer & Schwechheimer, 2015).

GNC and *GNL* act redundantly in the regulation of developmental processes such as stomata development, chloroplast differentiation and chlorophyll accumulation (**Illustration 1**). While the gradual loss of Arabidopsis LLM-domain B-GATA factors results in a gradual increase in the strengths of the respective phenotypes, the antagonistic phenotype is often observed when *GNC* and *GNL* are overexpressed, arguing for a strong dosage-dependency of GATA-controlled biological processes (Behringer et al, 2014; Klermund et al, 2016). One such gene dosage-dependent phenotype is the change in chlorophyll accumulation between mutants and overexpressors. Whereas LLM-domain B-GATA loss-of-function mutants exhibit a strong decrease in greening, their overexpressing lines induce enhanced greening throughout the plant, which is especially promoted at the base of the hypocotyl (Behringer et al, 2014; Ranftl et al, 2016; Bastakis et al, 2018). The transcriptional regulation of greening by *GNC* and *GNL* occurs at different stages of the tetrapyrrole pathway through the control of several subunits of the Mg-chelatase enzyme, GE-

NOMES UNCOUPLED (GUN) factors, and together with GOLDEN-LIKE 1 (GLK1) and GLK2, among others (Bastakis et al, 2018). In brief, the tetrapyrrole pathway begins with the synthesis of 5-aminolevulinic acid (ALA) from glutamate, leading to protoporphyrin IX (Tanaka et al, 2011). In this stage, the combined actions of Mg-chelatase, GUN4 and GUN5 catalyse the insertion of a magnesium ion, which will tip the balance towards the formation of chlorophyll (Tanaka et al, 2011).

LLM-domain B-GATA factors also regulate chloroplast formation and size. First, ectopic expression of GNC in dark-grown seedlings promotes the differentiation of proplastids to etioplasts, as indicated by the presence of prolamellar bodies (PLB) and prothylakoids (PT) (Chiang et al, 2012). In wild type seedlings grown in the dark, proplastids are not yet differentiated into plastids. In the light, GNC and GNL do not modulate chloroplast differentiation (Chiang et al, 2012; Zubo et al, 2018; An et al, 2020), but control the number and size of chloroplasts (Hudson et al, 2011; Chiang et al, 2012; Richter et al, 2013b; Ranftl et al, 2016; Bastakis et al, 2018). Overexpression of GNC leads to an increase in the number and size of chloroplasts, whereas *gnc gnl* mutants have smaller chloroplasts (Hudson et al, 2011; Chiang et al, 2012). In addition, GATA factors act downstream of CK on regulating chloroplast division. The CK-induced expression of *GNL* is compromised in ARABIDOPSIS RESPONSE REG-

ULATOR 1 (ARR1) and ARR12 loss-of-function mutants *arr1* and *arr12* (Chiang et al, 2012). Thus, the effects of CK on chloroplast division cannot be observed in *arr1 arr12* and *gnc gnl* mutants (Chiang et al, 2012). In sum, GNC and GNL are key regulators of chloroplast development, integrating light and hormone pathways (**Illustration 1**).

GNC and GNL also promote starch accumulation in the light, possibly as a result of increased chloroplast number and increased photosynthesis rate (Hudson et al, 2011; Hudson et al, 2013; Zubo et al, 2018; An et al, 2020). In *Arabidopsis thaliana*, as well as in *Populus trichocarpa*, the single- and double-mutants *gnc*, *gnl* and *gnc gnl* accumulated less starch than in wild type leaves, whereas GNCox and GNLox accumulated more starch (Hudson et al, 2011; Zubo et al, 2018; An et al, 2020). The differences observed in starch accumulation correlated to differences in chlorophyll accumulation. For instance, *gnc gnl* leaves accumulated clearly less chlorophyll than wild type leaves, and contained less starch (Hudson et al, 2011; Zubo et al, 2018). Furthermore, in fungi, GATA factors regulate genes involved in starch, cellulose and hemicellulose degradation like the glucoamylase and the α -amylase genes (He et al, 2018).

Another dosage-dependent phenotype of GNC and GNL is the formation of stomata in cotyledons and hypocotyls through direct regulation of SPEECHLESS (SPCH) (Klermund et al,

2016). The effects of the GATA factors on stomata formation are light-dependent, and act downstream of PIF factors. Thus, overexpression of GNC in the *pifq* background, promotes stomata formation in the dark (Klermund et al, 2016).

GATA factors are also known to modulate the change in the angle of lateral shoots emerging from the primary inflorescence (Richter et al, 2010; Ranftl et al, 2016). The lateral shoots of *GATA* mutants emerge with a steeper angle from the primary inflorescence than in the wild type, whereas the emergence angles from lateral shoots in the GNL overexpression lines are strongly increased (Richter et al, 2010; Behringer et al, 2014; Ranftl et al, 2016). In addition to changes in the angle of emergence,

GNC and GNL overexpression lines display changes in cotyledon and leaf shape, petiole length and most importantly, plant growth (Behringer et al, 2014). Strong overexpression of GNC and GNL results in smaller plants and severely delayed flowering (Behringer et al, 2014).

PLANT TROPISMS

Plants integrate a wide range of signals that allow them to adapt to their environment. Roots, shoots, branches and leaves are modified structurally in order to have the right shape, orientation and mechanical resistance to grow towards the light, orientate against gravity and gather necessary nutrients.

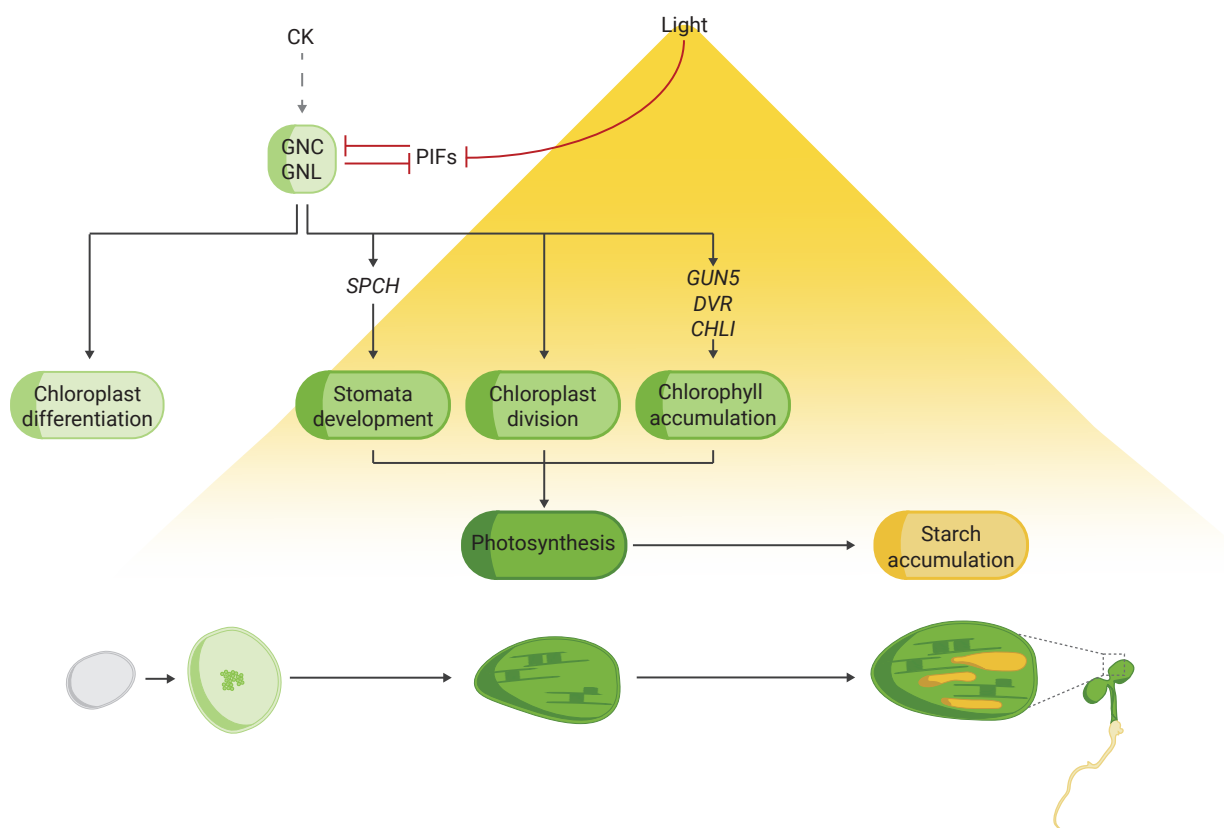


Illustration 1: Regulation of LLM-domain B-GATA factors GNC and GNL on chloroplast biogenesis, chlorophyll accumulation and stomata development. Abbreviations: cytokinin (CK), GATA, NITRATE-INDUCIBLE CARBON METABOLISM INVOLVED (GNC), GNC-LIKE (GNL), PHYTOCHROME INTERACTING FACTOR (PIF), GENOMES UNCOUPLED 5 (GUN5), DIVINYLYL CHLOROPHYLLIDE 8-VINYLYL-REDUCTASE (DVR), MAGNESIUM CHELATASE I (CHLI), SPEECHLESS (SPCH).

Gravitropism

During skotomorphogenic growth in the dark, seedling roots grow towards the gravity vector, referred as positive gravitropism; while their hypocotyls elongate away from gravity, which is referred as negative gravitropism (Kiss, 2000; Sato et al, 2015). Gravitropism comprises four sequential processes: gravity perception, signal formation, signal transduction and asymmetric cell elongation (Morita & Tasaka, 2004; Nakamura et al, 2019). In the first step, and according to the starch-statolith hypothesis, plastids sediment in the direction of gravity due to the force of gravity exerted on high-density starch granules (**Illustration 2**) (Nakamura et al, 2019). Amyloplasts that function as statoliths are located in the hypocotyl endodermis and in the root columella (Kiss et al, 1989; Christie & Murphy, 2013). It is known that the endodermal cell layer in the shoot and the columella cells in the root are essential for the correct perception of gravity, thus disrupting these tissues results in reduced gravitropism (Blancaflor & Masson,

2003). Moreover, mutants responsible for the formation of the endodermis, such as SCARECROW (SCR), exhibit defects in the perception of gravity (Fukaki et al, 1998; Tasaka et al, 1999; Kim et al, 2011).

Amyloplasts sediment in the direction of gravity due to the mass of starch granules. It is known that the strength of the gravitropic responses is, amongst others, dependent on the content of starch (Kiss et al, 1998). Supporting the starch-statolith hypothesis, the PHOSPHOGLUCOMUTASE1 (PGM1) mutant *pgm1*, which is not able to synthesize starch, exhibits reduced gravitropism (Kiss et al, 1998; Weise & Kiss, 1999). On the other hand, an increase in starch accumulation leads to stronger gravitropic responses in the hypocotyl and the root (Vitha et al, 2007). The developmental stage of plastids also modulates the perception of gravity. PIFs convert amyloplasts into plastids with etioplasmic or chloroplastic features (Kim et al, 2011). The gradual loss of PIF factors results in defective amyloplasts that contain smaller starch granules, and thus, reduced

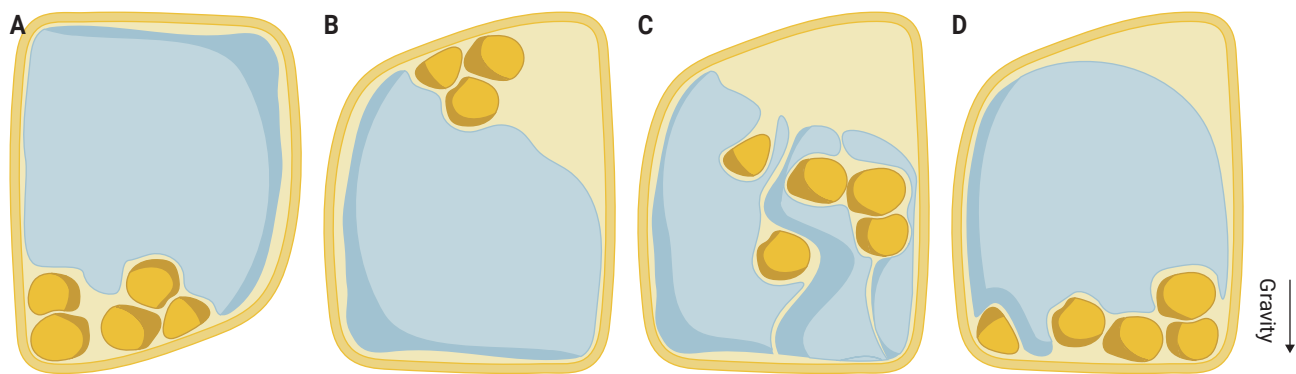


Illustration 2. Model of the starch-statolith hypothesis. A. Starch granules at the base of the cell. B. Starch granules start to sediment in the direction of gravity, after reorientation of the plant. C. The sedimentation process occurs via transvacuolar strands and actin filaments, which act as a restraining mesh. D. Starch granules settle at the bottom of the cell, compressing the cytoskeleton and peripheral ER, releasing calcium ions.

hypocotyl gravitropism in the dark (Kim et al, 2011; Kim et al, 2016).

Additional studies suggest that the association of amyloplasts with actin filaments (Palmieri & Kiss, 2005; Song et al, 2019) and endoplasmatic reticulum (ER) (Leitz et al, 2009) enhance gravitropism. Although the mechanisms regulating gravity perception are not yet fully understood, it is clear that an increased content of starch in endodermal and root columella cells, enhances gravitropic responses.

Gravitropism and phototropism

In the light, plants use phototropin-mediated phototropism to orient their growth towards the light for optimal photosynthesis (Briggs & Christie, 2002; Christie & Murphy, 2013). Phototropins are plasma-membrane associated kinases that are activated by blue light, and play important roles in regulating chloroplast movements, stomatal opening and leaf positioning (Inoue et al, 2010; Legris & Boccaccini, 2020; Legris et al, 2021; Labuz et al, 2022).

In the light, the angle of hypocotyl and root growth results from the additive sum of gravitropic and phototropic responses (Hangarter, 1997). In hypocotyls, positive phototropism dominates over negative gravitropism, whereas in the root negative phototropism and positive gravitropism are equal (Vitha et al, 2000). When the respective inputs do not act in the same direction, plants have to find a balance between

phototropic and gravitropic growth (Hangarter, 1997). Hence, decreased gravitropism in wild type seedlings grown on clinostats (Nick & Schafer, 1988), or as a result of reduced content of starch in the *pgm1* mutant (Vitha et al, 2000), leads to increased phototropic responses (Nick & Schafer, 1988; Vitha et al, 2000).

STARCH METABOLISM

Starch is the most abundant storage carbohydrate on Earth (Nakamura et al, 2022). Hence, it is not surprising that starch plays a central role in all living organisms. In most vascular plants, starch in photosynthetic active cells, referred to as transitory starch, accumulates during the day and its degraded on the following night in order to provide a continuous supply of carbohydrates during cellular respiration (Streb & Zeeman, 2012). In non-photosynthetic cells, starch accumulates in tissues like tubers to serve as a long-term carbohydrate storage (Reyniers et al, 2020), or in endodermal and root columella cells to aid in gravity perception (Kiss et al, 1989).

Starch synthesis

Starch consists of amylose and amylopectin (Zeeman et al, 2002). Amylose is composed of linear chains of α -1,4-linked D-glucose residues, whereas amylopectin is branched through additional α -1,6-linked D-glucoses (**Illustration 3**) (Seung, 2020). Neighbouring chains of amylopectin form clusters of double helices

that pack into crystalline lamellae, enabling starch to become insoluble (Streb & Zeeman, 2012; Apriyanto et al, 2022). The branching points of amylopectin form rather an amorphous lamella, that alternates with the crystalline lamellae, resulting in high-order growth rings (**Illustration 3**) (Seung, 2020). Whereas amylopectin accounts for 70-90% of the starch granule mass, amylose represents only 10-30% (Streb & Zeeman, 2012). Amylose is not necessary for starch granule formation, therefore, it can be considered as a filling between the amylopectin matrix (**Illustration 3**) (Seung, 2020).

In the light, the precursor for starch biosynthesis is withdrawn from the Calvin cycle in the form of fructose-6-phosphate (F6P), and converted sequentially to glucose-6-phosphate (G6P) and glucose-1-phosphate (G1P) by the activities of PHOSPHOGLUCOSE ISOMERASE (PGI) and PGM1 (**Illustration 4**) (Funfgeld et al, 2022). Additionally, sugars located in storage tissues can be delivered to the starch pathway through the activity of invertases and sucrose synthases that cleave sucrose into G6P, F6P and UDP-glucose (Fernie et al, 2002). In the cytosol, UDP-glucose is converted to G1P by UDP-glucose pyrophosphorylase or transported into the Golgi lumen, where it is essential for pectin and hemicellulose biosynthesis (Saez-Aguayo et al, 2021). The flux of carbon into starch biosynthesis is tightly regulated by the plastidial ADP-GLUCOSE PYROPHOSPHORYL-

ASE (AGPase), which catalyses the conversion of G1P to ADP-glucose (ADPGlc) (**Illustration 4**). In *Arabidopsis thaliana*, AGPase encodes 2 small subunits: APS1 and APS2; and 4 large subunits: APL1 – APL4. The loss-of-function mutant *adg1 adg2* contains little amounts of starch (Funfgeld et al, 2022). ADPGlc serves as a glucosyl donor, forming new α -1,4 glucosidic linkages by the activity of starch synthases (Streb & Zeeman, 2012). GRANULE BOUND STARCH SYNTHASE1 (GBSS1) elongates glucan molecules in a processive-manner, forming amylose (Seung et al, 2020), whereas soluble starch synthases (SS1, SS2 and SS3) add glucose residues to the non-reducing ends of an already existing chain, forming amylopectin (**Illustration 4**). Furthermore, branching enzymes (BEs) introduce branch points into

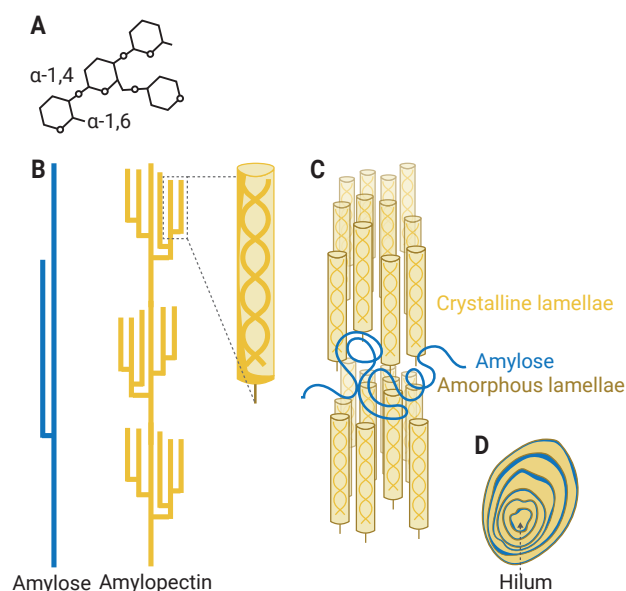


Illustration 3. Structure and components of the starch granule. A. Chains of α -1,4- and α -1,6-linked glucosyl residues. B. Linear chains of amylose (α -1,4-link) and branched chains of amylopectin (α -1,6-link). Neighbouring chains of amylopectin form clusters of double helices that pack into crystalline lamellae. C. and D. The branching points of amylopectin form rather an amorphous lamella, that alternates with the crystalline lamellae, resulting in high-order growth rings.

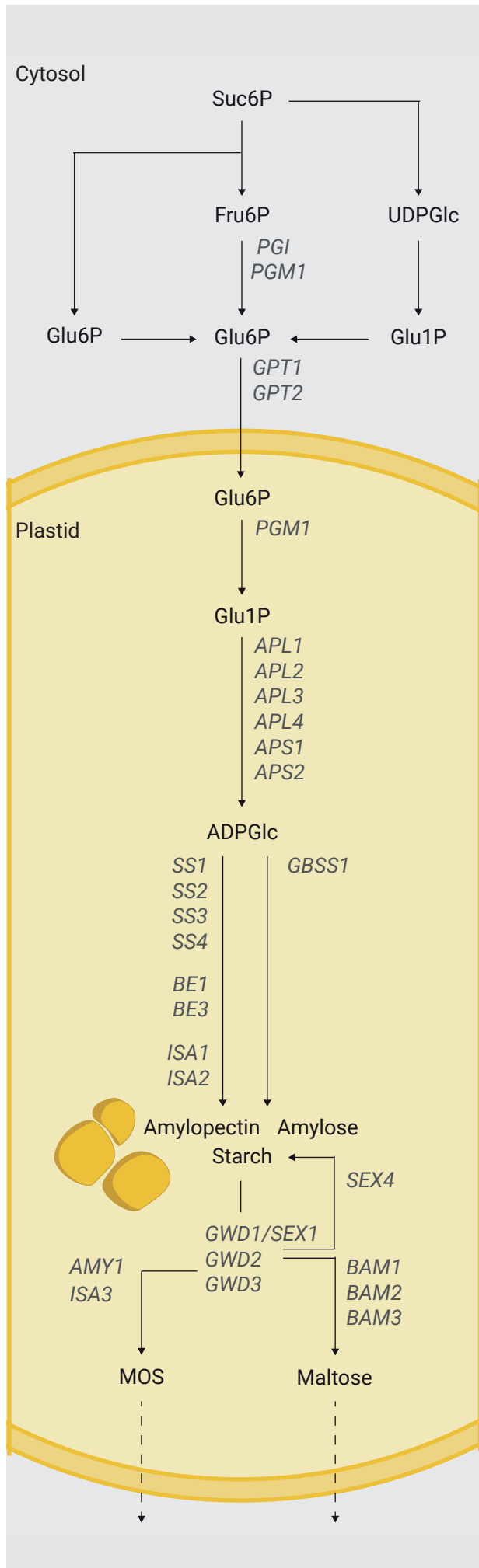
the elongated amylopectin chains, contributing to the final structure of amylopectin (**Illustration 4**) (Delvalle et al, 2005; Zhang et al, 2008; Lu et al, 2015; Seung et al, 2020; Gamez-Arjona & Merida, 2021).

Starch granule initiation

The knowledge on how starch granules initiate is currently scarce, but appears to involve the coordination of a specialised set of proteins. Granules emanate from a central core, known as hilum, by the activity of a starch synthase isoform (SS4) (Tetlow & Bertoft, 2020). Unlike other starch synthases, SS4 has a long N-terminal region involved in shaping the morphology of starch granules (Lu et al, 2018). The loss-of-function *ss4* mutant has 1 or 2 starch granules per chloroplast, that acquire a rounded morphology, rather than 4 flattened-starch granules per chloroplasts observed in wild type plants (Roldan et al, 2007). It is thought that SS4 is responsible for elongating de-novo glucan chains by interacting with PROTEIN TARGETING TO STARCH 2 (PTST2) (Tetlow & Bertoft, 2020). Members of the PTST family contain a carbohydrate-binding domain that delivers suitable substrates to SS4 (Apriyanto et al, 2022). Recently, further proteins have been identified in the regulation of starch granule initiation. MAR-BINDING FILAMENT-LIKE PROTEIN1 (MFP1) and PROTEIN INVOLVED IN STARCH INITIATION (PII1) interact with PTST2, and loss of both proteins results in a reduction of starch

granule number (Seung et al, 2018). In addition, proteins involved in maltose metabolism also modulate starch granule initiation, for example ALPHA-GLUCAN PHOSPHORYLASE1 (PHS1) and DISPROPORTIONATING ENZYME2 (DPE2). Additional loss of both proteins in the *ss4* background results in perfectly spherical granules aberrant in size (Malinova & Fettke, 2017; Apriyanto et al, 2022).

Little is known about the molecular mechanisms controlling starch granule morphology. The fact that starch granules differ vastly among species, and even among tissues from the same organism, hinders the general understanding. In cereals, it is common that starch granules emerge from a single initiation event, and therefore, each individual granule, referred to as simple-type granule, contains a hilum (Toyosawa et al, 2016; Li et al, 2017; Hawkins et al, 2021). Wheat endosperm contains simple-type granules, but deficiency of SS4 results in the formation of compound granules due to multiple initiations per amyloplast (Hawkins et al, 2021). On the other hand, the endosperm of wild type rice contains compound polyhedral starch granules, but loss of SS3 and SS4 leads to single round granules (Toyosawa et al, 2016). In Arabidopsis, a recent study focusing on transitory starch, suggests that starch granules in chloroplasts arise from multiple coalescent initiations (Burgy et al, 2021).



Starch degradation

At night, when the synthesis of sucrose is limiting, plants break down starch in order to provide a continuous supply of carbohydrates. Starch degradation begins with the phosphorylation of glucosyl residues of amylopectin through the enzymatic activity of α -GLUCAN WATER DIKINASE (GWD1) and PHOSPHOGLUCAN WATER DKINIASE (PWD) (**Illustration 4**) (Streb et al, 2012). The activity of GWD1 is necessary for the correct degradation of starch, and hence the *gwd1/sex1* (*starch excess1*) mutant accumulates high amounts of starch (Yu et al, 2001). The phosphorylated residues are then removed by the action of STARCH EXCESS 4 (SEX4) (Mak et al, 2021). After disrupting the amylopectin double helices and solubilizing the starch granule surface, the combined action of α -amylases (AMYs), β -amylases (BAMs), debranching enzymes (DBEs) and isoamylases (ISAs) allow the hydrolysis of glucan chains and release of maltose to the cytosol (**Illustration 4**) (Yu et al, 2001; Flutsch et al, 2020; Feike et al, 2022). Maltose is then further metabolised by PHS1, DPE1 and DPE2 into glucose (**Illustration 4**) (Abt & Zeeman, 2020).

Illustration 4. Starch synthesis and degradation pathway. Abbreviations: sucrose-6-phosphate (Suc6P), fructose-6-phosphate (Fru6P); UDP-glucose (UDPGlc); glucose-6-phosphate (Glu6P); glucose-1-phosphate (Glu1P); ADP-glucose (ADPGlc); maltooligosaccharides (MOS); PHOSPHOGLUCOSE ISOMERASE (PGI); PHOSPHOGLUCOMUTASE1 (PGM1); GLUCOSE 6-PHOSPHATE TRANSLOCATOR (GPT1); ADP GLUCOSE PYROPHOSPHORYLASE LARGE SUBUNIT (APL); ADP GLUCOSE PYROPHOSPHORYLASE SMALL SUBUNIT (APS); STARCH SYNTHASE (SS); BRANCHING ENZYME (BE); ISOAMYLASE (ISA); GRANULE BOUND STARCH SYNTHASE (GBSS); STARCH EXCESS4/LAFORIN-LIKE1 PHOSPHOGLUCAN PHOSPHATASE (SEX4); GLUCAN WATER DIKINASE (GWD); STARCH EXCESS1 (SEX1); ALPHA-AMYLASE (AMY); ISOAMYLASE (ISA); BETA-AMYLASE (BAM).

PLASTID DEVELOPMENT

Plants contain a wide diversity of plastids, which perform highly specific functions (Pyke, 2013). Plastids develop from an undifferentiated type of plastid, referred to as proplastid, found in meristematic cells (**Illustration 5**) (Choi et al, 2021). In the dark, proplastids differentiate to leucoplasts or etioplasts. Leucoplasts are storage plastids located in non-photosynthetic tissues, which account for starch-filled amyloplasts, lipid- and terpenoid-filled elaioplasts, and protein-filled proteinoplasts; whereas etioplasts are found in photosynthetic tissues and characterized by a crystalline PLB consisting of lipids and protochlorophyllide, and PTs (Pyke, 2010; Choi et al, 2021). Plastids are highly interconvertible in response to developmental and environmental responses. For instance, leucoplasts can differentiate to chloroplasts, and vice versa (**Illustration 5**) (Choi et al, 2022). Unfortunately, the knowledge about how amyloplasts transition to chloroplasts is scarce.

The transition from etioplasts to chloroplasts is the most studied, and occurs during de-etiolation via negative regulators of photomorphogenesis such as CONSTITUTIVE PHOTOMORPHOGENIC1 (COP1), SUPPRESSOR OF phyA (SPA) and DE-ETIOLATED1 (DET1) (Xu, 2020; Choi et al, 2021). Upon light exposure, plant photoreceptors inhibit the COP1-SPA E3 ubiquitin ligase complex, releasing early light re-

sponsive proteins like ELONGATED HYPOCOTYL 5 (HY5) and LONG HYPOCOTYL IN FARD-RED1 (HFR1) (Xu, 2020). Among others, HY5 and HFR1 induce the expression of positive regulators of photomorphogenesis. Simultaneously, the degradation of PIF factors induce the expression of two families of transcription factors; first, the GLK family, and second LLM-domain B-GATA factors (Chiang et al, 2012; Bastakis et al, 2018; Zubo et al, 2018). GLK and GATA factors are thus considered as positive regulators of chloroplasts development.

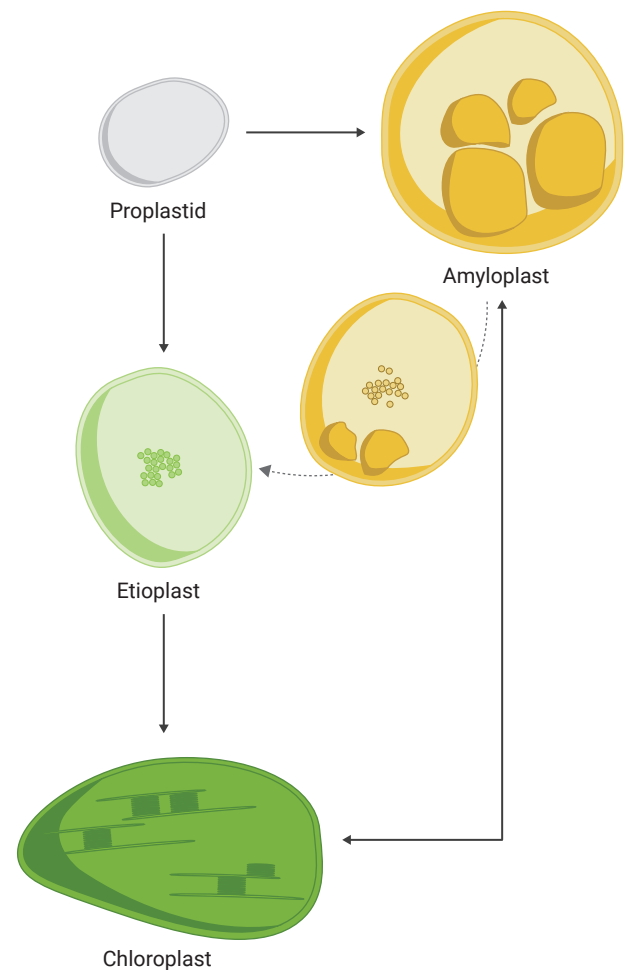


Illustration 5. Differentiation of plastids to amyloplasts and chloroplasts. Plastids develop from an undifferentiated type of plastid, referred to as proplastid, found in meristematic cells. In the dark, proplastids differentiate to etioplasts and amyloplasts, and upon illumination, etioplasts convert to chloroplasts.

03

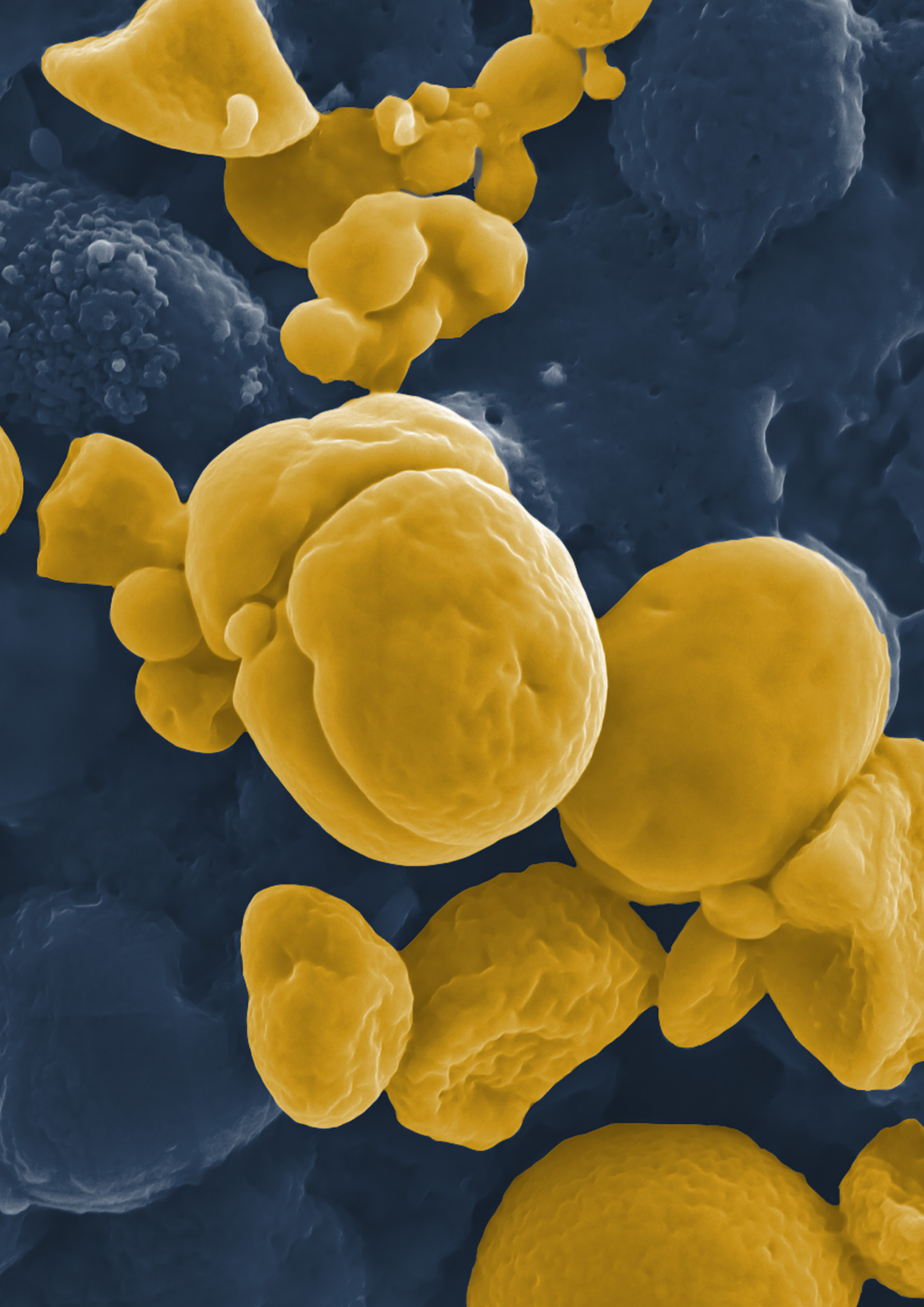
OBJECTIVES

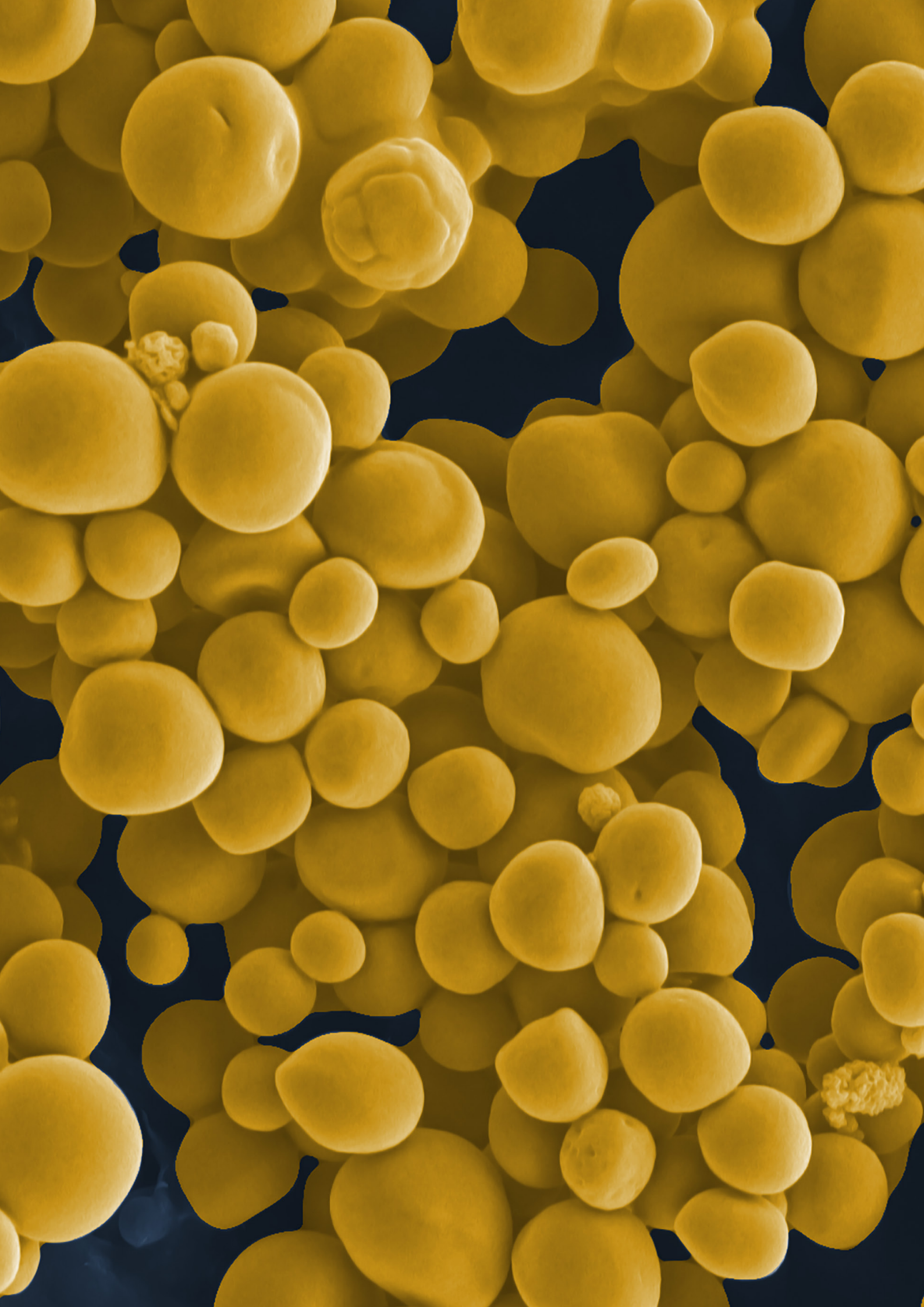
First, the aim of my dissertation was to examine whether defects in the emergence angle of inflorescences observed in *GATA* mutants and overexpression lines, were related to defects in gravity perception. The branching angle in *gnc gnl*, *GNCox* and *GNLox* plants has been previously reported and quantified (Richter et al, 2010; Behringer et al, 2014; Ranftl et al, 2016), however, the mechanism behind this phenotype is not understood. To start with, I performed a series of gravitropism assays in the shoots, hypocotyls and roots of *gnc gnl* and *GNLox* seedlings and plants, and I observed similar defects compared to those defects observed in inflorescences (Ranftl et al, 2016). These results indicated that gravitropism is disturbed in the *GATA* genotypes analysed.

It is known that the perception of gravity requires the sedimentation of starch granules. Thus, I performed an RNA sequencing experiment with seedlings grown in the dark, in order to gain further insight into the regulation of *GNC* and *GNL* on starch accumulation. The transcriptional analysis revealed that genes involved

in starch metabolism are differentially regulated in *gnc gnl* and *GNLox* seedlings. Although most of the studies on starch focus on transient starch in the chloroplasts of *Arabidopsis thaliana*, or storage starch in the grains of cereals, the knowledge regarding endodermal starch, where gravity perception occurs, is rather incomplete. Therefore, the succeeding aim of my dissertation was to examine the regulation of *GNC* and *GNL* on starch granule growth, in specialized cells involved in gravity perception. Combining genetic, transcriptomic, metabolomic and physiological studies, I uncovered and characterized a role of the *GATA* factors on starch granule initiation and growth, transitory starch accumulation, as well as amyloplast differentiation.

Ultimately, I integrated the novel knowledge obtained in this work, with previous studies on chlorophyll accumulation, chloroplast development and stomata development, concluding that *GATA* factors balance between gravitropism and phototropism, and modulate carbon assimilation and storage.





04

MATERIALS AND METHODS

BIOLOGICAL MATERIAL

All experiments were performed in *Arabidopsis thaliana* ecotype Columbia (Col-0). The *gnc* (SALK_001778) and *gnl* (SALK_003995) single and double mutants, the GNL overexpression line GNLox, as well as the *pif1-1 pif3-3 pif4-2 pif5-3 (pifq, phytochrome interacting factor quadruple)* and *pifq* GNLox, were previously described (Richter et al, 2010; Klermund et al, 2016). *arc5-2* (SAIL_71_D11), *sex1-8* (SALK_077211) and *ss4-1* (SALK_096130) were obtained from the Nottingham Arabidopsis Stock Centre (NASC) (Roldan et al, 2007) (Mahlow et al, 2014). *pgm1-1* was generously provided by Christian Frankhauser (Lausanne, Switzerland) (Periappuram et al, 2000; Lariguet et al, 2003) and ptA5-3 (*CaMV35S::TP_{BCS3A}-GFP::NOS*) by Ryuichi D. Itoh (Okinawa, Japan) (Niwa et al, 1999; Fujiwara et al, 2018). Homozygous mutant combinations were isolated from segregating populations by

PCR-based genotyping with oligonucleotides. In addition, successful *pgm1-1* cloning was confirmed by iodine staining. To confirm successful ptA5-3 cloning, fluorescence was verified with an Olympus SZX16 stereofluorescence microscope (Olympus, Shinjuku, Tokyo, Japan) using an excitation wavelength of 488 nm and emission at 507 nm.

Marchantia polymorpha ecotype BoGa, the CRISPR/Cas9-generated mutants *Mpb-gata1-1* and *Mpb-gata1-2*, and the overexpression line *MpB-GATAOX3* were generously provided by Peter Schröder (Lehrstuhl für Systembiologie der Pflanzen, Technische Universität München, Freising, Germany).

Seedlings were cultivated on sterile half-strength Murashige and Skoog ($\frac{1}{2}$ MS) medium (Duchefa, Harlem, The Netherlands), when specified supplemented with glucose, fructose, sucrose or sorbitol. Seedlings were, unless specified otherwise, grown in the dark in growth chambers (Sanyo, Osaka, Japan) at 21°C. When grown in the light, plants were grown in growth chambers (Sanyo, Osaka, Japan) at 21°C under white-fluorescent light ($120 \mu\text{mol m}^{-2} \text{s}^{-1}$) with a 12 hrs light / 12 hrs dark or 16 hrs light / 8 hrs dark photoperiod. Gemmae were cultivated on sterile half-strength Gamborg's B5 medium containing 1.4% plant agar (Duchefa, Harlem, Netherlands) under

white-fluorescent light ($60 \mu\text{mol m}^{-2} \text{s}^{-1}$) with a 16 hrs light / 8 hrs dark photoperiod.

TRANSCRIPTOMICS

RNA-sequencing

For RNA-seq, 3-days-old wild type, *gnc gnl* and GNLox seedlings were grown in the dark on sucrose free and 1% sucrose-supplemented $\frac{1}{2}$ MS medium. Liquid nitrogen-frozen seedlings were disrupted in a Tissue Lyser2 (Qiagen, Hilden, Germany) and total RNA was extracted from entire seedlings using a NucleoSpin RNA kit (Macherey-Nagel, Düren, Germany). RNA quantity and quality were determined with a 2100 Bioanalyzer Microfluids System (Agilent,

Allele	Description	ID	Sequence
<i>arc5-2</i>	<i>arc5-2</i> SAIL71 forward	SAIL_71_D11	TGTGTTGGATGCCCTTAAGAC
<i>arc5-2</i>	<i>arc5-2</i> SAIL71 reverse	SAIL_71_D11	TGTCACCTGATGAAGGAAAGG
<i>gnc</i>	<i>gnc</i> SALK1778 forward	SALK_001778	TTTGATCTTGCACTTTTTTGGC
<i>gnc</i>	<i>gnc</i> SALK1778 reverse	SALK_001778	GCCAAGATGTTTGTGGCTAAC
<i>gnl</i>	<i>gnl</i> SALK3995 forward	SALK_003995	AAGAACAACCACATTGTTGGG
<i>gnl</i>	<i>gnl</i> SALK3995 reverse	SALK_003995	AAGGCGATTATTACCACCAGC
<i>pgm1-1</i>	<i>pgm1-1</i> Trp192 forward		GGTTTCCGCTGTAATCAGGA
<i>pgm1-1</i>	<i>pgm1-1</i> Trp192 reverse		CTGACCACTGCTGTAATTGAAC
<i>pks4-2</i>	<i>pks4-2</i> GABI312 forward	GABI_312E01	TTGGGTTCCACAAAATCAAAC
<i>pks4-2</i>	<i>pks4-2</i> GABI312 reverse	GABI_312E01	ATTCAGAACCGGTTTAATCGG
<i>sex1-8</i>	<i>sex1-8</i> SALK77211 forward	SALK_077211	GGAGAAGACACGACCACAGTC
<i>sex1-8</i>	<i>sex1-8</i> SALK77211 reverse	SALK_077211	TTTGAAAAGCCTTTGTTGCAG
<i>ss4-1</i>	<i>ss4-1</i> SALK96130 forward	SALK_096130	GTGACATTACTTGAGGAGCGG
<i>ss4-1</i>	<i>ss4-1</i> SALK96130 reverse	SALK_096130	GCGTCTGAAATCATCTTGCTC
35S	CaMV35S promoter forward		CAAGACCCTTCCTCTATATAAGG
GFP	GFP forward		CTGCTGGAGTTCGTGAC
LB3	SAIL		TAGCATCTGAATTTTCATAAC- CAATCTCGATACAC
LBb1.3	SALK		ATTTTGCCGATTTTCGGAAC
O8474	GABI		ATAATAACGCTGCGGACATCTACATT

Table 1. List of oligonucleotides used for PCR-based genotyping.

Santa Clara, CA). Libraries were generated with the Illumina stranded mRNA Kit (Illumina, San Diego, CA) and single-ended sequencing was performed on a NovaSeq 6000 (Illumina, San Diego, CA). Reads were mapped to the region of the TAIR10 release of the *Arabidopsis thaliana* Col-0 genome (www.arabidopsis.org) using the default settings of the CLC Genomics Workbench (Qiagen, Düren, Germany). Differentially expressed genes (DEGs) were filtered by a false discovery rate (FDR) < 0.05. The RNA-seq data is available at Gene Expression Omnibus (<https://www.ncbi.nlm.nih.gov/geo/>) under accession number GSE205524.

Venn diagrams were generated using the default settings of the CLC Genomics Workbench (Qiagen, Düren, Germany) in order to compare the overlap of differentially expressed genes.

Gene ontology (GO) analysis was performed using the PANTHER algorithm at TAIR and the enriched set of differentially expressed genes was retrieved according to their biological function (Lamesch et al, 2012). For a hierarchical clustering of GO term categories, the complete list of ontology term categories was summarized based on semantic similarity measures (SemRel) using the REVIGO algorithm (Supek et al, 2011). Similarity coefficients were converted into distances using the DendroUPGMA tool (Garcia-Vallve et al, 2000) and dendrograms were visualized with the Java TreeView

software (Saldanha, 2004).

The list of genes obtained from the GO analysis was uploaded to the STRING database in order to annotate the corresponding protein-protein interactions (Szklarczyk et al, 2017). Networks were built using the Cytoscape software (Shannon et al, 2003) including expression and ontology information.

METABOLOMICS

Purification of starch granules

Starch granules were purified from liquid nitrogen-frozen seedlings grown in the dark on sucrose-free and 1% sucrose-supplemented $\frac{1}{2}$ MS medium. Seedlings were homogenized with a tissue blender in 2 ml ice-cold extraction buffer (50 mM Tris-HCl, pH 8.0; 0.2 mM EDTA, 0.5% Triton X-100). The homogenate was filtered through Miracloth (Merck, Darmstadt, Germany) and pelleted by centrifugation at 2,500 *g* for 15 mins. The pellet was resuspended in 1 ml extraction buffer, containing 0.5% SDS (sodium dodecyl-sulphate). Subsequently, the pellet was washed 5 times with distilled water and re-pelleted by centrifugation at 2,500 *g* for 10 mins to remove excess SDS.

Starch quantification

Starch was quantified with the Megazyme Total Starch HK Assay Kit (Megazyme, Bray, Ireland) from 200 mg liquid nitrogen-frozen seedlings grown in the dark on sucrose-free and 1% sucrose-supplemented $\frac{1}{2}$

MS medium, and harvested at the specified time points. Plant material was disrupted until homogeneous with a Tissue Lyser2 (Qiagen, Hilden, Germany). The tissue was then incubated in 80% ethanol for 5 mins, and insoluble material was pelleted by centrifugation at 10,000 *g* for 5 mins. The supernatant was discarded and the ethanol extraction was repeated once. The starch-containing pellet was transferred to a 15 ml glass tube and starch quantification was performed according to the manufacturer's instructions (Megazyme, Bray, Ireland).

Liquid Chromatography tandem Mass Spectrometry

Tre6P, other phosphorylated intermediates and organic acids were extracted with chloroform-methanol and generously measured by John Lunn (Max Plank Institute of Molecular Plant Physiology, Potsdam, Germany) by anion-exchange high-performance liquid chromatography coupled to tandem mass spectrometry (Lunn et al, 2006).

PHENOMICS

Tropism assays

For hypocotyl and root gravitropism responses, seedlings were grown for 2 days in the dark on vertically oriented ½ MS plates. Since the genotypes examined here affected hypocotyl growth in the dark due to defects in negative gravitropism, seedling hypocotyls were straightened away

from the gravity vector, in safe green light, before the plates were turned by 90° and grown for an additional 24 hrs. Subsequently, photographs were taken with a Sony A6100 digital camera (Sony, Berlin, Germany) and the bending of hypocotyls was measured from the digital images using the Fiji ImageJ software (Schindelin et al, 2012). Because cotyledon position influences the degree of negative hypocotyl gravitropism, only seedlings with their cotyledons pointing in the bending direction were included in the quantification (Khurana et al, 1989).

For shoot gravitropism, plants were grown in a growth chamber on soil until their primary inflorescences reached 10 cm. Then plants were placed horizontally for 1 hr in a dark-chamber to determine negative shoot gravitropism and to prevent interference from phototropic responses. Inflorescence bending was determined from digital photographs using the Fiji ImageJ software, as described above.

For the analysis of the growth direction, seedlings were grown for 3 days on vertically oriented ½ MS plates in the dark or illuminated with undirected far-red light (2.5 $\mu\text{mol m}^{-2} \text{s}^{-1}$), as specified. The growth angle of hypocotyls was determined from digital photographs using the Fiji ImageJ software, as described above.

To determine the interaction between hypocotyl negative gravitropism and phototropism, seedlings were grown for 2 days in the dark on

vertically oriented plates on $\frac{1}{2}$ MS and straightened as described above. Plates were then turned by 90° and grown for 6 hrs with unilateral blue light illumination ($1 \mu\text{mol m}^{-2} \text{s}^{-1}$) from above or below, as specified. Seedling hypocotyl bending was determined from digital photographs using the Fiji ImageJ software, as described above.

Physiological assays

For rosette area measurements plants were grown for 2 weeks in the soil on sucrose-free, 1% glucose-, 1% fructose-, 1% sucrose- and 1% sorbitol-supplemented $\frac{1}{2}$ MS medium, as specified, and in the light. Photographs were taken with a Sony A6100 digital camera (Sony, Berlin, Germany) and images analysed with the Fiji ImageJ software (Schindelin et al, 2012).

The branching angles were measured from cauline nodes and leaf-bearing nodes that reached, at least, 0.5 cm length from 5-weeks-plants grown in the soil.

Iodine staining

For the imaging of starch granules by light microscopy, starch granule preparations were dispersed in distilled water, stained with Lugol's solution and glycerol (1:1 v/v), mounted and imaged with an Olympus BX61 light microscope (Olympus, Shinjuku, Tokyo, Japan).

For the imaging of starch distribution in seedlings, 3-days-old dark-grown seedlings were stained

for 1 min with Lugol's solution, and destained for 5 min with distilled water. Stained seedlings were imaged as described above.

Plants grown in soil were harvested at the end of the day (EoD) or at the end of the night (EoN), and immediately transferred to hot EtOH 80% until chlorophyll was removed. Then plants were stained for 1 min with Lugol's solution, and destained for 5 mins with distilled water. Stained plants were imaged with a Sony A6100 digital camera (Sony, Berlin, Germany).

MICROSCOPY

Confocal laser scanning microscopy

Confocal laser scanning microscopy was performed with an Olympus FV1000 (Olympus, Shinjuku, Tokyo, Japan) using an excitation wavelength of 488 nm and emission at 520 to 720 nm, after cell wall- and starch granule-staining with mPS-PI (modified pseudo-Schiff reagent-propidium iodide) (Truernit et al, 2008). Chlorophyll was detected using the parameters described above, while EGFP was detected using an excitation wavelength of 488 nm and emission at 507 nm.

Starch granule size was measured from the digital images using the Fiji ImageJ software (Schindelin et al, 2012), considering the starch granule area (μm^2) as a proxy for starch granule size of individual starch granules. High-magnification images of mPS-

PI-stained starch granules allowed to distinguish between several starch granules in one amyloplast.

To qualitatively assess the morphology of granules and chloroplasts, 3D rendering was created from z-stacks using the 3Dscript plugin from the Fiji ImageJ software (Schmid et al, 2019). For the fractionation of fluorescence, 3D-rendered images were first converted to 8-bit. Then the threshold was adjusted to black and white, and the area fraction measured with the Fiji ImageJ software (Schindelin et al, 2012) as a proxy of chloroplast density.

Scanning electron microscopy

For SEM analysis, starch granules were sputter-coated for 90 secs with a gold alloy and imaged at 5.0 kV in a JEOL JSM-7200F field emission scanning electron microscope.

Transmission electron microscopy

Samples were prepared, embedded and mounted, as well as images were generously obtained by Niccolò Mossesso and Erika Isono (Universität Konstanz, Constance, Germany).

Hypocotyls from 5-days-old dark-grown *Arabidopsis* seedlings were high-pressure frozen in a Leica EM ICE high-pressure freezer (Leica, Wetzlar, Germany). Frozen samples were freeze-substituted in a Leica EM AFS2 (Leica, Wetzlar, Germany) in 2.5% OsO₄ in acetone for 41 hrs at -90°C. Subsequently, the temperature was gradually increased to 0°C. Hypocotyls were then infiltrated with

Epoxy Embedding Medium (EPON) (Fluka Chemie, Buchs, Switzerland) for ultrastructural analyses. 70 nm ultra-thin sections were mounted on copper grids (Plano GmbH, Wetzlar, Germany) coated with Pioloform (Wacker-Chemie, Munich, Germany) and stained with saturated Uranyl Acetate (Merck, Darmstadt, Germany) at 4°C, followed by 0.4% lead citrate in 0.2% NaOH. Alternatively, samples were stained with Uranyl-Less (Science Services, Munich, Germany) and 0.4% lead citrate in 0.2% NaOH. The sections were imaged in a Jeol 2100 Plus electron microscope (Jeol, Freising, Germany) operated at 120 kV.

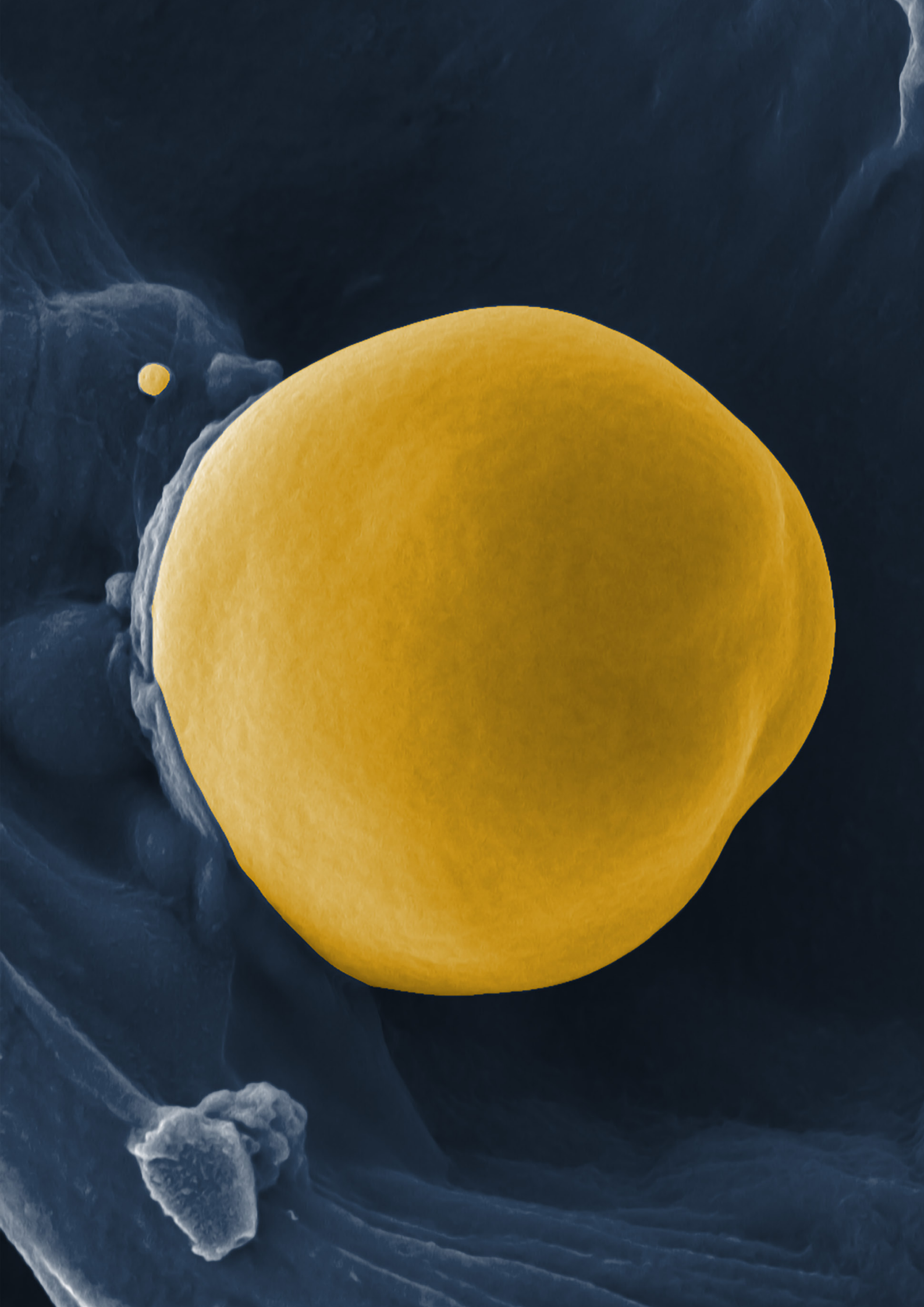
05

CHAPTER 1

GNC AND GNL REPRESS GRAVITROPISM

In 2010, Quirin L. Ranftl (Lehrstuhl für Systembiologie der Pflanzen, Technische Universität München, Freising, Germany) reported that the lateral shoots of *Arabidopsis thaliana* mutants emerge with a steeper angle from the primary inflorescence than in the wild type, whereas the emergence angles from lateral shoots in *GATA* overexpression lines are strongly increased (Richter et al, 2010; Behringer et al, 2014; Ranftl et al, 2016). To examine whether these defects are related to defects in shoot negative gravitropism, I measured the shoot bending responses of 25-days-old wild type, *gnc gnl* and GNLox inflorescences grown in the light, 1 hr after turning them by 90° (**Figure 1A**). To avoid interference from phototropic responses the experiment was performed in the dark. After 1 hr, while wild type plants had reoriented their inflorescence by 60°, *gnc gnl* had already reoriented to 90° (**Figure 1A and B**). On the contrary, GNLox had reoriented only by 30°

(**Figure 1A and B**). Inflorescences start to reorient upwards after an initial lag period of 30 mins (**Figure 2**) (Tasaka et al, 1999; Xia et al, 2021). In the double mutant, inflorescences are already reorienting after 15 mins, and bending rapidly after 30 to 45 mins, thus achieving full reorientation in 1 hr (**Figure 1A and B, and Figure 2**). These results indicate that *GNC* and *GNL* are negative regulators of negative gravitropism in the shoot. I then analysed negative gravitropism in hypocotyls of 2-days-old wild type, *gnc gnl* and GNLox seedlings grown in the dark on ½ MS medium. The hypocotyl bending angle was increased in *gnc gnl* and decreased in GNLox, compared to the wild type (**Figure 1C and E**). Addition of 1% sucrose to the medium enhanced gravity perception in all three genotypes, but the respective differences were maintained (**Figure 1D and E**). Thus, *GNC* and *GNL* repress gravity perception in the hypocotyl.



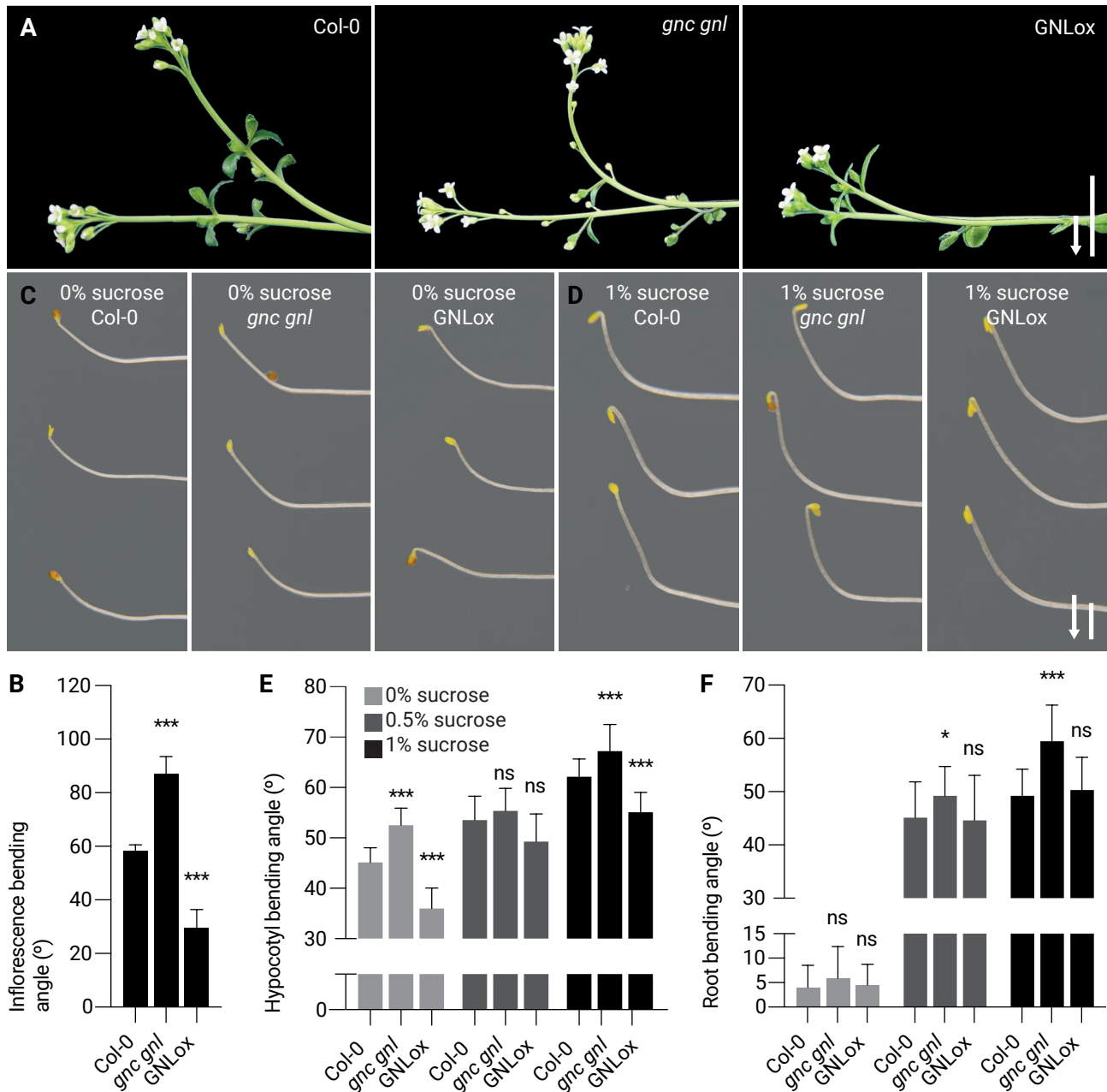


Figure 1. *GNC* and *GNL* repress gravitropism. **A.** Overlay of two representative photographs of 25-days-old *Arabidopsis thaliana* wild type, *gnc gnl* and GNLox inflorescences before, and 1 hr after turning the plants by 90°. The arrow indicates the direction of the gravity vector. Scale bar = 1 cm. **B.** Average and standard deviation of inflorescence bending angles (a) as detected in the experiment shown in (A) and measured from 10 wild type, *gnc gnl* or GNLox plants. **C.** and **D.** Representative photographs of *Arabidopsis thaliana* wild type, *gnc gnl* and GNLox hypocotyls from 2-days-old seedlings grown on sucrose-free ½ MS medium (C) and 1% sucrose-supplemented ½ MS medium (D), as specified, 24 hrs after reorienting the seedlings by 90°. The arrow indicates the direction of the gravity vector. Scale bar = 1 mm. **E.** Average and standard deviation of the hypocotyl bending angle (a) as detected in the experiment shown in (C) from 50 wild type, *gnc gnl* or GNLox seedlings. **F.** Average and standard deviation of the root bending angle (a) from 50 wild type, *gnc gnl* or GNLox seedlings 24 hrs after turning the seedlings by 90°. Student's *t*-test: *, *p* 0.05; ***, *p* 0.001; ns, not significant.

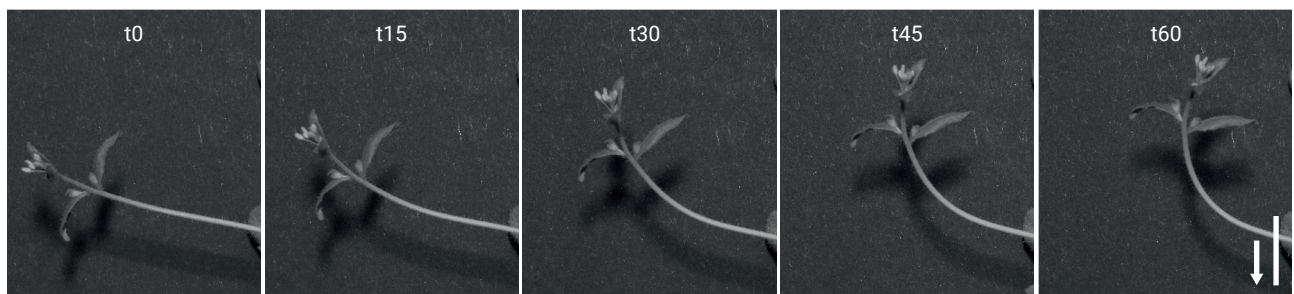


Figure 2. Gravotropism in the inflorescences of *gnc gnl* plants. **A.** Photographs of 25-days-old *Arabidopsis thaliana gnc gnl* inflorescences, acquired every 15 min during a 1 hr time period. The arrow indicates the direction of the gravity vector. Scale bar = 1 cm.

When I analysed positive gravitropism, the root bending in *gnc gnl* mutants was subtly increased compared to the wild type, but this difference became more pronounced and statistically significant upon sucrose treatment (**Figure 1F**). Thus, *GNC* and *GNL* also repress gravity perception in the root.

Contrary to the differences observed from seedlings grown with 1% sucrose, addition of 0.5% sucrose did not provide compelling information (**Figure 1E and F**). Therefore, the following experiments were performed only on sucrose-free and 1% sucrose-supplemented $\frac{1}{2}$ MS medium to reduce the number of conditions analysed.

Sucrose treatment rescues disrupted gravitropism in *GNL*ox seedlings, but not in *pifq* seedlings

Phytochromes inhibit hypocotyl negative gravitropism through the phosphorylation of PIF1, PIF3, PIF4 and PIF5 (Kim et al, 2011; Yang et al, 2020), which in turn, modulate the expression of the GATA factors (Richter et al, 2010; Richter et al, 2013a; Richter et al, 2013b). To evaluate whether the differences observed in positive gravitropism were a consequence of the repression that PIF factors exert on *GNC* and *GNL*, I measured the growth direction of 3-days-old wild type, *gnc gnl* and *GNL*ox seedlings

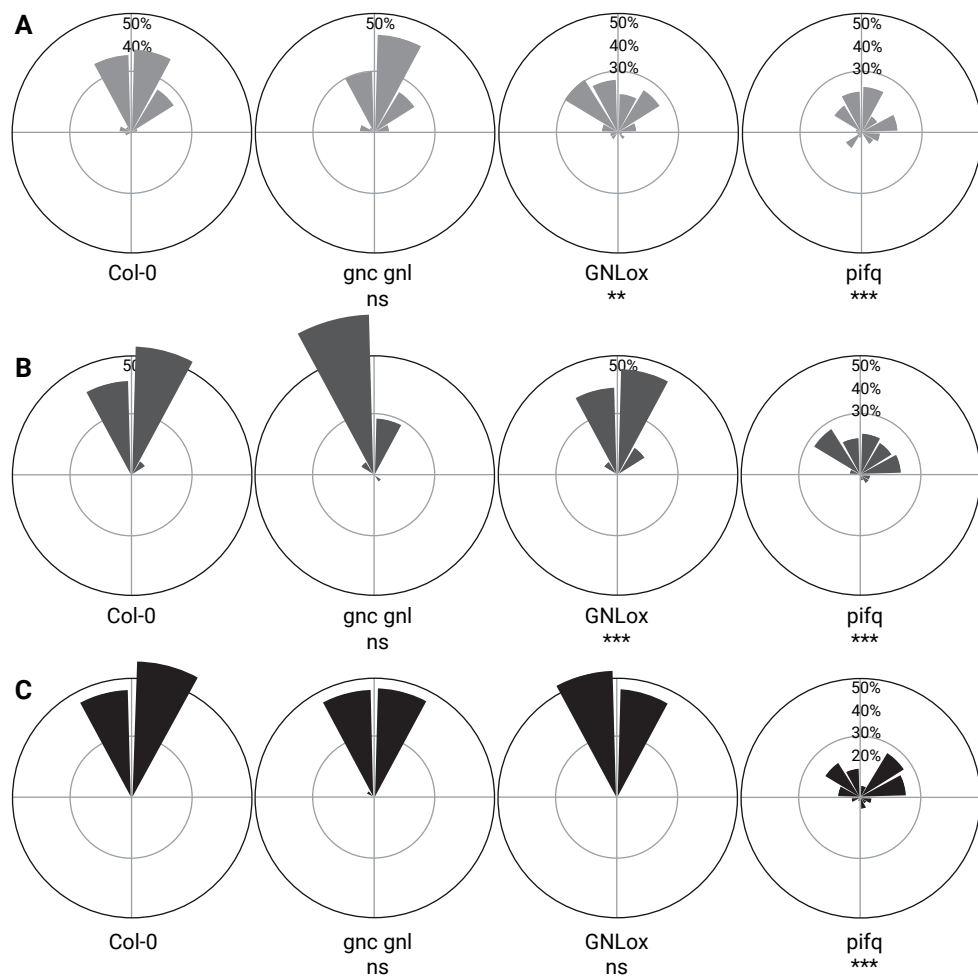


Figure 3. *GNC* and *GNL* repress gravitropism independently of PIF factors. A – C. Growth direction of 3-days-old *Arabidopsis thaliana* wild type, *gnc gnl*, *GNL*ox and *pifq* hypocotyls grown vertically on sucrose-free $\frac{1}{2}$ MS medium (A and B) and 1% sucrose-supplemented $\frac{1}{2}$ MS medium (C). Seedlings were illuminated with undirected far-red light (A) or grown in the dark (B and C). Diagrams are sectioned in a 30° interval. N = 50. For Student's *t*-test: **, *p* 0.01; ***, *p* 0.001; ns, not significant; means of the absolute value of the angle were compared.

grown on vertical plates in the dark or in far-red light. In contrast to the experiment described above, seedlings were not straightened against the gravity vector, but the distribution of angles was directly measured. Hypocotyls of wild type seedlings grew upwards against the gravity vector when grown in the dark on sucrose free and 1% sucrose-supplemented $\frac{1}{2}$ MS medium (**Figure 3B and C**). However, in far-red light, wild type seedlings oriented less against the gravity vector, indicating disrupted gravitropism (**Figure 3A**). The double-mutant *gnc gnl* displayed a similar response to the wild type in all three conditions (**Figure 3**). On the other hand, GNLox seedlings grown in far-red light or in the dark without sucrose, were more agravitropic than the wild type (**Figure 3A and B**). Addition of 1% sucrose to the medium restored the disrupted gravitropic response, and GNLox seedlings grew upwards (**Figure 3C**). The *pifq* mutant showed a more pronounced agravitropic response in far-red light and in the dark without sucrose compared to GNLox (**Figure 3A and B**). Addition of 1% sucrose did not restore the gravitropic defects, indicating that *GNC* and *GNL* repress negative gravitropism independently of the PIFs.

GATA FACTORS REGULATE THE EXPRESSION OF GENES INVOLVED IN STARCH METABOLISM

To examine whether gene expression

differences can provide insights into the molecular cause for the differential gravitropism responses, I performed an RNA-seq analysis with 3-days-old *Arabidopsis thaliana* wild type, *gnc gnl* and GNLox seedlings grown in the dark on $\frac{1}{2}$ MS medium. In this work, I largely focused on seedlings grown in the dark. On the one side, this allowed me using tropic responses as a physiological readout for the observed changes in starch granule accumulation, and on the other side, to avoid the interference from impaired chlorophyll accumulation in the *GATA* genotypes analysed (Bastakis et al, 2018), and from transitory starch synthesis and degradation during day-night cycles (Zeeman et al, 2002).

As expected, the expression of *GNC* and *GNL* was reduced in the double mutant, while the expression of *GNL* in GNLox was higher compared to the wild type (**Figure 4A**). Applying a false discovery rate (FDR) < 0.05, I identified 1876 upregulated and 1312 downregulated genes in *gnc gnl*, as well as 2046 upregulated and 2204 downregulated genes in GNLox (**Figure 4B and C**). As shown in the Venn diagrams, a total of 204 genes were shared between DEGs upregulated in *gnc gnl* and downregulated in GNLox (**Figure 4B**), whereas 140 genes were shared between DEGs downregulated in *gnc gnl* and upregulated in GNLox (**Figure 4C**).

Next, I performed a GO analysis, and identified Thalianol metabolism (GO 0080003), Starch metabolism (GO

0005982) and Amino acid metabolism (GO 0006520) as the 3 most enriched GO categories among the 204 genes shared between DEGs upregulated in *gnc gnl* and downregulated in GNLox (**Figure 4B and D**). The most enriched term category, referred to as Thalianol metabolism, accounted only for 3 genes, thus leading to false-positive enrichment (Fulcher et al, 2021). When subtracting Thalianol metabolism, then Starch metabolism was the most enriched GO category among genes differentially regulated between *gnc gnl* and GNLox seedlings grown in the dark (**Figure 4D**). Additionally, the term categories Re-

sponse to auxin (GO 0009733), Developmental growth (GO 0048589) and Response to stimulus (GO 0009416) represented the 3 most enriched categories among the 140 genes shared between DEGs downregulated in *gnc gnl* and upregulated in GNLox (**Figure 4C and E**).

In summary, a total of 344 genes were antagonistically regulated between *gnc gnl* and GNLox (**Figure 4B and C**). From these, genes involved in starch metabolism were strongly enriched, indicating a role of *GNC* and *GNL* in the regulation of starch accumulation.

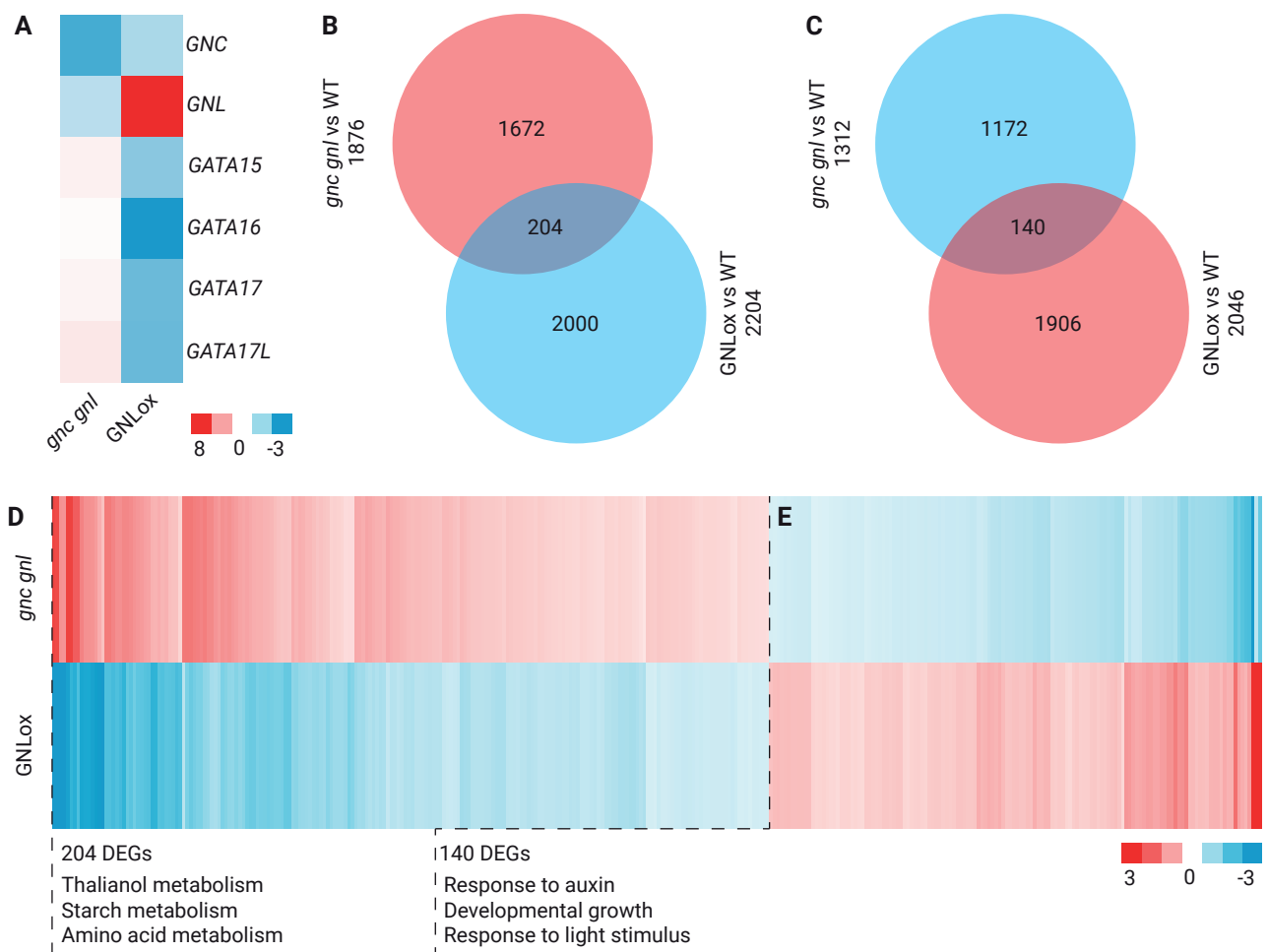


Figure 4. Expression profile of *gnc gnl* and GNLox seedlings grown in the dark. **A.** Heat map representation of the expression of LLM-domain B-GATA factors from 3-days-old *Arabidopsis thaliana* *gnc gnl* and GNLox seedlings grown in the dark. **B.** and **C.** Venn diagrams comparing the genes upregulated in *gnc gnl* and downregulated in GNLox (**B**), or downregulated in *gnc gnl* and upregulated in GNLox (**C**). **D.** and **E.** Heat map representation of 204 DEGs (**D**) and 140 DEGs (**E**) identified in the diagrams shown in (**B** and **C**), displaying the 3 most enriched GO term categories for each set of DEGs. Colour scale represents Log₂ fold change values filtered by FDR < 0.05.

Starch metabolism genes are upregulated in *gnc gnl* seedlings

The perception of gravity induces negative gravitropism in the endodermis of hypocotyls and shoots, and positive gravitropism in root columella cells (Christie & Murphy, 2013). Considering that gravity perception is promoted by the sedimentation of starch granules, the differential regulation of starch metabolism genes might explain the defects observed in the perception of gravity described above (**Figure 1**) (Kiss et al, 1989; Christie & Murphy, 2013).

To further characterize the most enriched term categories from genes upregulated in *gnc gnl* (**Figure 5A**), I generated a protein-protein interaction network using the STRING database (**Figure 5B**). A total of 110 candidate proteins distributed in 5 distinct but highly interactive clusters. In Chapter 2, I will discuss the clusters associated with Photosynthesis light harvesting and Stomata development in more detail.

The cluster associated with Starch metabolism was constituted by 16 proteins, which encompassed a wide range of functions such as starch anabolism, including subunits of AGP-ase and SS1; starch catabolism proteins like SEX4; starch granule development as of LIKE EARLY STARVATION (LESV); and sugar transport with FRUCTOKINASE (FRKs) or the maltose transporter MALTOSE EXCESS (MEX1) (**Appendix 1**). To have a more comprehensive understanding

of the regulation that GNC and GNL exert on starch, the genes associated to starch metabolism were represented along the starch pathway (**Figure 5C**). Clearly, I detected an increased expression of *PGM1*, of 3 genes encoding for the large (*APL*) and small (*APS*) subunits of *AGP-ase*, of *GBSS* and *SEX4*. Most important, *SS1*, *BE1* as well as two isoamylases (*ISA1* and *ISA2*) were antagonistically regulated between the double mutant and the overexpressor (**Figure 5C**). Upregulation of these genes may lead to increased starch synthesis, and differential starch accumulation, which in turn may be causal for the tropism phenotypes of *gnc gnl* and, conversely, of *GNLox* (**Figure 1**).

Sucrose does not impact the expression profile of starch metabolism genes

Taking into account that addition of 1% sucrose to the medium enhanced the bending of hypocotyls and roots in the *GATA* genotypes analysed (**Figure 1**), I further explored the role of *GATA* factors in starch metabolism by performing a complementary RNA-sequencing experiment with 3-days-old *Arabidopsis thaliana* wild type, *gnc gnl* and *GNLox* seedlings grown in the dark, but this time on 1% sucrose-supplemented $\frac{1}{2}$ MS medium.

First, I assessed the sucrose responsiveness at the gene level. I selected 3 well characterized sucrose-induced genes: *6-PHOSPHOGLUCONATE DEHYDROGENASE 3* (*PGD3*), *ARABI-*

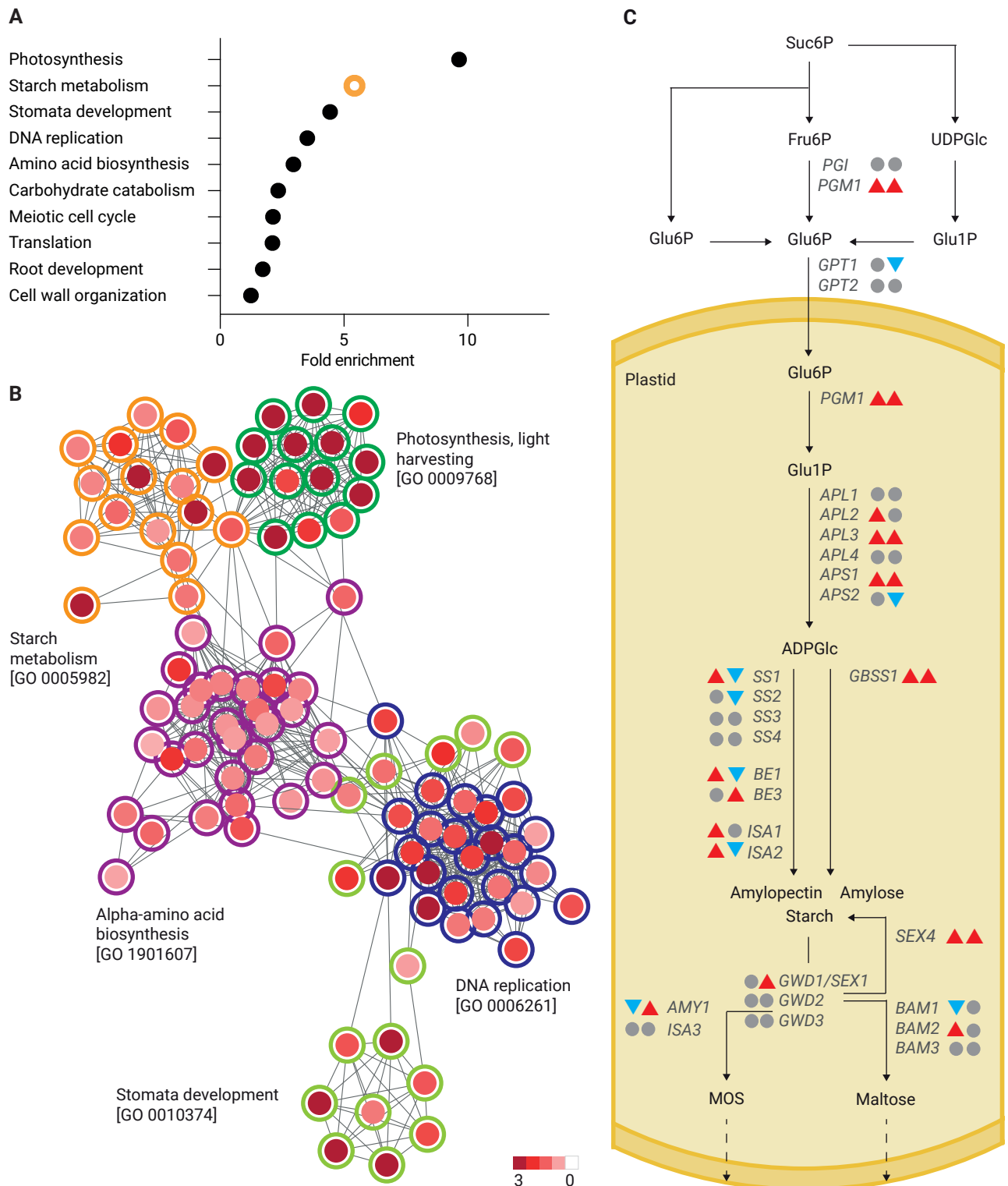


Figure 5. Starch metabolism genes are differentially regulated in *gnc gnl*. **A.** Graph displaying the GO enrichment analysis of the 10 most strongly regulated GO term categories among the genes up-regulated in 3-days-old *Arabidopsis thaliana gnc gnl* seedlings grown in the dark. **B.** STRING network analysis of the genes belonging to the five most prominent GO term categories as shown in (A). Photosynthesis, light harvesting (green), starch metabolism (yellow), stomata development (bright green), DNA replication (blue) and alpha-amino acid biosynthesis (violet). Network nodes and colour scale represent Log_2 fold change values, filtered by $\text{FDR} < 0.05$. **C.** Graphical display of the starch anabolism and catabolism pathway. Arrowheads symbolize genes upregulated (red) or downregulated (blue) in *gnc gnl* (left) and GNLox (right) using $\text{FDR} < 0.05$ as filtering criteria. Abbreviations: sucrose-6-phosphate (Suc6P), fructose-6-phosphate (Fru6P); UDP-glucose (UDPGlc); glucose-6-phosphate (Glu6P); glucose-1-phosphate (Glu1P); ADP-glucose (ADPGlc); maltooligosaccharides (MOS); PHOSPHOGLUCOSE ISOMERASE (PGI); PHOSPHOGLUCOMUTASE1 (PGM1); GLUCOSE 6-PHOSPHATE TRANSLOCATOR (GPT1); ADP GLUCOSE PYROPHOSPHORYLASE LARGE SUBUNIT (APL); ADP GLUCOSE PYROPHOSPHORYLASE SMALL SUBUNIT (APS); STARCH SYNTHASE (SS); BRANCHING ENZYME (BE); ISOAMYLASE (ISA); GRANULE BOUND STARCH SYNTHASE (GBSS); STARCH EXCESS4/LAFORIN-LIKE1 PHOSPHOGLUCAN PHOSPHATASE (SEX4); GLUCAN WATER DIKINASE (GWD); STARCH EXCESS1 (SEX1); ALPHA-AMYLASE (AMY); ISOAMYLASE (ISA); BETA-AMYLASE (BAM).

DOPSIS *GLUCOSE-6-PHOSPHATE/PHOSPHATE TRANSLOCATOR (GPT2)* and a putative phosphofructokinase (*AT1G20950*); and 3 sucrose-repressed genes: *DARK INDUCIBLE 6 (DIN6)*, *DORMANCY-ASSOCIATED PROTEIN-LIKE 1 (DRM1)* and a putative cold acclimation protein (*AT4G37220*) (Gonzali et al, 2006). As expected, *PGD3*, *GPT2* and *AT1G20950* were upregulated in wild type, *gnc gnl* and GNLox, whereas *DIN6*, *DRM1* and *AT4G37220* were downregulated, thus verifying the quality of the sucrose treatment (**Figure 6A**).

Next, I characterized the effect of sucrose in the *GATA* genotypes. Applying an FDR < 0.05, I identified 1901 upregulated and 2317 downregulated genes in *gnc gnl*, as well as 2487 up-

regulated and 2856 downregulated genes in GNLox (**Figure 6C and D**). From these, *GNC* and *GNL* were downregulated in *gnc gnl*, and *GNL* strongly upregulated in the over-expression line (**Figure 6B**). A total of 137 genes were shared between DEGs upregulated in *gnc gnl* and downregulated in GNLox (**Figure 6C**), and 137 genes were shared between DEGs downregulated in *gnc gnl* and upregulated in GNLox (**Figure 6D**). I performed a GO analysis of the genes antagonistically regulated between *gnc gnl* and GNLox, and found Cell wall modification (GO0042545), Cell wall biogenesis (GO0042546) and Polysaccharide metabolism (GO0005976) as the 3 most enriched GO term categories among the 137 genes from DEGs downregulated in *gnc gnl* and

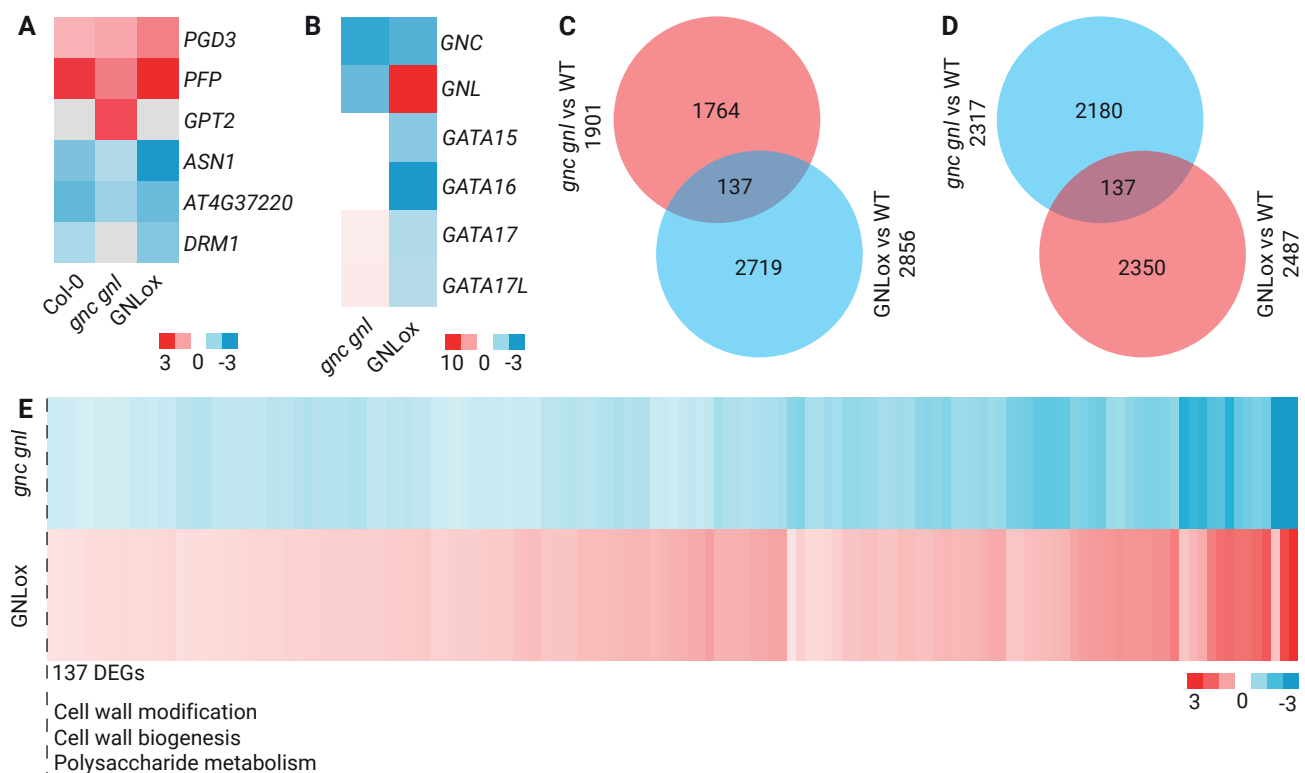


Figure 6. Expression profile of *gnc gnl* and GNLox seedlings grown in the dark with 1% sucrose-supplemented medium. **A.** Heat map representation of sucrose-modulated genes from 3-days-old *Arabidopsis thaliana gnc gnl* and GNLox seedlings grown in the dark on 1% sucrose-supplemented ½ MS medium. **B.** Heat map representation of the expression of LLM-domain B-GATAs genes of *gnc gnl* and GNLox seedlings. **C.** and **D.** Venn diagrams comparing the genes upregulated in *gnc gnl* and downregulated in GNLox (**C**), or downregulated in *gnc gnl* and upregulated in GNLox (**D**). **E.** Heat map representation of 137 DEGs identified in the diagram shown in (**D**) displaying the 3 most enriched GO term categories.

upregulated in GNLox (**Figure 6E**). Unfortunately, no significant GO term categories could be identified from DEGs upregulated in *gnc gnl* and downregulated in GNLox. The term categories Cell wall modification, Cell wall biogenesis and Polysaccharide metabolism will be also discussed in more detail in Chapter 2.

The antagonistic regulation of starch metabolism genes between *gnc gnl* and GNLox was not conserved upon sucrose treatment, thus I then aimed to understand whether sucrose impacts the expression of genes involved in starch metabolism. I performed an in-depth analysis with the RNA-seq data obtained from genes upregulated in *gnc gnl*, from seedlings grown without sucrose (**Figure**

4) and with 1% sucrose (**Figure 6**). I identified 1323 genes that were modulated by sucrose, and 578 genes not induced by sucrose treatment (**Figure 7A**). The GO terms Starch metabolism (GO 0005982) and Stomata development (GO 0010374) were enriched among the 578 genes not induced by sucrose (**Figure 7**), whereas Plastid transcription (GO0042793) and translation (GO0032544) were enriched among the 1323 genes differentially expressed upon treatment with sucrose (**Figure 7A**). Thus, treatment with 1% sucrose does not impact the expression profile of starch metabolism genes in *gnc gnl* seedlings grown in the dark.

Comparative transcriptomics reveals a significant conservation in the differential regulation of starch metabolism genes between *Arabidopsis thaliana* and *Marchantia polymorpha*

Bryophytes is the collective name for early land plant lineages, including mosses, like *Physcomitrium patens*, hornworts and liverworts, such as *Marchantia polymorpha*. This taxonomic division possess all the characteristic from land plant evolution, however lacks vascular tissue and true roots, differentiating vascular plants from bryophytes.

Aiming to better understand the role of B-GATA factors on starch metabolism in plant evolution, I compared the transcriptome of *Arabidopsis thaliana* (**Figure 4**) with the tran-

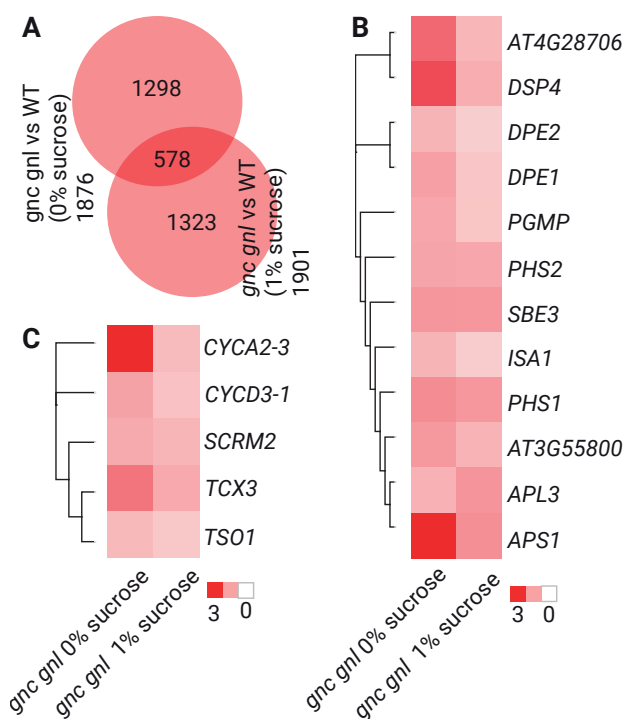


Figure 7. Sucrose does not impact the expression profile of starch metabolism genes in *gnc gnl*. **A.** Venn diagram comparing genes upregulated in *Arabidopsis thaliana gnc gnl* seedlings grown in the dark on sucrose-free and on 1% sucrose ½ MS medium. **B.** and **C.** Heat map representation of genes belonging to the GO term category Starch metabolism (**B**) and Stomata development (**C**), identified in the diagram shown in (**A**). Colour scale represents Log₂ fold change values, filtered by FDR < 0.05.

scriptome of *Marchantia polymorpha* (**Figure 8**). Noteworthy, the CRISPR/Cas9-generated mutants *Mpb-gata1-1* and *Mpb-gata1-2*, the overexpression line *MpB-GATAOX3* as well as the transcriptomic data of *Marchantia polymorpha* were generously provided by Peter Schröder (Lehrstuhl für Systembiologie der Pflanzen, Technische Universität München, Freising, Germany).

Applying a false discovery rate (FDR) < 0.05, we identified 13 differentially expressed genes involved in starch metabolism (**Figure 8A**). Similarly than in *Arabidopsis thaliana*, in the *GATA4* mutants *Mpb-gata1-1* and *Mpb-gata1-2*, I detected an increased expression of starch anabolism genes encoding for the large (*APL*) or small (*APS*) subunits of AGP-ase, isoamylases (*ISA*) and branching enzymes (*BE2*); starch catabolism genes like *SEX4* and *GWD1*; and the maltose transport encoding

gene *MEX1* (**Figure 8A**). On the other hand, most of these genes were down-regulated, or not significantly enriched in the overexpressor *MpB-GATA3OX*. The clear antagonistic regulation between mutants and the overexpressor line, and the high similarity with the transcriptomic profile of *gnc gnl* and *GNLox* in *Arabidopsis thaliana* reveals conserved and specific features of the GATA factors on starch metabolism.

In an attempt to examine starch distribution in *Marchantia polymorpha* I stained the rhizoids of 3-weeks-old wild type (BoGa), *Mpb-gata1-1* and *Mpb-gata1-2* grown in the light on ½ MS Gamborg's B5 medium (**Figure 8B**). However, as described in previous studies (Koide et al, 2020), no visible starch was detected along the rhizoid, nor in the rhizoid cap of wild type, *Mpb-gata1-1* and *Mpb-gata1-2* plants (**Figure 8B**).

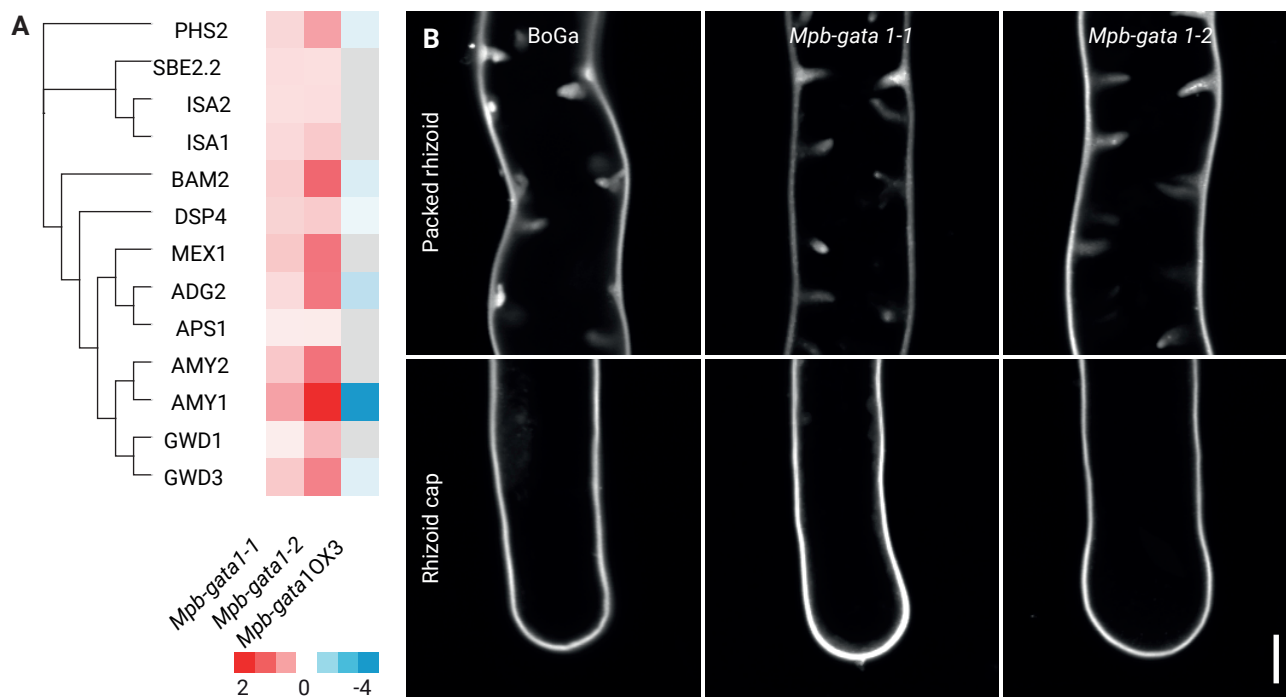


Figure 8. Starch metabolism genes are differentially regulated in *Marchantia polymorpha* *Mpb-gata1-1*, *Mpb-gata1-2* and *MpB-GATAOX3*. **A.** Heat map representation of *Marchantia polymorpha* *Mpb-gata1-1*, *Mpb-gata1-2* and *Mpb-gata1OX3* orthologs, belonging to the GO term category starch metabolism and identified from 3-days-old *Arabidopsis thaliana* seedlings as shown in (Figure 5). **B.** Representative confocal microscopy images of mPS-PI-stained rhizoids from 3-weeks-old *Marchantia polymorpha* plants grown in ½ Gamborg's B5 medium containing 1.4% plant agar. Scale bar = 10 µm.

THE NUMBER AND SIZE OF STARCH GRANULES ARE ALTERED IN *gnc gnl* AND GNLOX SEEDLINGS

Because gravity perception is promoted by the sedimentation of starch granules (Kiss et al, 1989; Christie & Murphy, 2013), I examined starch granule size and number in hypocotyl endodermis and root columella cells of wild type, *gnc gnl* and GNLOx seedlings grown in the dark (Figure 9). Starch granule size was increased in *gnc gnl*, and strongly decreased in GNLOx (Figure 9A, C, E and F). On

sucrose-containing medium, starch granule size increased in all genotypes but the respective differences between the genotypes were maintained (Figure 9B, D, E and F). Singularly, in GNLOx seedlings grown with 1% sucrose the size of endodermal starch granules did not exceed the size of granules in wild type seedlings grown without sucrose (Figure 9, B, E and F). Therefore, I concluded that the GATA factors repress starch granule growth in endodermal and columella cells.

At the same time, I noticed that the number of starch granules was

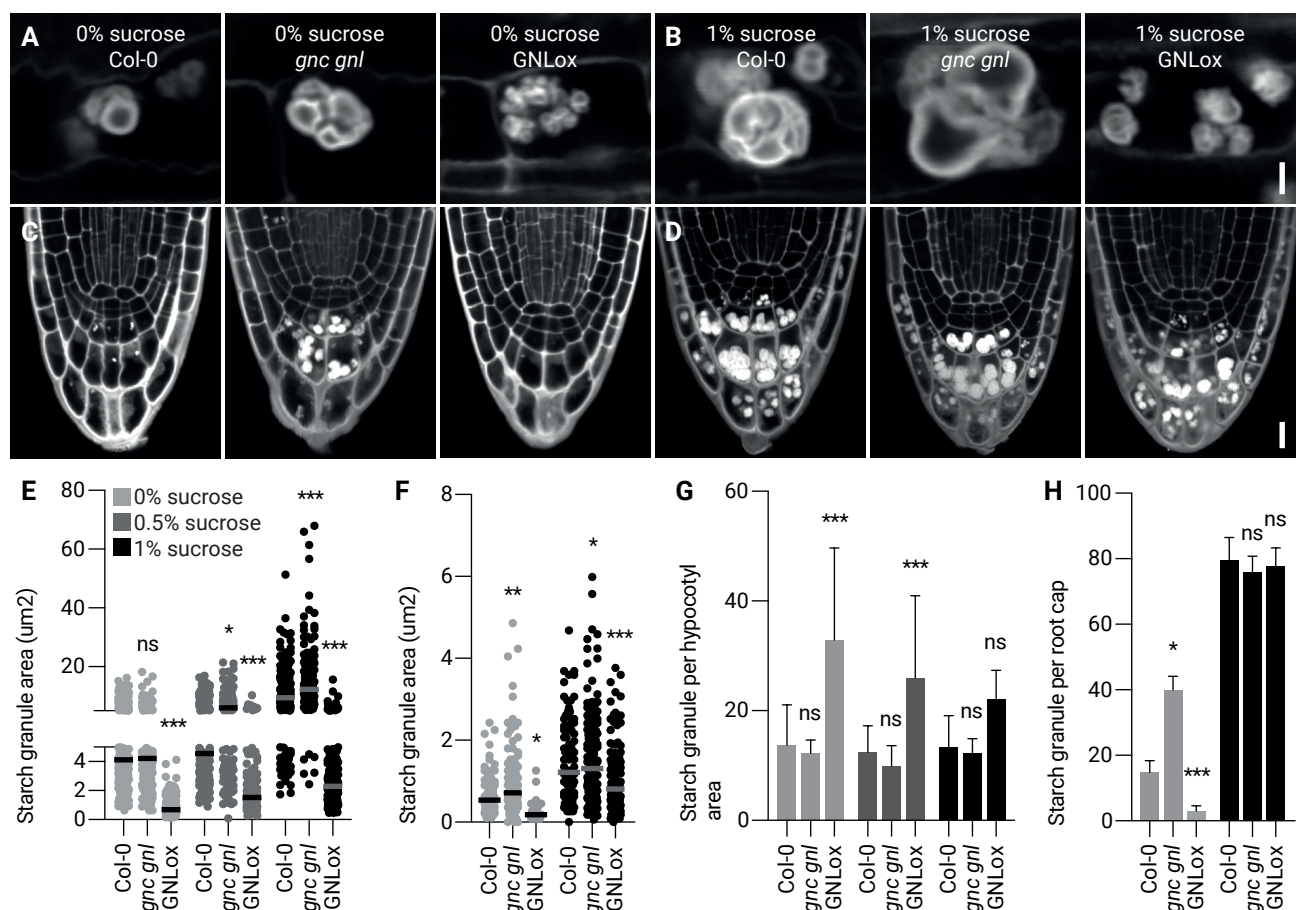


Figure 9. GNC and GNL repress starch granule growth. A – D. Representative confocal microscopy images of mPS-PI-stained starch granules from the hypocotyl endodermis cells (A and B) and the columella cells in the root tip (C and D) from 5-days-old *Arabidopsis thaliana* wild type, *gnc gnl* and GNLOx seedlings grown in the dark on sucrose-free ½ MS medium (A and C) and 1% sucrose-supplemented ½ MS medium (B and D), as specified. Scale bar = 5 and 20 µm. E. and F. Graphs displaying the starch granule area (µm²) as a proxy for starch granule size of individual starch granules, from 5-days-old seedlings grown on 0%, 0.5% and 1% sucrose-supplemented ½ MS medium, as detected in (A – D). N 200. G. and H. Graphs displaying average and standard deviation of starch granule number per field from hypocotyl endodermis cells (G) and the entire root columella (H) from 5-days-old seedlings grown on 0%, 0.5% and 1% sucrose-supplemented ½ MS medium, as detected in (A – D). N 10; Student's t-test: *, $p \leq 0.05$; **, $p \leq 0.01$; ***, $p \leq 0.001$; ns, not significant.

strongly increased in GNLox hypocotyl endodermal cells and, slightly but not significantly, decreased in *gnc gnl*, suggesting that GATA factors may also promote starch granule initiation in the endodermis (**Figure 9A and G**). Upon addition of 1% sucrose, the number of starch granules in GNLox decreased significantly, suggesting a possible correlation be-

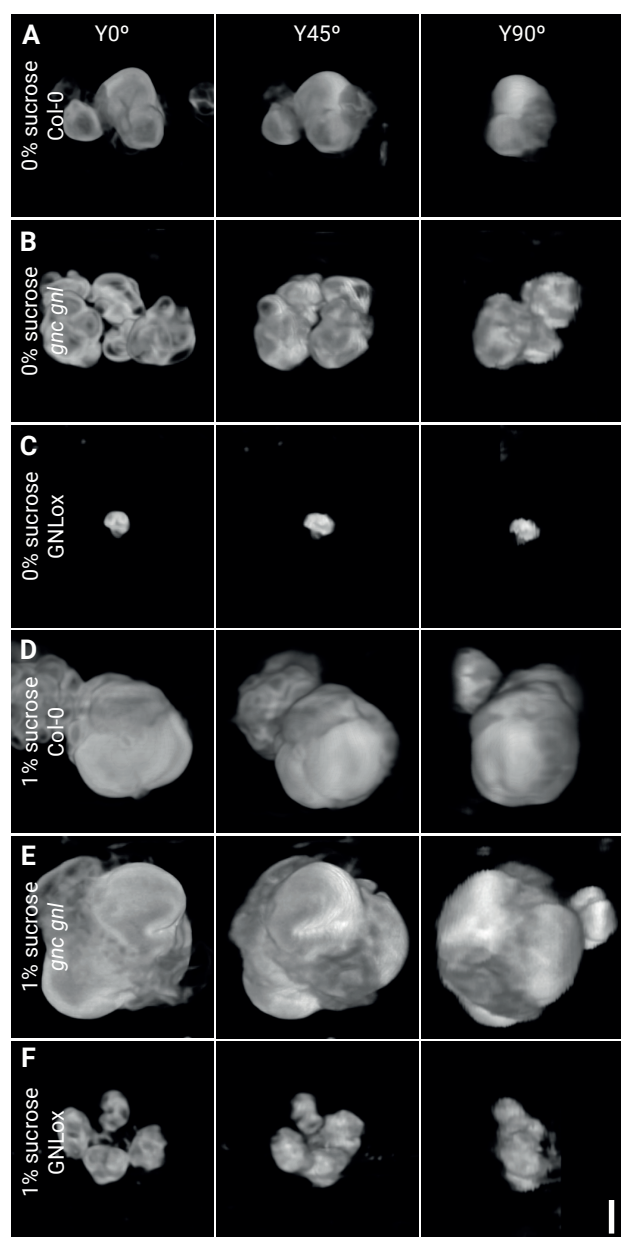


Figure 10. Starch granule morphology is altered in the dark. A – F. 3D reconstruction of representative confocal z-stacks with multi-view (Y0°, Y45° and Y90°) of mPS-PI-stained starch granules of the hypocotyl endodermis cells from 5-days-old *Arabidopsis thaliana* wild type, *gnc gnl* and GNLox seedlings grown in the dark on 0% sucrose-free ½ MS medium (A – C) and 1% sucrose-supplemented ½ MS medium (D – F), as specified. Scale bar = 5 μm.

tween starch granule size and number (**Figure 9B and G**). On the contrary, granule number was strongly decreased in GNLox root columella cells, whereas *gnc gnl* mutants accumulated a significantly increased number of starch granules (**Figure 9C and H**). On 1% sucrose, all genotypes produced more starch granules than on sucrose-free medium, and the differences between the genotypes disappeared (**Figure 9D and H**). In summary, I concluded that *GNC* and *GNL* induce starch granule initiation in endodermal cells.

The size of starch granules in root columella cells was reduced compared to granules located in hypocotyl endodermal cells (**Figure 9E and F**). Unfortunately, visualization of starch granules under the CLSM lead to poor detection of small starch granules located in root columella cells. Thus, the number of starch granules quantified in wild-type and GNLox root columella cells might not be representative of the total amount of starch granules in the root (**Figure 9H**).

Starch granule morphology undergoes alterations in the dark

To qualitatively assess the morphology of starch granules in the endodermis I generated 3D renders from z-stacks of endodermal starch granules (**Figure 10**). Starch granule size was increased in *gnc gnl* and strongly decreased in GNLox, in line with my previous analyses (**Figure 9 and 10**). Remarkably, in all genotypes starch

granules acquired a spherical morphology rather than the well-characterized flattened discoid morphology of granules located in chloroplasts from cotyledons, stomata and rosette leaves (Burgy et al, 2021; Liu et al, 2021b; Lim et al, 2022). The spherical morphology of granules was enhanced on 1% sucrose-supplemented $\frac{1}{2}$ MS medium, primarily in wild type and *gnc gnl* cells. A closer look revealed that the surface of starch granules in *gnc gnl* was not uniform, but included granules fused together (Figure 10E). These results support the hypothesis for a role of *GNC* and *GNL* in starch granule initiation and development, and indicates that the morphology of starch granules from seedlings grown in the dark differs from light-grown plants.

GNC and GNL independently repress starch granule growth, regardless of PIF factors

To examine whether *GNC* and *GNL* repress starch granule growth downstream of PIFs, I measured starch granule size and number in the hypocotyl endodermis of dark-grown wild type, *GNLox*, *pifq* and *pifq GNLox* seedlings (Figure 11). On sucrose-free $\frac{1}{2}$ MS medium, the size of starch granules in *GNLox*, *pifq* and *pifq GNLox* was clearly reduced compared to wild type (Figure 11A). However, in *pifq* endodermal cells starch granules were slightly, but significantly, bigger than those in *GNLox* and *pifq GNLox* (Figure 11A). Addition of 1% sucrose to the medium increased the size of

starch granules in all genotypes and enhanced the differences between *pifq* and *GNLox*, *pifq GNLox* (Figure 11A). Importantly, there were no significant differences between *GNLox* and *pifq GNLox* upon treatment with sucrose (Figure 11A).

Concurrently, the number of starch granules in *GNLox* and *pifq GNLox* hypocotyl endodermal cells was strongly increased, whereas in *pifq* were decreased (Figure 11B). As described above, the addition of sucrose to the medium leads to a reduced number of starch granules in *GNLox* (Figure 9), and to some extent in *GNLox pifq* (Figure 11B). However, no significant decrease was observed in wild type and *pifq* hypocotyl endodermal cells. Taken together, these results favour the conclusion that *GNC* and *GNL* promote starch granule initiation in the hypocotyl endodermal cells, independently of the PIFs.

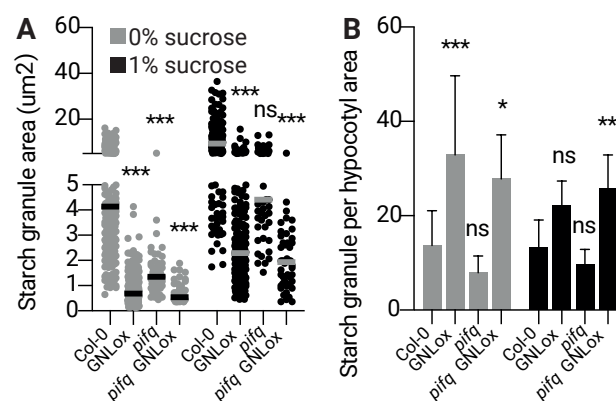


Figure 11. GNC and GNL repress starch granule growth independently of PIF factors. **A.** Graph displaying the starch granule area (μm^2) as a proxy for starch granule size of individual starch granules from hypocotyl endodermis cells from 5-days-old *Arabidopsis thaliana* wild type, *gnc gnl*, *GNLox*, *pifq* and *pifq GNLox* seedlings grown in the dark on sucrose free $\frac{1}{2}$ MS medium and 1% sucrose-supplemented medium, as specified. N 200. **B.** Graph displaying average and standard deviation of starch granule number per field from hypocotyl endodermis cells from 5-days-old seedlings grown on 0% and 1% sucrose, as specified. N 10; Student's t-test: *, $p \leq 0.05$; **, $p \leq 0.01$; ***, $p \leq 0.001$; ns, not significant.

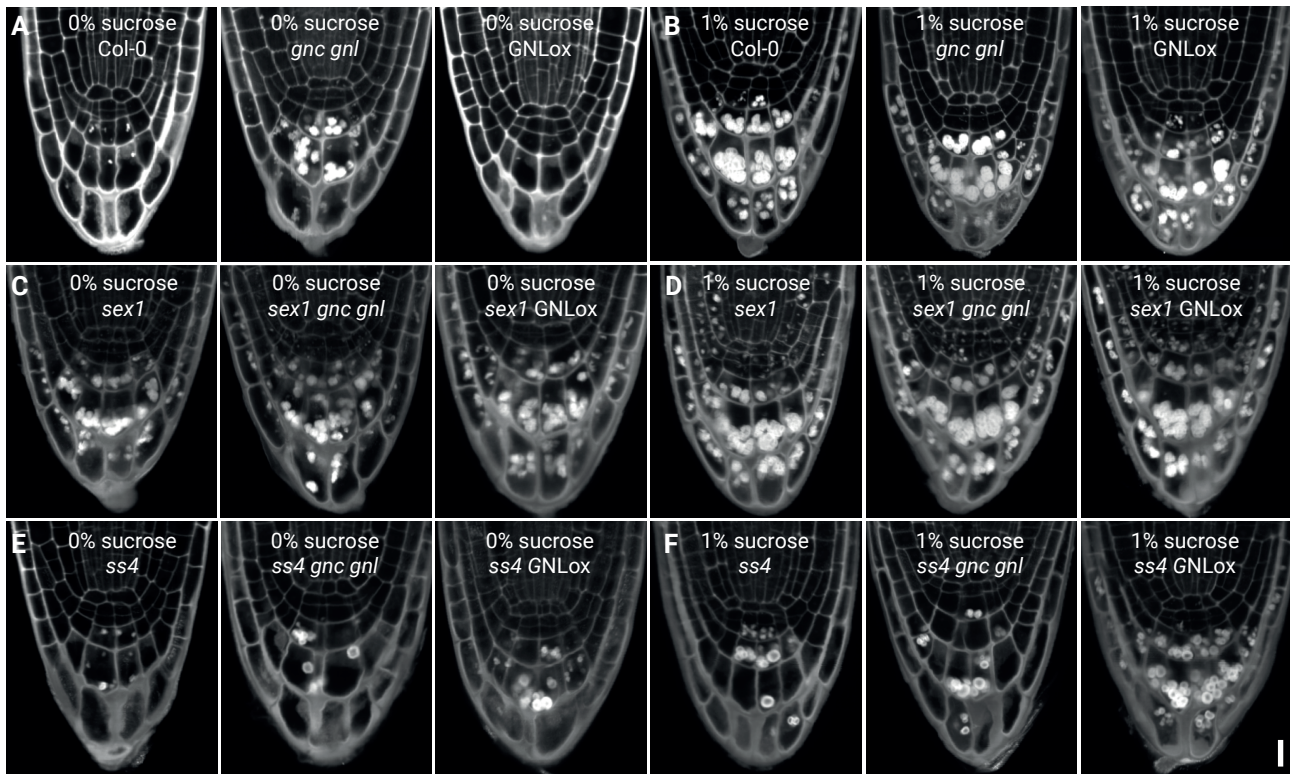
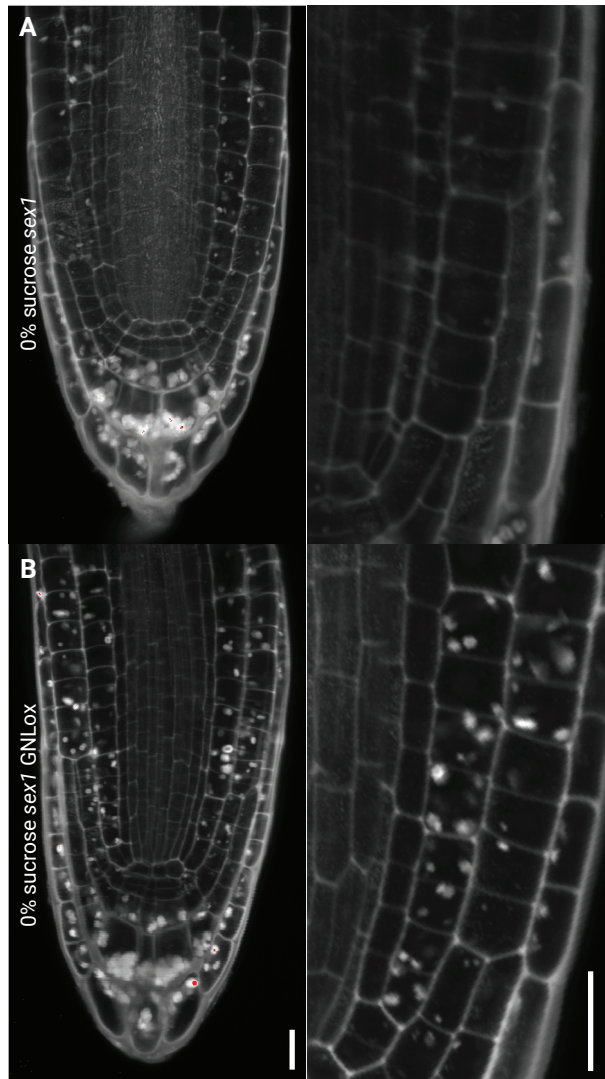


Figure 12. *GNC* and *GNL* repress starch granule growth in a *SEX1*- and *SS4*-dependent manner. A – F. Representative confocal microscopy images of mPS-PI-stained starch granules from the columella cells in the root tip from 5-days-old *Arabidopsis thaliana* seedlings from the specified genotypes, grown in the dark on sucrose-free ½ MS medium (A, C and E) and 1% sucrose-supplemented ½ MS medium (B, D and F), as specified. Scale bar = 20 μm. Wild type, *gnc gnl* and *GNL*ox images are identical to those shown in Figure 13.



GNC* and *GNL* repress starch granule growth in a manner dependent on *SEX1* and *SS4

The number, size and shape of starch granules is affected by the rate of initiation and the relative abundance of amylose and amylopectin (Burgy et al, 2021; Merida & Fettke, 2021). Starch degradation is initiated by amylopectin phosphorylation through *GWD1*, which adds phosphate groups to glucosyl residues. *GWD1* enables the high-ordered glucan chains at the starch granule surface to become more soluble (Mahlow et al, 2014). In the *GWD1* mutant *sex1*, besides a high accu-

Figure 13. *sex1* *GNL*ox accumulates more starch granules in non-columella cells. A – B. Representative confocal microscopy images of mPS-PI-stained starch granules from the columella cells in the root tip from 5-days-old *Arabidopsis thaliana* seedlings from *sex1* (A) and *sex1* *GNL*ox (B), grown in the dark on sucrose-free ½ MS. Scale bar = 20 μm.

mulation of starch due to impaired starch degradation (Yu et al, 2001), granules have irregular edges as a consequence of uneven metabolism (Edner et al, 2007; Liu et al, 2021b). On the other hand, SS4 promotes starch granule initiation and thereby determines starch granule number, but it also has an influence on granule shape (Crumpton-Taylor et al, 2013; Merida & Fettke, 2021). Rather than the multiple flatter granules that can be found in wild type plants, *ss4* mutants produce only one round granule per amyloplast. Therefore, and taking into consideration the available literature, I investigated the role of GNC and GNL, in combination with SS4 and GWD1 on the regulation of starch granule morphology.

In line with previous publications, on sucrose-free $\frac{1}{2}$ MS medium, *sex1* roots accumulated clearly more starch than wild type in columella cells (**Figure 12C**). After mPS-PI staining, I did not observe striking differences between *sex1* and *sex1 gnc gnl*, whereas in *sex1 GNLox* starch accumulated in columella cells but also in non-columella cells, such as lateral columella, epidermal and cortex cells (**Figure 12C and 13**). On 1% sucrose *sex1*, *sex1 gnc gnl* and *sex1 GNLox* accumulated starch in most of the cell files (**Figure 12D**).

In *ss4* roots, starch granules acquired the previously described characteristic round morphology (**Figure 12E and F**) (Merida & Fettke, 2021). Larger starch granules were observed in *ss4 gnc gnl*, and strikingly, also in *ss4 GN-*

Lox, possibly by promoting starch accumulation and granule initiation (**Figure 12E**). On sucrose-supplemented $\frac{1}{2}$ MS medium, the number of starch granules increased in all genotypes, enhancing the differences between *ss4* and *ss4 GNLox*, which accumulated large starch granules in columella cells, but also smaller granules in non-columella cells (**Figure 12E and F**). Therefore, I concluded that GNC and GNL repress starch granule growth in a SEX1- and SS4-dependent manner.

STARCH GRANULE INITIATION IS REPRESSED BY GNC AND GNL

As previously described, the morphology and number of starch granules is differentially regulated in *gnc gnl* and the GNL overexpression line (**Figure 9 and 10**). Nevertheless, the poor resolution in highly magnified images made it difficult to properly analyse the surface of starch granules. Therefore, I extracted and purified starch from entire seedlings, grown in the dark for 3 days on sucrose-free and 1% sucrose-supplemented $\frac{1}{2}$ MS medium, as specified. Then, I examined the starch granules by scanning electron microscopy (SEM) (**Figure 14**). In line with my previous observations, starch granule size was increased in preparations from *gnc gnl*, at least when seedlings were grown on 1% sucrose (**Figure 14A, D and G**). In turn, GNLox repressed granule size in both sucrose-free and sucrose-supplemented medium (**Figure**

14A, D and G). These results indicate once more that GATA factors repress granule growth or prevent granule initiation. In addition, in all 3 genotypes, starch granules adopted again a spherical morphology, thus reinforcing the idea that seedlings grown in the dark produce spherical granules, rather than flattened or discoid granules found in chloroplasts. The fact that starch was extracted from entire seedlings clearly indicates that the spherical morphology is not characteristic of hypocotyl endo-

dermal and root columella cells, but rather an effect of starch granules from seedlings grown in the dark.

Increased starch granule size could also be detected in *sex1 gnc gnl* and *ss4 gnc gnl*, even though granule size was already enlarged in *sex1* and *ss4* single mutants, respectively (**Figure 14B - I**). Across all genotypes and on both growth media tested, starch granule size was increased in the *gnc gnl* mutant. On the other hand, GNLox repressed granule size in the wild type and in *sex1* GNLox, but not

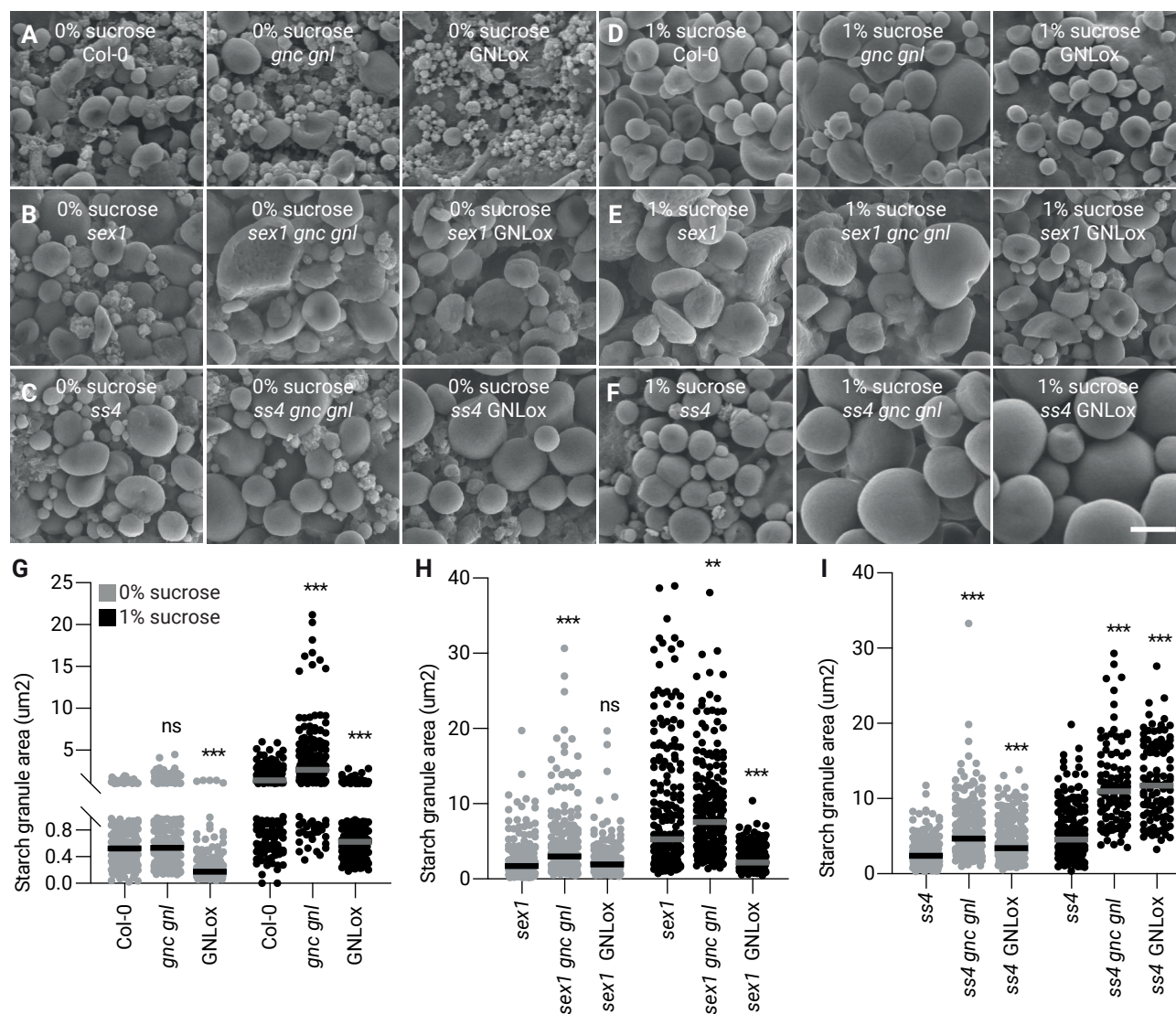


Figure 14. GNC and GNL repress starch granule initiation. **A - F.** Representative scanning electron microscopy images of starch granules prepared from 5-days-old *Arabidopsis thaliana* seedlings from the specified genotypes, grown in the dark on sucrose-free ½ MS medium (A, C, E) and 1% sucrose-supplemented ½ MS medium (B, D, F). Scale bar = 250 µm. **G. - I.** Scatter plots of individual starch granule area measurements as a proxy for granule size, as well as their average from the experiment shown in (A - F). N = 200; Student's *t*-test: ***, p 0.001; **, p 0.01; ns, not significant.

in *ss4* GNLox, where aberrant starch granules reached 10 times the size detected in the wild type (**Figure 14B - I**). Interestingly, the irregular surface described in *sex1* mutants was enhanced in *sex1 gnc gnl* (**Figure 14B**), whereas in *ss4*, *ss4 gnc gnl* and *ss4* GNLox, granules were uniform (**Figure 14C and F**).

GNC and GNL repress starch granule initiation in a manner dependent on SS4

Iodine staining provides further insight about the content and distribution of amylose and amylopectin (Blennow et al, 2003; He et al, 2020; Hawkins et al, 2021). Light microscopy and appropriate concentrations of iodine allow visualization of the hilum, where the starch granule initiates, and concentric rings (Blennow et al, 2003; Cai et al, 2014).

To better understand how starch granules initiate in *gnc gnl* and GNLox, I stained starch preparations for 1 hr with Lugol's solution and glycerol (1:1 v/v), to avoid staining gradients as a result of iodine diffusion. Wild type granules stained purple and were composed of 1 individual starch granule (**Figure 15A**). In turn, granules in *gnc gnl* stained darker than wild type granules, suggesting higher concentrations of amylose (Blennow et al, 2003) and contained, in some cases, several granules

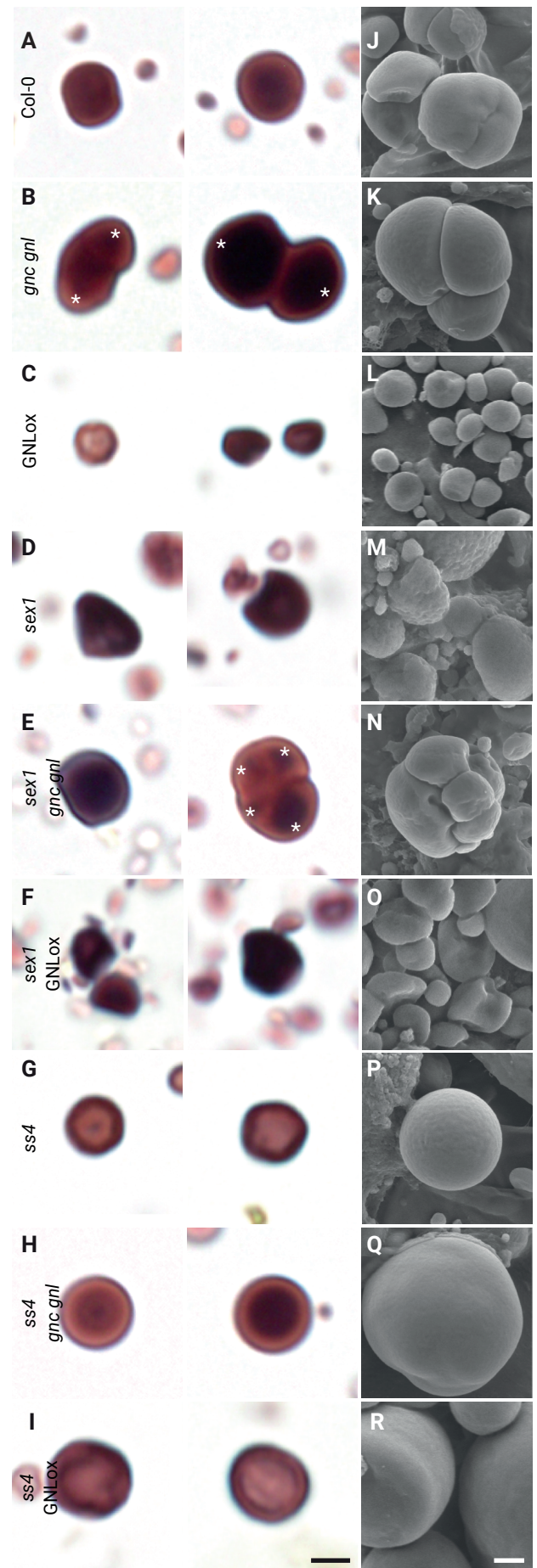


Figure 15. GNC and GNL repress starch granule in a SS4-dependent manner. A. – I. Representative images of iodine-stained starch granules detected by light microscopy prepared from 5-days-old *Arabidopsis thaliana* seedlings from the specified genotypes, grown in the dark on sucrose-free ½ MS medium. Scale bars = 2.5 µm. The asterisks indicate individual granules in a compound granule. **J. – R.** Representative scanning electron images of starch granules prepared from 5-days-old *Arabidopsis thaliana* seedlings from the specified genotypes, grown in the dark on sucrose-free ½ MS medium. Scale bars = 1µm.

fused together (**Figure 15B**). On the contrary, granules in GNLox stained pale and contained only one individual starch granule (**Figure 15C**). The preparations in *sex1* and *sex1* GNLox contained irregular shaped granules, as previously noted by SEM analysis (**Figure 14B**), and stained darker than the wild type, due to higher concentrations of amylose (**Figure 15D and F**) (Yu et al, 2001). Interestingly, I detected two types of starch granules in *sex1 gnc gnl*: first, darker and irregular granules resembling those found in the single *sex1* mutant, but also fused granules that stained lighter (**Figure 15E**). Most of the compound granules in *sex1 gnc gnl* contained 4 to 5 fused granules, adopting the form of a spherical sector, whereas the compound granules in *gnc gnl* contained up to 3 fused granules, and adopted a spherical morphology (**Figure 15B and E**). On the other hand, *ss4* preparations did not show iodine-staining differences compared to the wild type, since the ratio of amylose and amylopectin is not affected in the mutant (**Figure 15G**) (Szydlowski et al, 2009). Also, starch granules in *ss4 gnc gnl* and *ss4* GNLox stained purple (**Figure 15H and I**). Remarkably, no compound granules were found in *ss4 gnc gnl*. Thus, I concluded that *GNC* and *GNL* repress starch granule initiation in an SS4-dependent manner. Furthermore, the GATA factors might modulate the composition of starch, as indicated by iodine staining.

ECTOPIC EXPRESSION OF *GNL* REPRESSES TRANSITORY STARCH DEGRADATION

Having portrayed the role of the GATA factors in starch granule initiation and development in the hypocotyl endodermal and root columella cells, and at the whole-seedling level, it remained to be examined whether *GNC* and *GNL* modulate the total content of starch. First, I stained entire dark-grown seedlings in an attempt to visualize the pattern of starch distribution in the *GATA* genotypes analysed, and then I quantified the total content of starch in entire seedlings. However, I did not note any obvious differences in starch accumulation between the wild type, *gnc gnl* and GNLox (**Figure 16A and D**).

I next examined starch accumulation in the *sex1* and *ss4* backgrounds (**Figure 16B and C**). As previously described, the single *sex1* mutant accumulated more starch than wild type (Zeeman et al, 1998), hence exhibiting stronger staining in all cell files (**Figure 16B**). On $\frac{1}{2}$ MS medium, *sex1 gnc gnl* and *sex1* GNLox accumulated significantly less starch than *sex1*, but more starch than *gnc gnl* and GNLox (**Figure 16D**). The addition of sucrose to the medium restored starch accumulation in *sex1* GNLox (8.0 mg/g FW), reaching the levels in *sex1* (7.9 mg/g FW), but not in *sex1 gnc gnl* (**Figure 16B and D**). In turn, *ss4* accumulated less starch than wild type, on 1% sucrose-sup-

plemented $\frac{1}{2}$ MS medium (**Figure 16C and D**) (Crumpton-Taylor et al, 2013). Whereas *ss4* stained fainter than the wild type, *ss4 gnc gnl* and *ss4 GNLox* stained similarly to *gnc gnl* and GNLox (**Figure 16A and C**). Accordingly, *ss4 gnc gnl* and *ss4 GNLox* accumulated more starch than *ss4*, specially on 1% sucrose (**Figure 16D**). In summary, despite differences between the genotypes, the regulation of GNC and GNL on starch granule initiation does not impact the total content of starch in seedlings grown in the dark. Although I could not observe differences in the total amount of starch, I next examined the effects of GATA factors on transitory starch synthesis and degradation, to get further insight into possible feedback regulatory mechanisms. First, I measured starch in seedlings grown in the dark for 3 days on $\frac{1}{2}$ MS medium. The seedlings were first transferred for 2 hrs from sucrose-free to 1% sucrose-supplemented medium, in order to induce starch synthesis, and then following the re-transfer of these seedlings to sucrose-free medium (**Figure 17A**).

In this experiment, *gnc gnl* accumulated starch less efficiently (1.08 mg/g FW) than the wild type (1.49 mg/g FW) and GNLox (1.43 mg/g FW) (**Figure 17A**), indicating that GNC and GNL might contribute to transitory starch synthesis, at least when examined at the whole seedling level. When the seedlings were then re-transferred to sucrose-free medium, starch degradation in *gnc gnl* was comparable to

the wild type, while in GNLox, starch degradation was attenuated over a 6-hr period (**Figure 17A**). Therefore, *gnc gnl*, which had accumulated less starch on sucrose-containing medium, reached the initial levels of starch already after 2 hrs on sucrose-free medium, whereas the wild type had not yet reached this baseline after 8 hrs, at the end of the experiment (**Figure 17A**).

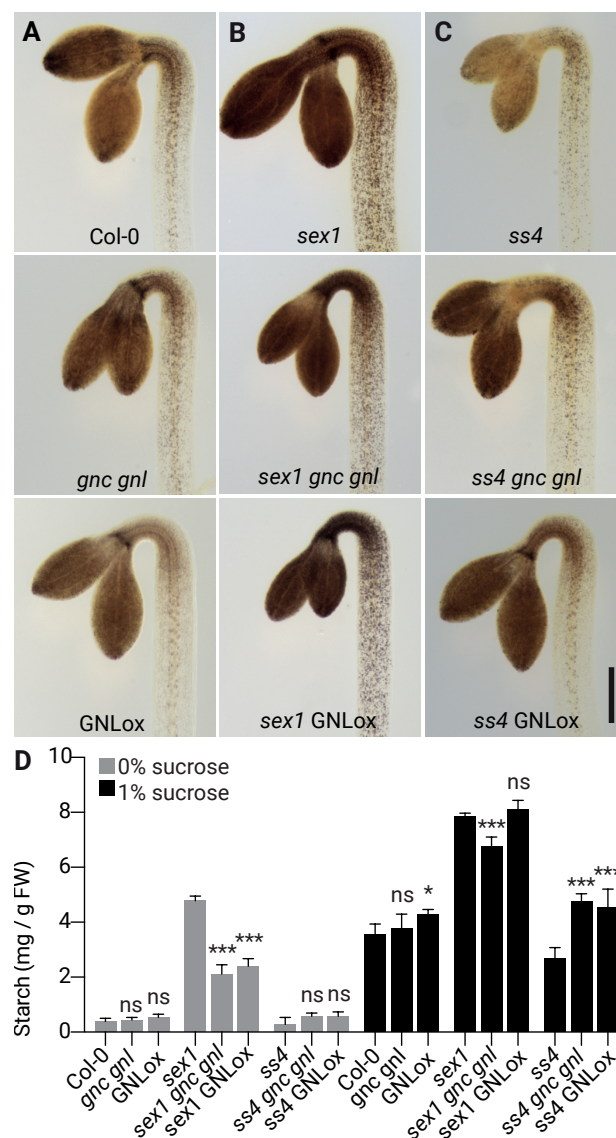


Figure 16. Differential effects of GNC and GNL on starch accumulation in the *sex1* and *ss4* backgrounds. A. – C. Representative images of 5-days-old *Arabidopsis thaliana* seedlings from the specified genotypes, grown in the dark on 1% sucrose-supplemented $\frac{1}{2}$ MS medium after iodine staining. Scale bar = 250 μ m. D. Graph displaying average and standard deviation of total starch content per g fresh weight (FW) in the specified genotypes of 5-days-old dark-grown seedlings grown in the dark on sucrose free $\frac{1}{2}$ MS medium and 1% sucrose-supplemented $\frac{1}{2}$ MS medium. Student's *t*-test: *, *p* 0.05; ***, *p* 0.001; ns, not significant.

In a complementary experiment, I grew seedlings on 1% sucrose-supplemented $\frac{1}{2}$ MS medium for 3 days in the dark, and then transferred them to sucrose-free conditions to examine starch degradation. The seedlings of all genotypes accumulated more starch on sucrose-containing medium (~ 3.8 mg/g FW) than on su-

crose-free medium (~ 0.6 mg/g FW). However, no clear differences were observed between the genotypes, well in line with the observations made after iodine staining (**Figure 16A**). After transferring the seedlings grown with sucrose to sucrose-free $\frac{1}{2}$ MS medium, I noted that starch degradation was accelerated in *gnc gnl* and attenuated in GNLox seedlings, when compared to the wild type (**Figure 17B**). Based on these observations, I concluded that *GNC* and *GNL* repress transitory starch degradation in the dark.

Transitory starch degradation is repressed by *GNC* and *GNL* at the whole-plant level, partially independent of chlorophyll accumulation

Plants generate sugars through photosynthesis that are stored in plastids in the form of starch, the main storage carbohydrate in plants (Zeeman et al, 2002). It has been previously reported that the B-GATA overexpression lines *GNCox* and *GNLox* have bigger chloroplasts, higher chlorophyll and thus, a higher photosynthesis rate (Chiang et al, 2012; Richter et al, 2013a; Behringer & Schwechheimer, 2015; Bastakis et al, 2018; Zubo et al, 2018). Therefore, it has been concluded that differences in starch accumulation in the *GATA* mutants are a direct effect of impaired greening (Hudson et al, 2011; Chiang et al, 2012; Zubo et al, 2018; An et al, 2020).

Bearing in mind that in the dark, the

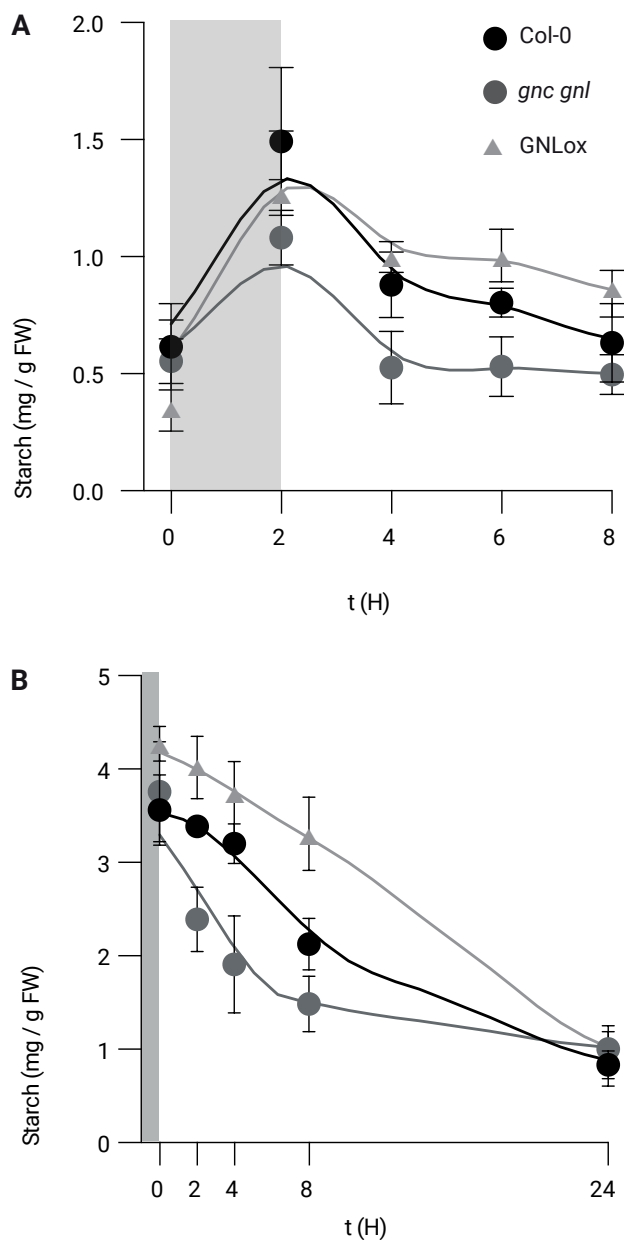


Figure 17. *GNC* and *GNL* regulate transitory starch degradation. **A. and B.** Graphs displaying the average and standard deviation of starch accumulation (A) after transfer of seedlings from sucrose-free to 1% sucrose-containing medium (grey area), followed by a retransfer to sucrose-free medium (white area), or (B) from growth on 1% sucrose-containing medium (grey area) to sucrose-free medium (white area). Shown are average and standard deviation from 6 biological replicate samples, with each biological replicate comprising hundreds of dark-grown seedlings.

effect of greening and photosynthesis is uncoupled from starch metabolism, and nevertheless, transitory starch degradation is still impaired in the *GATA* genotypes analysed, I

examined transitory starch accumulation in light-grown adult plants. 3-weeks-old plants were grown with a 12 hrs light / 12 hrs dark photoperiod, and samples harvested every 2



Figure 18. *GNC* and *GNL* regulate transitory starch degradation at the whole-plant level. Representative time course photographs of 3-weeks-old *Arabidopsis thaliana* wild type, *gnc gnl* and GNLox plants after iodine staining. Plants were grown with a 12 hrs light / 12 hrs dark photoperiod and samples harvested every 2 hrs, beginning at the End of Night (EoN) (Zt0). Scale bar = 2 cm.

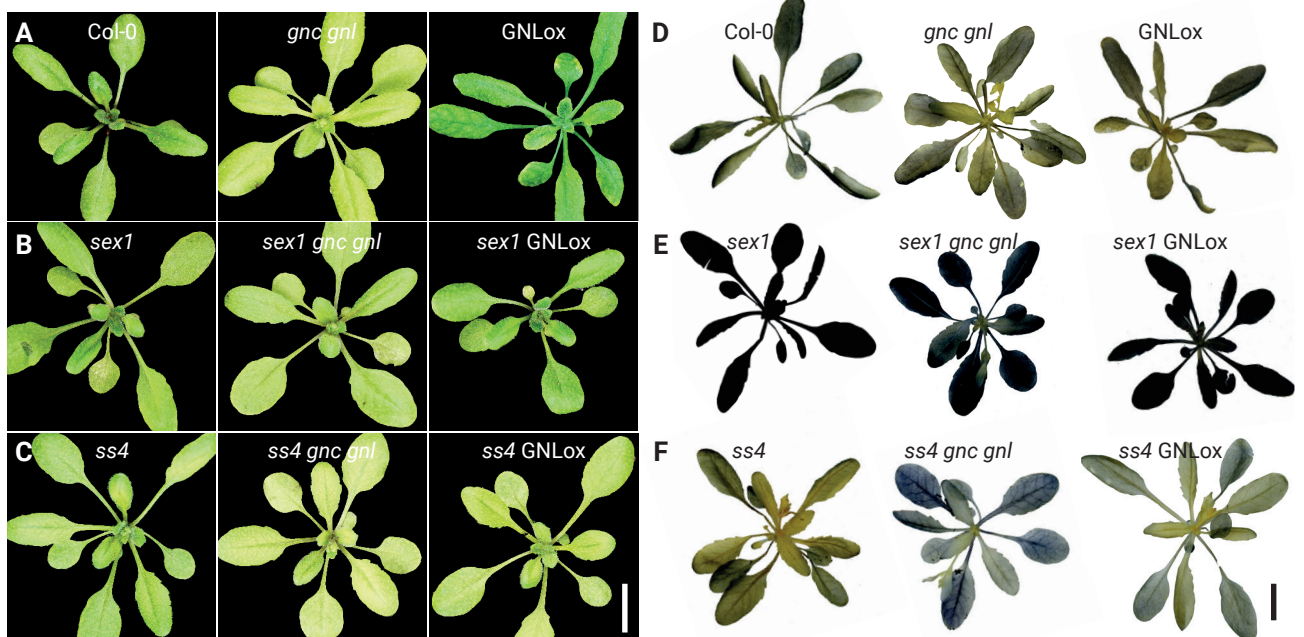


Figure 19. Differential effects of *GNC* and *GNL* on starch degradation in the *sex1* and *ss4* background at the whole-plant level. A. – C. Representative photographs of 3-weeks-old *Arabidopsis thaliana* plants of the specified genotypes. Scale bar = 2 cm. D. – F. Representative photographs of 3-weeks-old *Arabidopsis thaliana* plants of the specified genotypes after iodine staining. Plants were grown with a 12 hrs light / 12 hrs dark photoperiod and harvested at the End of Day (EoD). Scale bar = 2 cm.

hrs. At the End of Night (EoN / Zt0) all genotypes accumulated clearly less starch than during the light growth phase (ZT2 – 8) (**Figure 18**). However, *gnc gnl* plants accumulated less starch through the entire time course, compared to the wild type, as shown by iodine staining (**Figure 18**). By contrast, GNLox plants stained stronger, especially after 8 hrs of light exposure (**Figure 18**). Similarly to seedlings grown in the dark on sucrose-free medium, *gnc gnl* accumulated starch less efficiently, whereas GNLox accumulated more starch (**Figure 16 and 18**), providing further evidence that *GNC* and *GNL* repress transitory starch degradation.

To better understand whether in *GATA* mutants and overexpression lines, the differences in starch accumulation can fully attributed to impaired chlorophyll accumulation, I examined starch accumulation at the whole plant level in 3-weeks-old plants grown with a 12 hrs light / 12 hrs dark photoperiod, and compared iodine staining patterns to greening. I stained plants at the end of the light phase (End of Day, EoD), when starch accumulation reaches its peak (Zeeman et al, 2002) (**Figure 19**). As previously described (**Figure 18**) (Chiang et al, 2012; Zubo et al, 2018), Wild type and GNLox plants accumulated more starch than *gnc gnl* leaves (**Figure 19D**). In the *sex1* background, all three genotypes accumulated more starch than the wild type, hence staining stronger than wild type plants (**Figure 19E**) (Zeeman et al, 1998). Likewise, *sex1 gnc gnl* leaves

accumulated slightly less starch than *sex1*, also in accordance with the starch quantification performed in dark-grown seedlings (**Figure 16D and 19E**). On the contrary, *ss4*, *ss4 gnc gnl* and *ss4* GNLox accumulated less starch than the wild type, especially on juvenile leaves (**Figure 19F**) (Crumpton-Taylor et al, 2013).

When analysing chlorophyll accumulation, it became apparent that loss of *GNC* and *GNL* lead to reduced greening in the *sex1* and *ss4* backgrounds (**Figure 19A – C**). However, the content of starch in *gnc gnl*, *sex1 gnc gnl* and *ss4 gnc gnl* differed widely (**Figure 19D – F**). These results suggest that *GNC* and *GNL* repress transitory starch degradation independently of impaired chlorophyll accumulation (**Figure 19**). However, the effects of differential chlorophyll accumulation, and thus photosynthesis efficiency, cannot be uncoupled from starch metabolism in light-grown plants.

GNL independently repress starch synthesis, regardless of PGM1

PGM1 converts G6P to G1P. The loss-of-function mutant *pgm1* is often described as a starchless mutant, containing no obvious starch granules (Streb et al, 2009). The mutant phenotype clearly supports the starch-statolith hypothesis since it is partially agravitropic (Caspar et al, 1985; Kiss et al, 1989; Kawamoto et al, 2020). In addition to the genetic crosses generated with *sex1* and *ss4*, I also introduced the loss-of-function

mutant *pgm1* into the GNLox background, aiming to elucidate whether the GATA factors could play a role in early stages of starch synthesis. On sucrose-free and sucrose-supplemented $\frac{1}{2}$ MS medium, no starch granules could be observed in the hypocotyl endodermal and root columella cells of dark-grown *pgm1* and *pgm1* GNLox seedlings (**Figure 20A and B**), nor in any other cell file. Adult plants grown in the light manifested a reduction in growth, especially in *pgm1* GNLox (**Figure 20C**), and did not accumulate starch neither, hence not staining after exposure with iodine (**Figure 20D**).

I also introduced the *pgm1* mutant into the *gnc gnl* background. Unfortunately, after repeated attempts, I was not able to isolate a homozygous *pgm1 gnc gnl* line. Described below are the steps I followed while trying to isolate the homozygous triple mutant; to start with, I crossed homozygous *pgm1* and *gnc gnl* parental plants, and the resultant F1 progeny were allowed to self-pollinate. *PGM1* and *GNC* are close together in chromosome 5, thus linked segregation is to be expected. Aiming to bypass this inconvenience, I first isolated F2

plants containing homozygous *pgm1* and *gnc* alleles, and heterozygous *gnl* alleles. Plants were allowed to self-pollinate again.

To identify homozygous mutants, I first performed a phenotypic screening using iodine, since homozygous *pgm1* plants do not contain starch. Thus, these plants do not stain with iodine, whereas, wild type and heterozygous *pgm1* plants clearly show iodine staining. Next, I amplified the coding sequence of *PGM1* by PCR, and subsequently sequenced it, in order to identify the described recessive mutation present in *pgm1* (TGG, Trp-192 to TGA, STOP) (Periappuram et al, 2000). *GNC* and *GNL* were isolated through PCR-based screening of T-DNA insertions using specific primers (Table 1). The phenotypic and genetic screenings were repeated with F3 plants, unfortunately, despite using a large number of plants, no homozygous *pgm1 gnc gnl* mutants were identified.

Surprisingly, a certain number of F3 plants exhibited intermediate iodine staining, compared to the wild type and *pgm1* mutants, and were smaller than wild type plants. The reduction

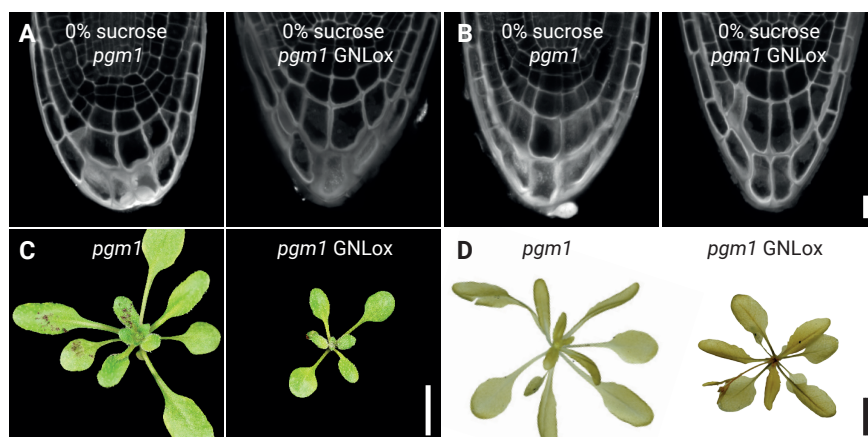


Figure 20. *GNL* regulates transitory starch accumulation independently of *PGM1*. **A.** and **B.** Representative confocal microscopy images of mPS-PI-stained columella cells in the root tip of 5-days-old *Arabidopsis thaliana pgm1* and *pgm1* GNLox seedlings grown in the dark on 0% sucrose-free (**A**) and 1% sucrose-supplemented $\frac{1}{2}$ MS medium (**B**). Scale bar = 5 μ m. **C** and **D.** Representative photographs of 3-week-old *Arabidopsis thaliana pgm1* and *pgm1* GNLox plants grown in the light (**C**) and after iodine staining (**D**). Scale bar = 2 cm.

in size is characteristic from plants that do not accumulate starch, as described for *pgm1* mutants (Stettler et al, 2009). As indicated by iodine staining, these plants contained less starch than *gnc gnl*, and were also smaller. I performed a genetic screening with these F3 plants, and I identified homozygous *gnc* and *gnl* alleles, but not the recessive mutation present in *pgm1*. These results suggest that in the *pgm1* mutant there are unknown mutations that segregate independently of *PGM1*.

ECTOPIC EXPRESSION OF *GNL* INDUCES THE DIFFERENTIATION OF AMYLOPLASTS TO ETIOPLASTS

Amyloplasts are derived from proplastids (Jarvis & Lopez-Juez, 2013) located in starch storage tissues and in gravity-sensing hypocotyl endodermal and root columella cells. The mechanisms regulating the cell type-specific division and differentiation of amyloplasts are not yet understood. In view of an apparent role of the GATA factors in chloroplast development, I next examined whether the differentiation of starch-accumulating amyloplasts was affected in *gnc gnl* or in GNLox.

In order to identify and characterize amyloplasts, I fluorescently labelled the plastid stroma of wild type, *gnc gnl* and GNLox by generating new genetic crosses with the transgenic line ptA5-3 (Fujiwara et al, 2018). The

construct expresses YFP fused to the transit peptide TP_{RBCS3A}, by the CaMV 35S promoter (Fujiwara et al, 2018). First, I analysed different tissues from ptA5-3 GNLox seedlings grown in the light or in the dark to have a better understanding of plastid distribution (**Figure 21**). As expected, fully developed and homogeneous chloroplasts localized in the cotyledons and hypocotyls of light-grown ptA5-3 GNLox seedlings, as indicated by the YFP signal and the accumulation of chlorophyll (**Figure 21A and B**). On the other hand, I observed a heterogeneity of plastids in the roots of light-grown seedlings and in most of the tissues grown in the dark (**Figure 21C - F**). Populations of plastids in the hypocotyls and roots of dark-grown seedlings were highly variable in their morphology and exhibited long stromules (**Figure 21E and F**) (Pyke, 2010; Pyke, 2011). The high frequency of stromules in ptA5-3 GNLox seedlings reassembled those in *arc5*, *arc6* and *atminE1* mutants (Fujiwara et al, 2018).

In order to identify amyloplasts, I directed the analysis towards starch-containing plastids located in columella cells, as identified by bright field (**Figure 22A and B**). I observed that in *gnc gnl*, amyloplasts were bigger than wild type, whereas in GNLox amyloplasts remained comparable or smaller to wild type (**Figure 22A and B**). Thus, GATA factors might repress amyloplast development in root columella cells.

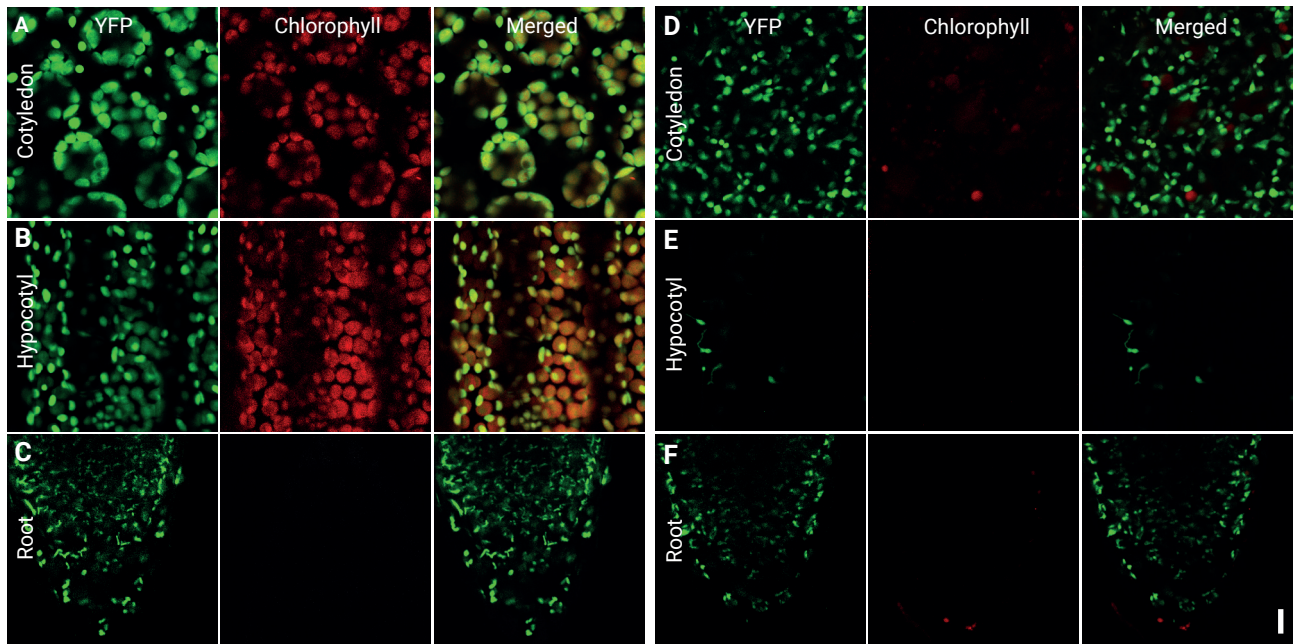


Figure 21. Plastid morphology in *ptA5-2* GNLox seedlings. A – F. Representative confocal microscopy images of plastid-targeted YFP and chlorophyll autofluorescence in the cotyledons (A and D), hypocotyl endodermis (B and E) and the root tip (C and F) of 5-days-old *Arabidopsis thaliana* *ptA5-3* GNLox seedlings grown in the light (A – C) or in the dark (D – F). Scale bar = 10 μ m.

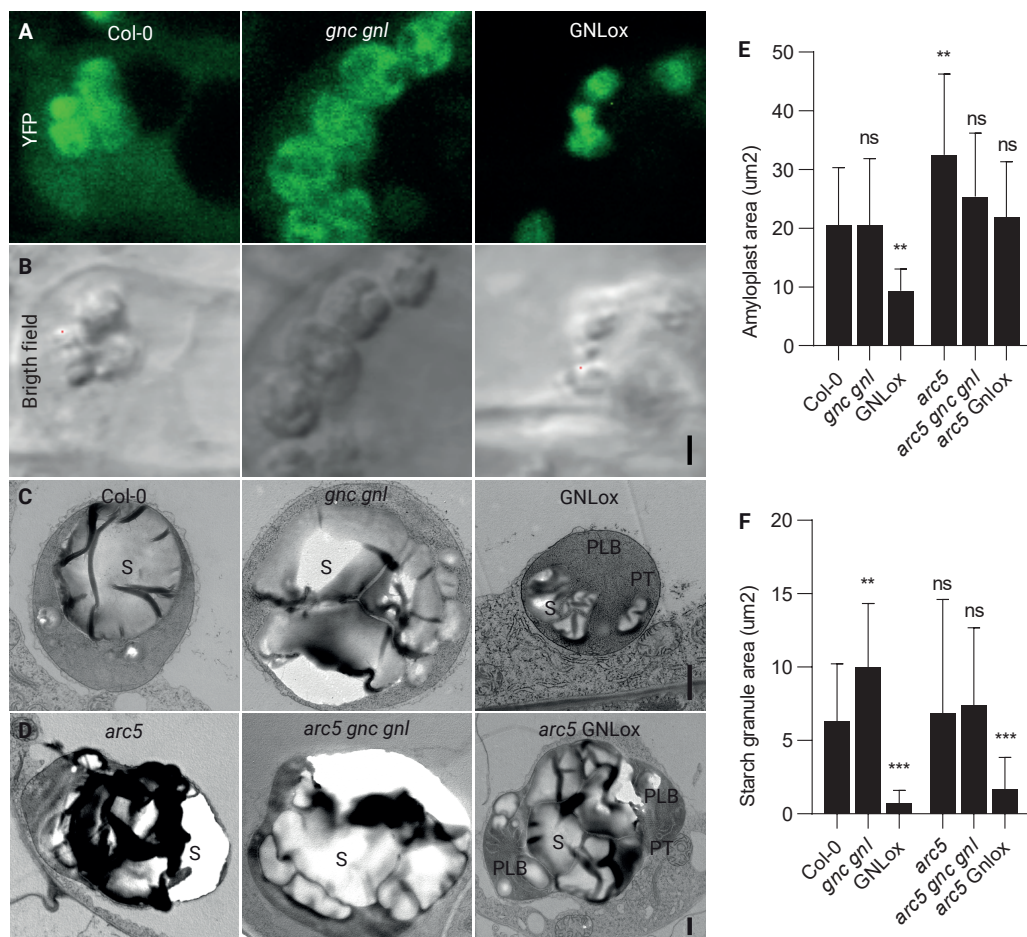


Figure 22. *GNC* and *GNL* regulate plastid differentiation. A. and B. Representative confocal microscopy images of plastid-targeted YFP (A) and bright field images (B) in the hypocotyl endodermis cells of 5-days-old *Arabidopsis thaliana* *ptA5-3*, *ptA5-3 gnc gnl* and *ptA5-3* GNLox seedlings grown in the dark. Scale bar = 2 μ m. C. and D. TEM images of representative amyloplasts from the hypocotyl endodermis of 5-days-old *Arabidopsis thaliana* seedlings of the specified genotype, grown in the dark. Abbreviations: S, starch granule; PLB, prolamellar body; PT, protothylakoid. Scale bar = 2 μ m. E. Graph displaying amyloplast area (μm^2) as a proxy for amyloplast size of individual amyloplast from hypocotyl endodermal cells, as shown in (C and D). N 50. F. Graph displaying starch granule area (μm^2) as a proxy for granule size of individual starch granules from hypocotyl endodermal cells, as shown in (C and D). N 50. Student's t-test: *, $p \leq 0.05$; **, $p \leq 0.01$; ***, $p \leq 0.001$; ns, not significant.

The growth of starch granules remains unaffected despite impaired amyloplast differentiation in GNLox seedlings

Chloroplasts division occurs via binary fission by a multiprotein complex which includes, among others, the ARC proteins. In the recessive *arc5* and *arc6* mutants, chloroplasts are enlarged and acquire a dumbbell morphology (Fujiwara et al, 2018; Sun et al, 2020). Taking into consideration that genes with a role in plastid development are differentially regulated in the *GATA* mutants (Bastakis et al, 2018), I introduced the *arc5* mutation into the *gnc gnl* and GNLox background to better understand the role of *GATA* factors in plastid division.

In collaboration with Erika Isono (Universität Konstanz, Constance, Germany), we examined amyloplasts in the hypocotyl endodermis by TEM (**Figure 22C and D**). Contrary to chloroplasts, amyloplasts in the double mutant were bigger than wild type and contained large starch granules that occupied most of the plastid stroma (**Figure 22C, E and F**). On the contrary, amyloplasts in GNLox contained smaller starch granules and interestingly, included prolamellar bodies (PLB) and protothylakoids (PT). These features are characteristic for etioplasts, but not for differentiated amyloplasts (**Figure 22C**). In addition, these undifferentiated amyloplasts appeared to be surrounded by endoplasmic reticulum (**Figure 22C**).

As expected, amyloplasts in *arc5*, *arc5 gnc gnl* and *arc5* GNLox were bigger in size than those in wild type, *gnc gnl* and GNlox respectively (**Figure 22C - E**). Although amyloplasts in *arc5* GNLox amyloplasts were bigger than in GNLox, still contained etioplasmic features, such as PLB and PTs, and most of the starch granules were small (**Figure 22D - F**). Introducing the *arc5* mutation in the *GATA* genotypes did not shed light into the regulation of *GNC* and *GNL* on plastid differentiation. However, it became apparent that the differences observed in starch granule size between the double mutant and the *GNL* overexpression line are not a consequence of defects in amyloplast development. In addition, *GNC* and *GNL* induce the conversion of plastids to etioplasts or pseudo-chloroplasts.

THE REGULATION OF *GNC* AND *GNL* ON STARCH GRANULE GROWTH AFFECT GRAVITROPISM

According to the starch-statolith hypothesis, starch-filled amyloplasts or statoliths, sediment in the hypocotyl endodermis or in the root columella during gravitropism, generating a signal that causes asymmetric growth (Kiss et al, 1989; Christie & Murphy, 2013).

The differences in starch granule size described previously in *gnc gnl* and GNLox (**Figure 9**) have an impact on how seedlings perceive gravity.

I computed a two-tailed Pearson r correlation using the values obtained from measuring the hypocotyl bending angle (**Figure 1**), starch granule size and starch granule number (**Figure 9**) and starch accumulation (**Figure 16**) in wild type, *gnc gnl* and GNLox seedlings grown in the dark on sucrose-free ½ MS medium (**Figure 23**). The gravitropic response of hypocotyls strongly correlated with the size of starch granules in endodermal cells (0.91), whereas the number of starch granules exhibited a negative correlation (-0.92). Clearly, the relation between the size and number of starch granules is inversely proportional in the endodermal cells studied (-1.00).

On the other hand, the content of starch did not impact the hypocotyl bending angle as much as the size and number of the granules did,

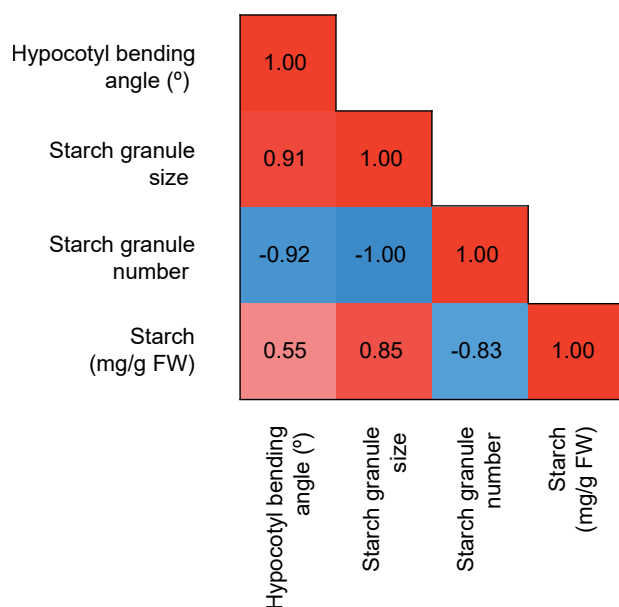


Figure 23. The regulation of GNC and GNL on starch granule growth affect gravitropism. Correlation matrix heat map representation of pairwise Pearson correlation coefficients. The correlation includes measurements of hypocotyl bending angle, starch granule size and number, and starch accumulation from *Arabidopsis thaliana* wild type, *gnc gnl* and GNLox seedlings grown in the dark, using the data presented in Figures 1, 9 and 16. Colour scale represents correlation coefficients.

since wild type, *gnc gnl* and GNLox accumulate similar amounts of starch (**Figure 23**).

I concluded that besides the content of starch, the size and number of starch granules also affect how plants perceive gravity.

The perception of gravity in the root is modulated by the repression exerted by GATA factors on starch granule growth

To understand whether differences in starch granule size and morphology directly impact gravity perception, I performed a root gravitropism assay in the wild type, *sex1* and *ss4* backgrounds. Increased root bending was detected in *sex1*, *sex1 gnc gnl* and *sex1* GNLox, both in sucrose-free and 1% sucrose-supplemented medium compared to wild type (**Figure 24**). In addition, the bending of *sex1* GNLox roots grown on sucrose-free medium increased compared to *sex1* (**Figure 24**). These results are well in line with previous studies showing that in *sex1* mutants, root bending increased due to higher accumulation of starch (Vitha et al, 2007). This can also explain the increased bending in *sex1* GNLox roots compared to *sex1*, which accumulate more starch granules in root columella and non-columella cells (**Figure 12 and 13**).

In *ss4*, *ss4 gnc gnl* and *ss4* GNLox, I did not detect significant differences compared to wild type, when seedlings were grown without sucrose (**Figure 24**). However, the bending of roots increased in 1% sucrose-sup-

plemented medium, compared to wild type (**Figure 24**). Non-significant differences in root bending were observed between *ss4* and *ss4 GNLox* (**Figure 24**). Thus, root gravitropism in the *ss4* background could be also modulated by the accumulation of starch granules in root columella cells.

The perception of gravity in the shoot is modulated by the repression exerted by *GNC* and *GNL* on starch granule growth

Providing further evidence that the defects observed in shoot negative gravitropism (Richter et al, 2010; Behringer et al, 2014; Ranftl et al, 2016) are a consequence of differences in starch granule size, morphology and number, I measured the emergence angle of lateral branches in the *sex1* and *ss4* backgrounds. First, as described (Ranftl et al, 2016), the double mutant emerged with a steeper angle, whereas the angle in *GNLox* was increased compared to the wild type (**Figure 25A and D**). Then, the lateral shoots of *sex1* and *sex1 gnc gnl* emerged with a similar angle than in wild type, whereas in *sex1 GNLox* the emergence angle notably steepened (**Figure 25B and D**). In the *ss4* background, all three genotypes emerged with an angle proximal to 80° (**Figure 25C and D**). While the emergence angle in *ss4 GNLox* was similar to *GNLox*, in *ss4 gnc gnl*, the angle increased more than 30 degrees (**Figure 25D**).

The differences I observed in the angle of emergence from the pri-

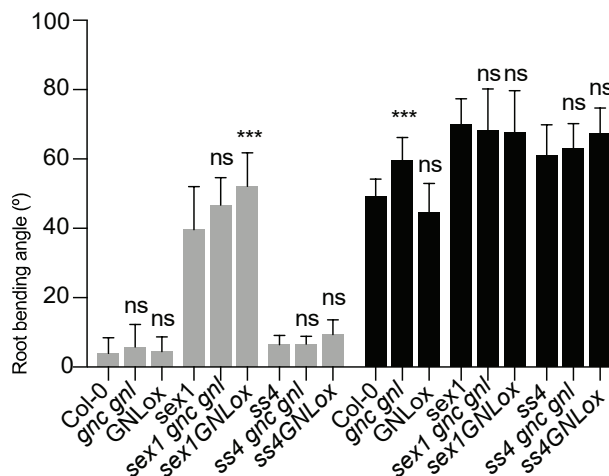


Figure 24. *GNC* and *GNL* modulate gravity perception in the root by repressing starch granule growth. Average and standard deviation of the root bending angle from >20 seedlings of the specified genotype, 24 hours after turning the seedlings by 90°. Wild type, *gnc gnl* and *GNLox* bar plots are identical to those shown in Figure 1. Student's t-test: *, p 0.05; ***, p 0.001; ns, not significant.

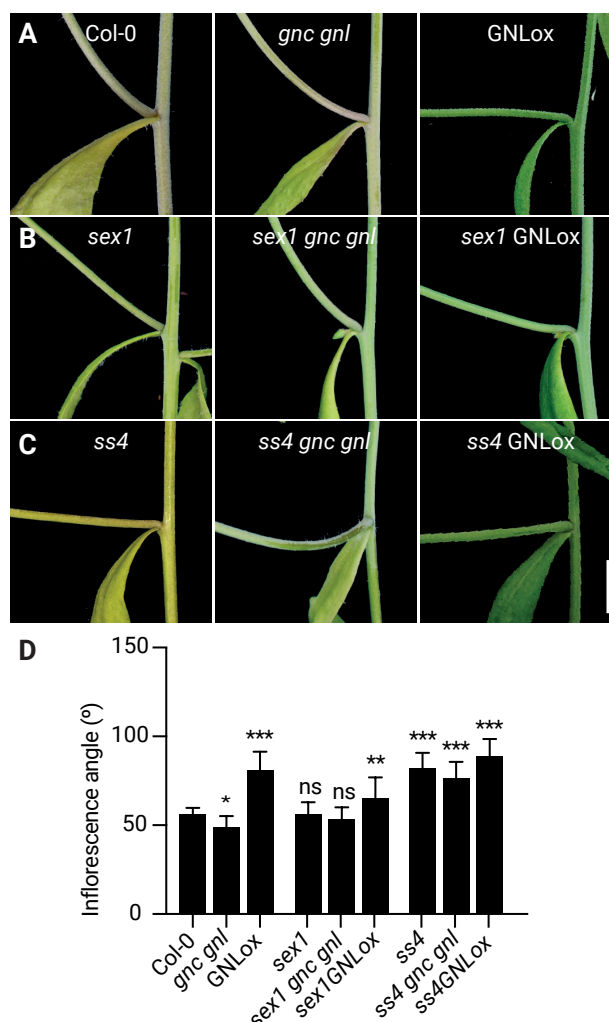


Figure 25. *GNC* and *GNL* modulate gravity perception in the shoot by repressing starch granule growth. A – C. Representative photographs of 6-week-old *Arabidopsis thaliana* cauline nodes of the specified genotypes. Plants were grown with a 12 hrs light / 12 hrs dark photoperiod. Scale bar = 0.5 cm. D. Average and standard deviation of the branch angles as detected in the experiment shown in (A – D) measured from at least 20 cauline nodes. Student's t-test: *, p 0.05; **, p 0.01; ***, p 0.001; ns, not significant.

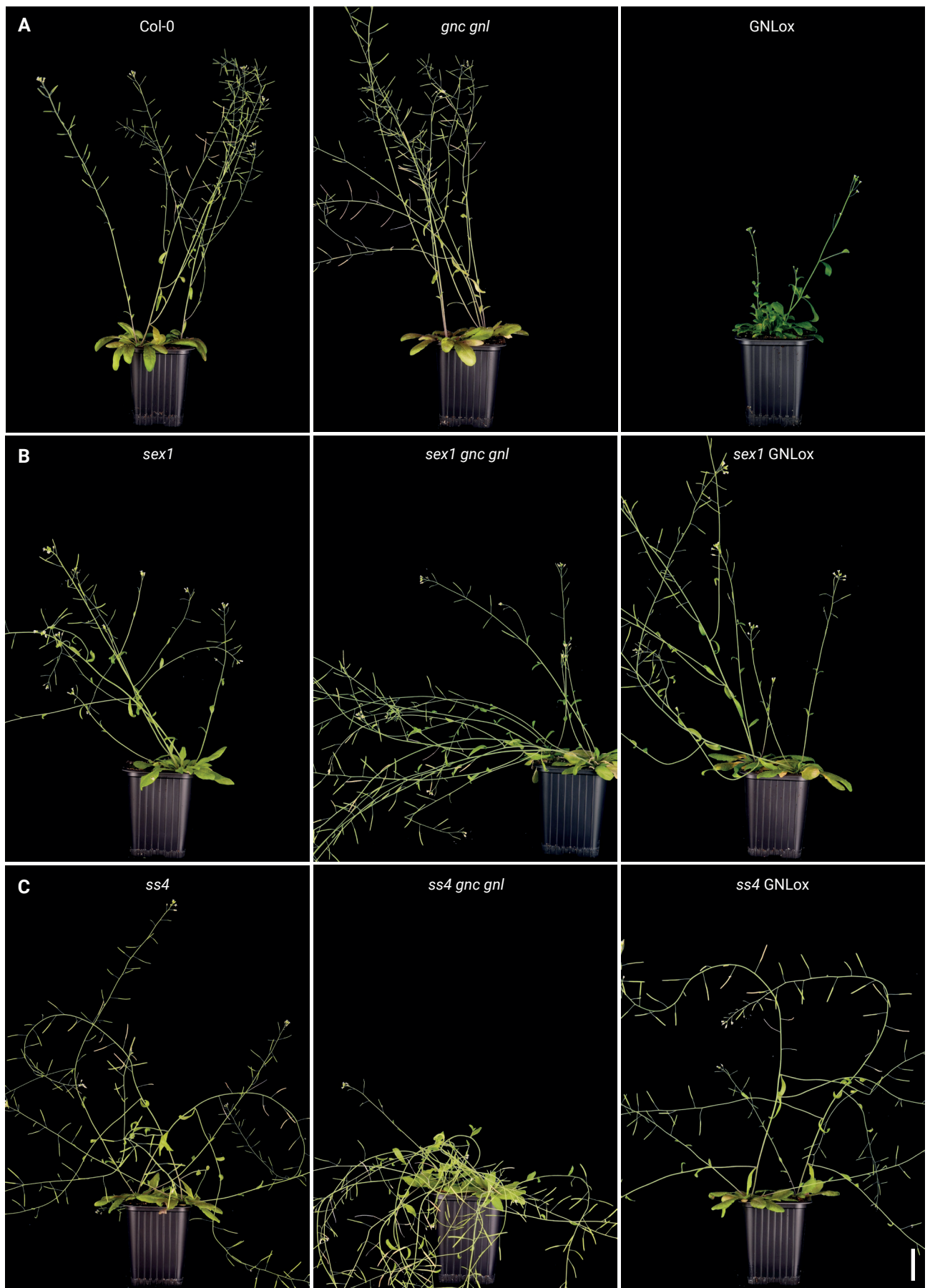


Figure 26. Differential effects of GNC and GNL on plant growth in the *sex1* and *ss4* backgrounds. A. Representative photographs of 6-weeks-old *Arabidopsis thaliana* plants of the specified genotype. Plants were grown with a 16 hrs light / 8 hrs dark photoperiod. Scale bar = 2 cm.

mary inflorescences shaped the morphology of whole inflorescences in 6-weeks-old plants (**Figure 26**). A steeper emergence angle led to tall and compact inflorescences (**Figure 26A and B**), whereas the increased angle observed in the GNLox and *ss4* backgrounds resulted in lower but more widespread plants (**Figure 26C**). Moreover, branches were thinner in the *gnc gnl* background, leading to pendent inflorescences (**Figure 26**). The stunted growth of GNLox (Behringer et al, 2014) was partially suppressed in *sex1* GNLox and *ss4* GNLox, however these mutants produced fewer inflorescences than their respective loss-of-function mutants. In conclusion, the repression of *GNC* and *GNL* on starch granule initiation,

morphology and accumulation, modulates the gravitropic responses not only in seedlings, but in whole plants.

GNC and GNL balance between gravitropism and phototropism

Light induces positive phototropic hypocotyl bending, e.g. when dark-grown seedlings are exposed to unilateral blue light. In the light, light and gravity regulate tropic responses but the two inputs may not always act in the same direction. The transcription of *GNC* and, particularly, that of *GNL* are light-induced and the repressive effects of *GNC* and *GNL* on starch formation may weaken the relative contribution of negative hypocotyl gravitropism on tropic responses in the light (Naito et al, 2007; Ranftl et al, 2016). I therefore tested the contribution of the B-GATA factors to tropic responses by exposing dark-grown seedlings to a phototropic and gravitropic stimulus. In the first experiment, I illuminated the seedlings from above with blue light such that phototropic and negative gravitropic hypocotyl bending would act in the same direction. In the second experiment, I provided the light from the bottom such that phototropic bending and negative gravitropic bending antagonize each other. Under these conditions, all genotypes responded uniformly by strongly bending the hypocotyls towards the light and away from the gravity vector (**Figure 27A and B**). In a second experiment, I provided the light from the bottom such that phototropic and gravitropic growth would antagonize each other. As expected, phototropic hypocotyl bending was dominant over negative gravitropism in this experiment (**Figure 27C and D**)

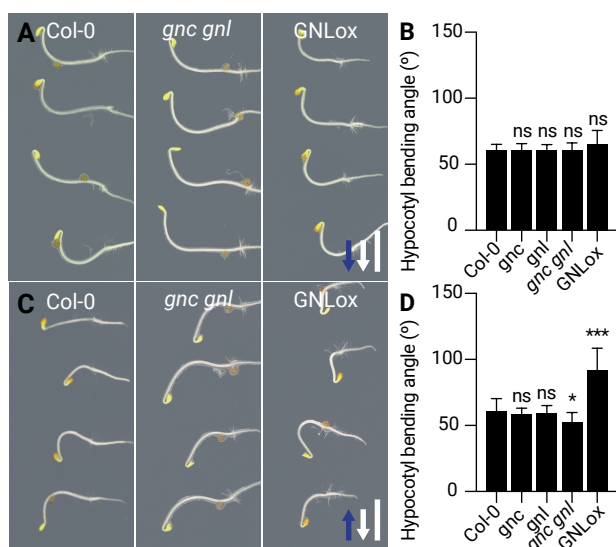
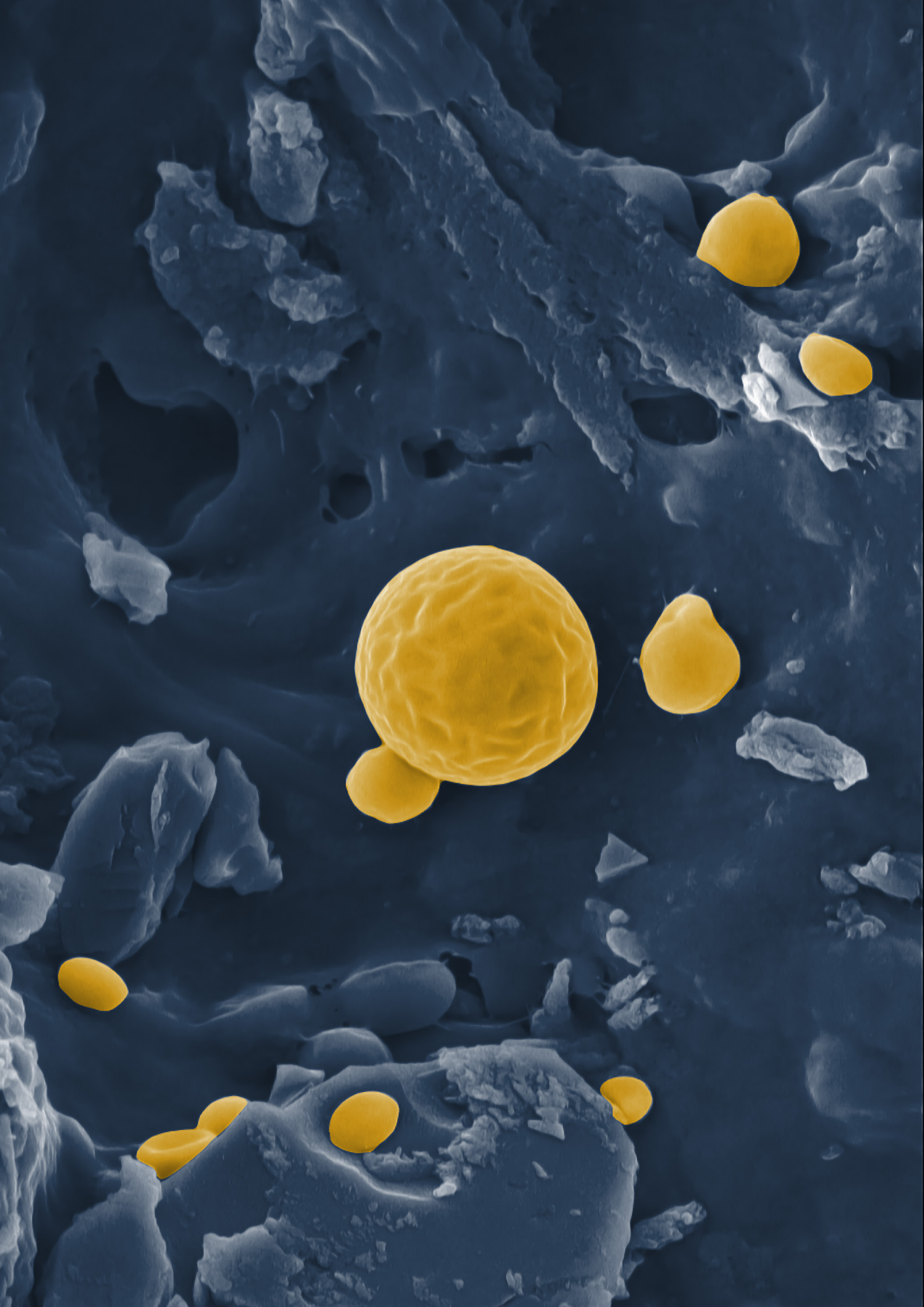


Figure 27. *GNC* and *GNL* balance between gravitropism and phototropism. **A.** and **C.** Representative photographs of 2-days-old *Arabidopsis thaliana* wild type (Col-0), *gnc gnl* and GNLox seedlings grown in the dark, 6 hrs after reorienting the seedlings by 90°. In (A and B), seedlings were illuminated with blue light from the top such that phototropic and negatively gravitropic hypocotyl bending would occur in the same direction. In (C and D), seedlings were illuminated from the bottom such that phototropic bending and negatively gravitropic bending antagonize each other. The white arrow indicates the direction of gravity, and the blue arrow the direction of light. Scale bar = 2 mm. **B.** and **D.** Graphs displaying the average and standard deviation of hypocotyl bending angles (α) as detected in the experiment shown in (A and C), including *gnc* and *gnl* single-mutants. N = 40. Student's *t*-test: *, $p < 0.01$; ***, $p < 0.001$; ns, not significant.

(Hangarter, 1997). However, the *gnc gnl* mutant bent less efficiently than the wild type, whereas GNLox bent more efficiently (**Figure 27C and D**). In correlation with my observation of increased and decreased starch granule growth in *gnc gnl* mutants and GNLox, respectively, I reasoned that the differential starch granule accumulation of these mutants may be causal for their differential tropic responses. Light regulation of *GNC* and *GNL* gene expression, and their effects on starch granule may thus help to decrease the contribution of negative gravitropic growth at the expense of positive phototropic growth for improved photosynthesis.



06

CHAPTER 2

GATA FACTORS REGULATE THE EXPRESSION OF GENES INVOLVED IN PHOTOSYNTHESIS AND STOMATA DEVELOPMENT

GATA factors are known to promote chlorophyll accumulation, chloroplast development as well as stomata formation in a light-dependent manner (Chiang et al, 2012; Klermund et al, 2016; Ranftl et al, 2016; Bastakis et al, 2018; Zubo et al, 2018). Under certain conditions, these effects can be induced in the dark (Chiang et al, 2012; Klermund et al, 2016).

To get additional insight into the biological functions of *GNC* and *GNL* in the dark, I performed a GO analysis with the transcriptional data obtained from *gnc gnl* and GNLox seedlings grown in the dark without sucrose (**Figure 4**). I determined that the 3 most enriched term categories among genes upregulated in *gnc gnl* were Photosynthesis (9.65-fold enrichment), Starch metabolism (5.43) and Stomatal development (4.44) (**Figure 28A**). The differential

regulation of photosynthesis and stomata development is well in line with previous reports that these GATA factors regulate greening and stomata development (Chiang et al, 2012; Klermund et al, 2016; Ranftl et al, 2016; Bastakis et al, 2018; Zubo et al, 2018). Moreover, Porphyrin compound catabolism (-8.19) is the most enriched category among genes downregulated in *gnc gnl* (**Figure 28B**), also in harmony with the role of *GNC* and *GNL* on chlorophyll biosynthesis (Ranftl et al, 2016; Bastakis et al, 2018; Zubo et al, 2018).

Unfortunately, the genes upregulated and downregulated in GNLox (**Figure 28 C and D**) lead to poor term enrichment (<2.5). However, the term category Response to auxin (2.53) and Cell wall organization (2.20) is, once more, matching previous reports about the regulation of GATA factors downstream of auxin, as well as the possible effect of *GNC* and *GNL* on cell wall biogenesis (Richter et al, 2010; Richter et al, 2013b; An et al, 2020).

As described in Chapter 1, to further characterize the most enriched term categories from genes upregulated in *gnc gnl*, I generated a protein-protein interaction network that included 110 candidate proteins (**Figure 5B**). The combination of gene expression data and network connectivity measures led to the identification of 3 specific clusters, associated with Photosynthesis light harvesting, Starch metabolism and Stomata development, and 2 larger but less specific clusters

belonging to Alpha-amino acid biosynthesis and DNA replication (**Figure 5B**) (Ballouz et al, 2017).

21 proteins associated with Stomata development, including the well-characterized proteins SPEECHLESS (SPCH) and SCREAM 2 (SCRM2), involved in the initiation of stomatal cell lineages (Chowdhury et al, 2021), and the transit peptide EPIDERMAL PATTERNING FACTOR2 (EPF2) and its partner TOO MANY MOUTHS (TMM), which control the initial spatial patterning of stomata (Yang & Sack, 1995; Hara et al, 2009). SPCH and SCRM2 directly induce the expression of *EPF2*, *TMM* and *BREAKING OF ASYMMETRY IN THE STOMATAL LINEAGE (BASL)* (**Appendix 1**) (Lau et al, 2014), whereas negatively regulate PIF4 (Lau et al, 2018). Genes involved in stomata proliferation and patterning, such as *BASL* and *STOMATAL DENSITY AND DISTRIBUTION1 (SDD1)* were also upregulated in *gnc gnl* seedlings grown in the dark (**Appendix 1**). GATA factors act downstream of PIFs and upstream of SPCH in regulating stomata formation in a light-dependent manner (Klermund et al, 2016). Thus, these results shed additional light into the regulation of GNC and GNL on stomata development in the dark.

Next, 13 out of the 15 proteins belonging to photosynthesis accounted for LIGHT HARVESTING COMPLEX (LHC) proteins, which serve, together with chlorophyll and xanthophylls, as the antenna complex of photosystem II (PSII) (**Appendix 1**) (Montane

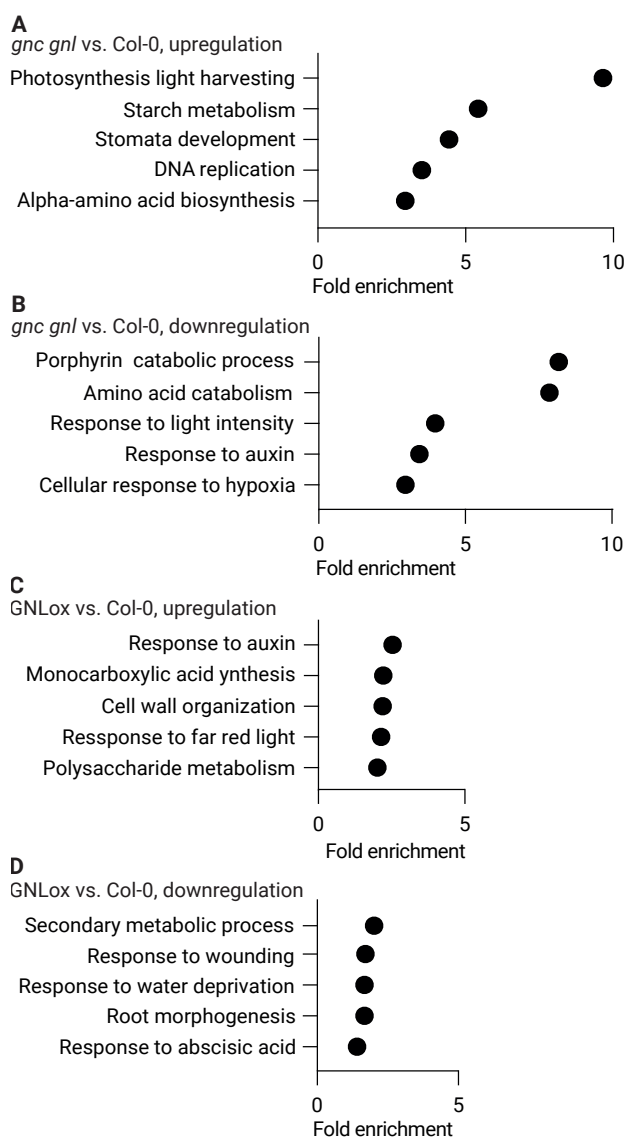


Figure 28. GO analysis of *gnc gnl* and GNLox seedlings grown in the dark. **A** – **D**. Graphs displaying the GO enrichment analysis of the 5 most strongly regulated GO term categories among genes upregulated in *gnc gnl* (**A**), downregulated in *gnc gnl* (**B**), upregulated in GNLox (**C**) and downregulated in GNLox (**D**). Scale represents enrichment values.

& Kloppstech, 2000; Pietrzykowska et al, 2014). In the dark, *LHC* levels are low, but their transcription is induced by light (Montane & Kloppstech, 2000; Pietrzykowska et al, 2014). Therefore, it remained unclear why their expression was upregulated in *gnc gnl* seedlings grown in the dark.

It is crucial to state that wild type, *gnc gnl* and GNLox seedlings used for the RNA-seq were grown in the same conditions, and samples harvested in an alternate manner, e.g., one plate included a biological replicate for each genotype, which consisted of hundreds of seedlings. Among all plates, each biological replicate was harvested alternating wild type – *gnc gnl* – GNLox. Taking into account that the expression of *LHCs* remains comparatively low in the wild type and GNLox, there appears to be no causal connection between exposure to light and their higher expression in *gnc gnl* seedlings. Furthermore, the transcript of *LHCs* is known to be regulated by chloroplast biogenesis

genes, such as *GUNs*. For example, the loss of *GUN1* results in an increase of *LCHBs* (Cottage et al, 2010). Because the expression of *GUNs* is known to be regulated by *GNC* and *GNL* (Bastakis et al, 2018), it is feasible to think that the differences observed in the transcript levels of *LHCs* are due to feed-back regulatory mechanism involving the *GATA* factors and chloroplast development genes.

In contrast to *LHCs*, genes from the Porphyrin catabolism category, like *NON-YELLOW COLORING 1 (NYC1)* and *ARABIDOPSIS THALIANA HEME OXYGENASE 1 (ATHO1)* were downregulated. A second protein-protein interaction network clearly depicted the antagonistic regulation between the light harvesting- and greening-proteins in the double mutant, showing that proteins involved in chlorophyll accumulation were downregulated in *gnc gnl* (**Figure 29**). This data is, once more, well in line with the pale greening phenotype described in *GATA* mutants (Ranftl et al, 2016; Bastakis et al, 2018).

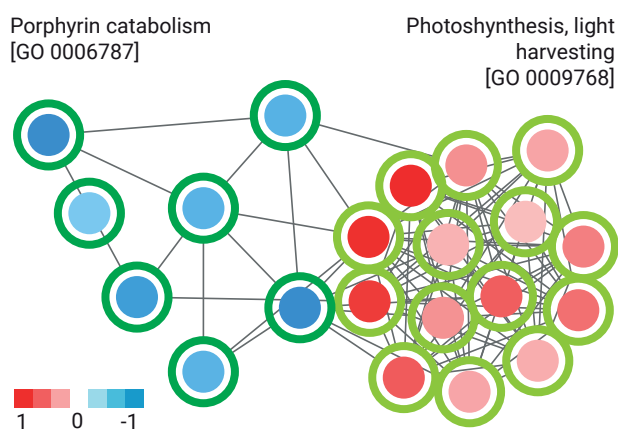
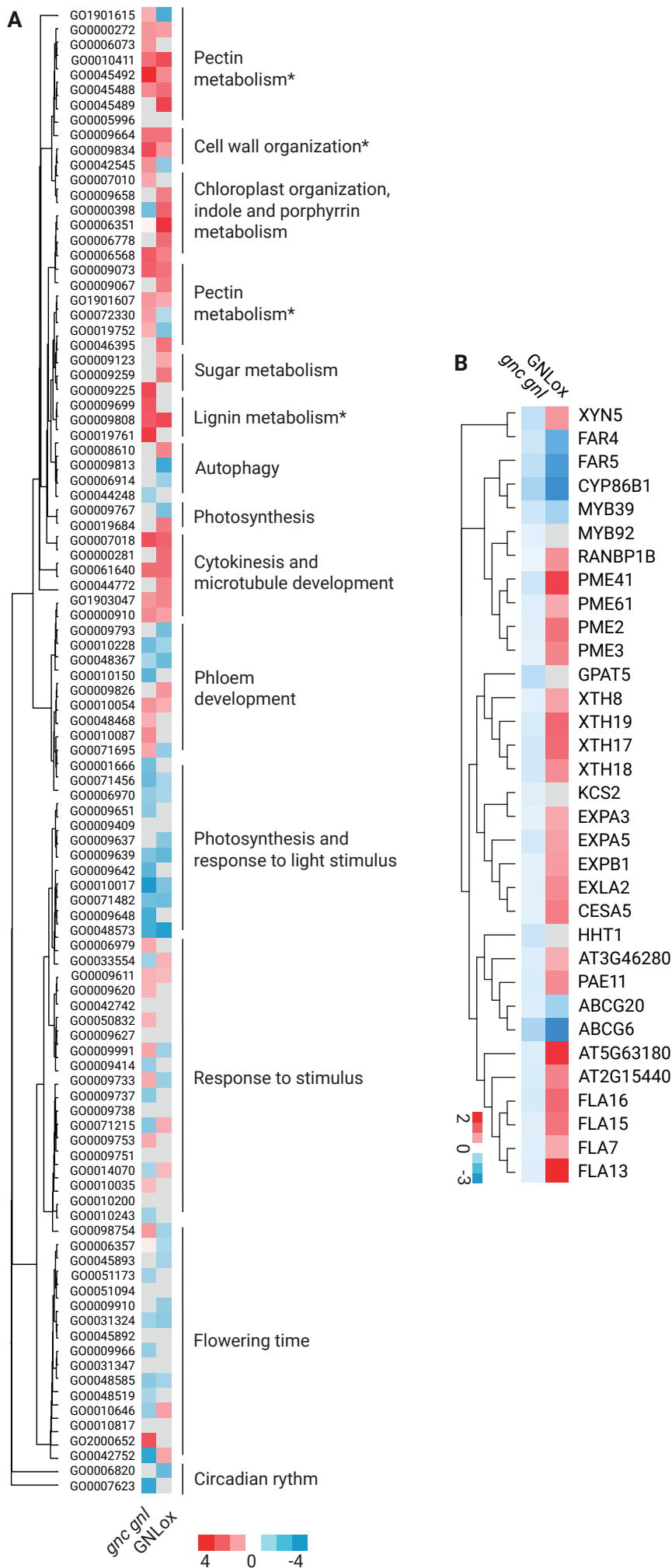


Figure 29. Photosynthesis and porphyrin catabolism genes are antagonistically regulated in *gnc gnl*. STRING network analysis of the genes differentially regulated in 3-days-old *Arabidopsis thaliana gnc gnl* seedlings grown in the dark, belonging to the GO term categories photosynthesis, light harvesting (bright green) and porphyrin catabolism (green). Network nodes and colour scale display Log_2 fold change values, filtered by $\text{FDR} < 0.05$.

CELL WALL BIOGENESIS MIGHT BE REGULATED BY GATA FACTORS

In Chapter 1 I identified that biological functions involved in the formation and modification of cell wall were antagonistically regulated between *gnc gnl* and GNLox seedlings grown in the dark with 1% sucrose (**Figure 6**). To gain insight into the role of *GATA* factors in cell wall formation I performed a GO



analysis for each dataset and clustered individual term categories according to ontology hierarchy, as described in available literature (Garcia-Vallve et al, 2000; Supek et al, 2011) (**Figure 30A**). Biological functions involved in cell wall biogenesis were strongly induced by sucrose, mainly the terms related to the biosynthesis of lignin and pectin. Interestingly, these GO terms were highly enriched in wild type and *gnc gnl*, but not significantly-enriched in GNLox (**Figure 30A**).

Then, I selected and filtered (FDR < 0.05) the DEGs associated with cell wall metabolism, including those belonging to the term categories Cell wall modification and Cell wall biogenesis (**Figure**

Figure 30. GNC and GNL regulate cell wall biogenesis. **A.** Hierarchical heat map representation of 99 clustered sucrose-modulated GO term categories among genes differentially regulated in 3-days-old *Arabidopsis thaliana gnc gnl* and GNLox seedlings grown in the dark on 1% sucrose-supplemented ½ MS medium. Colour scale represents term enrichment. The asterisks indicate term categories involved with cell wall metabolism. **B.** Heat map representation of genes belonging to the GO term categories cell wall modification and cell wall biogenesis from *gnc gnl* and GNLox seedlings, as shown in (E). Colour scale represents Log₂ fold change values filtered by FDR < 0.05.

6 and 30A). Most of the genes analysed were downregulated in *gnc gnl* but upregulated in GNLox, except for a group of genes involved in suberin biogenesis (**Figure 30B**). This group included genes associated with the synthesis of fatty acids and subsequent deposition of suberin, such as two members of the gene family encoding alcohol-forming fatty acyl-CoA reductases (*FAR4* and *FAR5*), *CYTOCHROME P450 (CYP86B1)*, two *MYB DOMAIN PROTEIN (MYB39* and *MYB92)* and two *ATP-BINDING CASSETTE (ABCG6* and *ABCG20)*, (Domergue et al, 2010; Pinot & Beisson, 2011; de Silva et al, 2021; Ichino & Yazaki, 2022). These results suggest a role for *GNC* and *GNL* in cell wall formation, more specifically in pectin and lignin biosynthesis.

In addition, pathways involved in cytokinesis, microtubule development, phloem development and responses to sucrose were as well, highly enriched (**Figure 30A**). These results are in accordance with previous studies, showing that sucrose induces cell wall formation, phloem development and general responses to sucrose (Gonzali et al, 2006). On the other hand, functions related to light perception, photosynthesis and flowering time were repressed by sucrose in all three genotypes (**Figure 30A**) (Price et al, 2004; Thum et al, 2004; Gonzali et al, 2006). Moreover, categories related to chloroplast organization, indole and porphyrin biosynthesis and autophagy were antagonistically regulated between *gnc gnl* and GNLox (**Figure 30A**). These results are again well in line with my previous obser-

vations that *GNC* and *GNL* regulate chloroplast division and chlorophyll accumulation, and provide further evidence that *GNC* and *GNL* regulate cell wall formation

SUGAR TRANSPORT AND ALLOCATION MIGHT BE REGULATED BY GATA FACTORS

Sugars produced during photosynthesis are retained in chloroplasts for sucrose and starch production (Zeeman et al, 2002; Streb & Zeeman, 2012). Defects on the translocation and accumulation of sugars negatively impact plant growth (Eom et al, 2015). In 2014, Carina Behringer (Lehrstuhl für Systembiologie der Pflanzen, Technische Universität München, Freising, Germany) reported that plants overexpressing LLM-domain B-GATA factors show cotyledon epinasty, chlorophyll accumulation, stunted growth and delay in flowering time (Behringer et al, 2014). These characteristics are already visible at the seedling stage (**Figure 31A**) and accompany the plants throughout their life cycle (Richter et al, 2013b; Behringer et al, 2014; Behringer & Schwechheimer, 2015).

While growing seedlings on sucrose-supplemented medium, it came to my attention that GNLox seedlings grown on 1% sucrose were able to suppress, at least, the stunted growth phenotype (**Figure 31A and B**). Addition of sucrose to the medi-

um led to more expanded cotyledons in the wild type and *gnc gnl*, and increased the skewing of roots in all three genotypes (**Figure 31A and B**) (Oliva & Dunand, 2007). While the cotyledons in GNLox remained unexpanded, the hypocotyl increased in size and the defects observed in root growth were suppressed (**Figure 31B**).

Next, I aimed to better understand whether the growth defects observed in the GATA overexpression lines were a result of defects in sugar accumulation. Wild type, *gnc gnl* and GNLox plants were grown in the light on ½ MS medium supplemented with 1% glucose, 1% fructose, 1% sucrose and 1% sorbitol, as specified. On sugar-free medium,

gnc gnl rosettes grew similarly to wild type, whereas GNLox rosettes reached only half the size of the wild type. (**Figure 31C and H**). Addition of 1% glucose or 1% fructose to the medium had an impact on the overall growth, resulting in smaller rosettes (Qian et al, 2020; Zhong et al, 2020), whereas 1% sucrose led to vigorous plants (**Figure 31D, E, F and H**). Plants that grew on sorbitol did not exhibit any growth differences compared to plants grown on sugar-free medium (**Figure 31G and H**). The differences in rosette size were maintained between the genotypes, except on 1% glucose and sucrose (**Figure 31H**). Addition of glucose and sucrose partially suppressed the stunted growth phenotype of GNLox

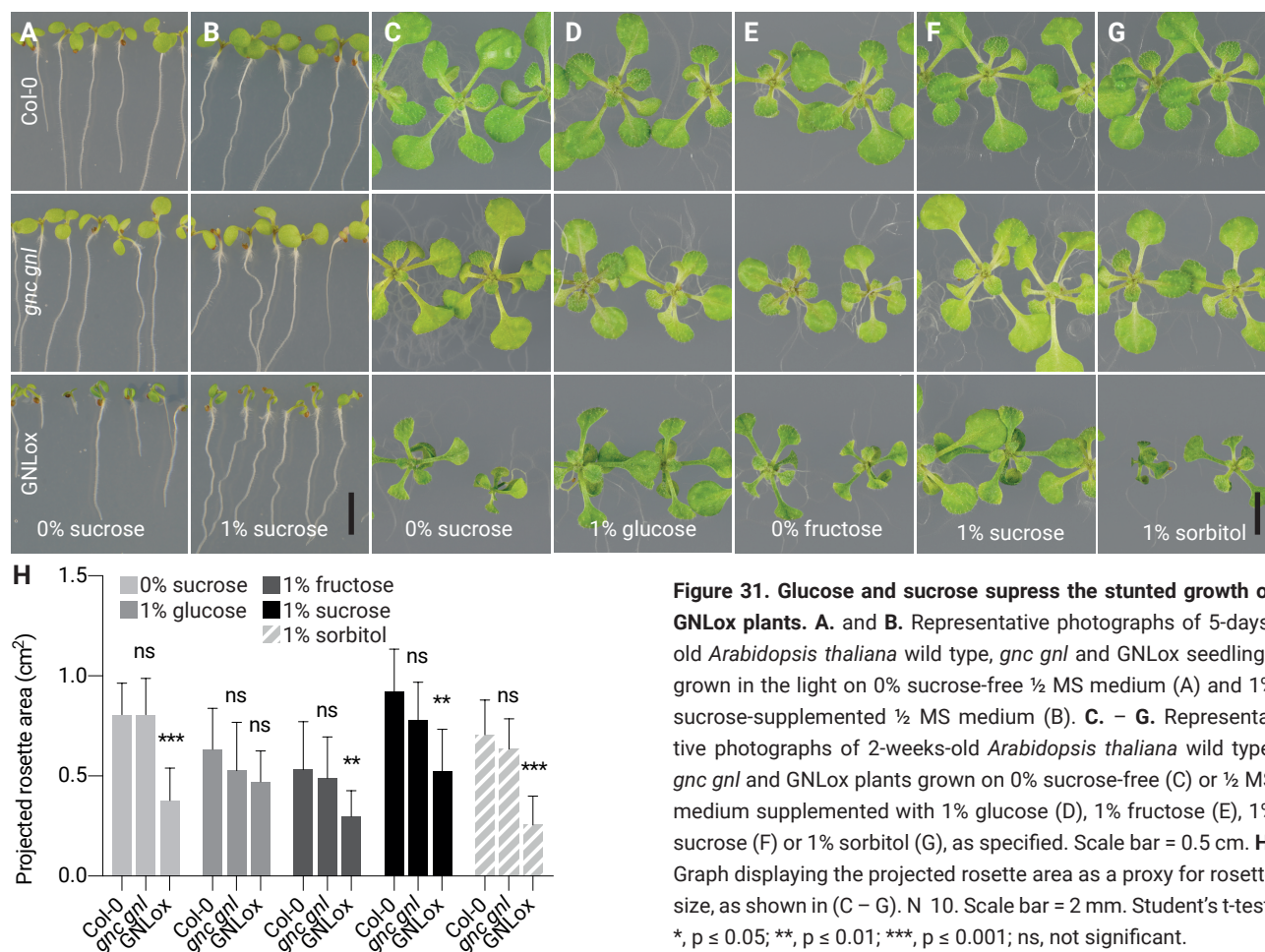


Figure 31. Glucose and sucrose suppress the stunted growth of GNLox plants. **A.** and **B.** Representative photographs of 5-days-old *Arabidopsis thaliana* wild type, *gnc gnl* and GNLox seedlings grown in the light on 0% sucrose-free ½ MS medium (A) and 1% sucrose-supplemented ½ MS medium (B). **C. – G.** Representative photographs of 2-weeks-old *Arabidopsis thaliana* wild type, *gnc gnl* and GNLox plants grown on 0% sucrose-free (C) or ½ MS medium supplemented with 1% glucose (D), 1% fructose (E), 1% sucrose (F) or 1% sorbitol (G), as specified. Scale bar = 0.5 cm. **H.** Graph displaying the projected rosette area as a proxy for rosette size, as shown in (C – G). N 10. Scale bar = 2 mm. Student’s t-test: *, p ≤ 0.05; **, p ≤ 0.01; ***, p ≤ 0.001; ns, not significant.

plants, suggesting that defects in the translocation and accumulation of glucose and/or sucrose impact, to some extent, the growth of plants overexpressing GATA factors.

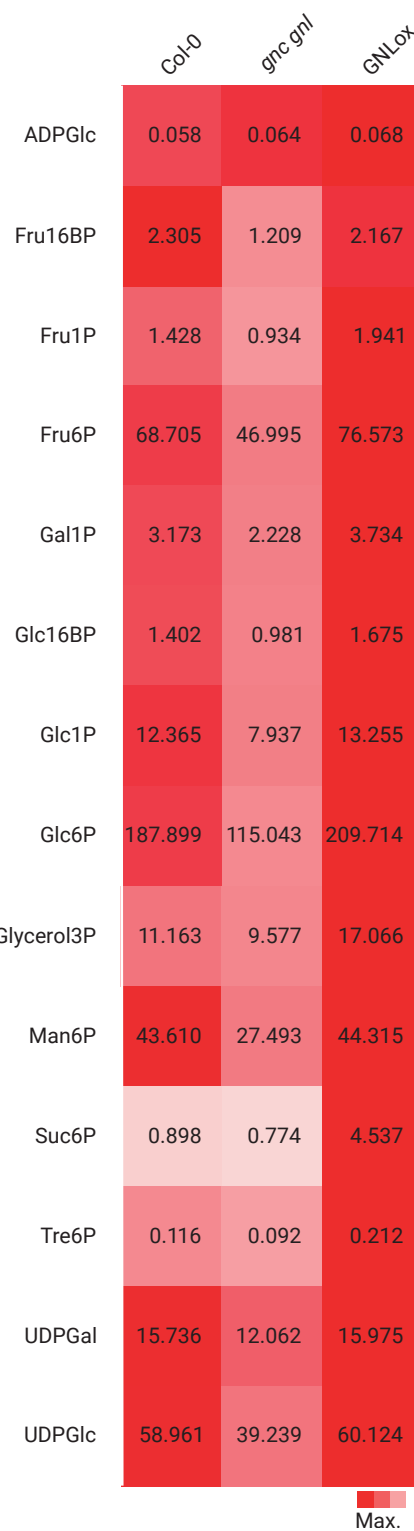
The flux of carbon into starch is tightly regulated in *gnc gnl* and GNLox

The enzyme AGPase controls the flux of carbon into starch metabolism in an allosteric manner. Mutants deficient in *PGI*, *PGM1* and *AGPase* have major reductions in the content of ADP-glucose and starch, whereas plants deficient in the translocation of sugars, for example the *SUCROSE SYNTHASE (SUS)* sextuple mutant *sus123456*, exhibit normal amounts of ADP-glucose and starch (Funfgeld et al, 2022)

Bearing in mind that the translocation and accumulation of sucrose might be impaired in the *GATA* genotypes analysed, I intended to exclude the possibility that a differential accumulation of sugars leads to defects on starch synthesis. In collaboration with John Lunn (Max Plank Institute of Molecular Plant Physiology, Potsdam, Germany), we performed an anion-exchange high-performance liquid chromatography coupled to tandem mass spectrometry (Lunn et al, 2006; Figueroa et al, 2016) with 3-days-old seedlings grown in the dark on 1% sucrose-supplemented ½ MS medium. Whereas *gnc gnl* accumulated less phosphorylated sugars than wild type, GNLox accumulated more sugars overall (Figure 32). Interestingly, the antagonistic accumulation

of sugars between *gnc gnl* and GNLox became more apparent when analysing glucose, sucrose and mannose (Figure 32). In *gnc gnl*, G1P and G6P were 1.5 times lower than in wild type seedlings, whereas Suc6P accumulated 5 times more in GNLox compared to wild type (Figure 32). Importantly, we could not observe differences in the content of ADP-glucose, indicating that the flux of carbon into starch is tightly regulated in *gnc gnl* and GNLox, despite defects in sugar allocation.

Figure 32. The flux of carbon into starch is tightly regulated in *gnc gnl* and GNLox. Heat map representation of the metabolite content of 3-days-old *Arabidopsis thaliana* wild type, *gnc gnl* and GNLox seedlings grown in the dark on 1% sucrose-supplemented ½ MS medium. Colour scale represents the content of metabolites in nmol / g FW.

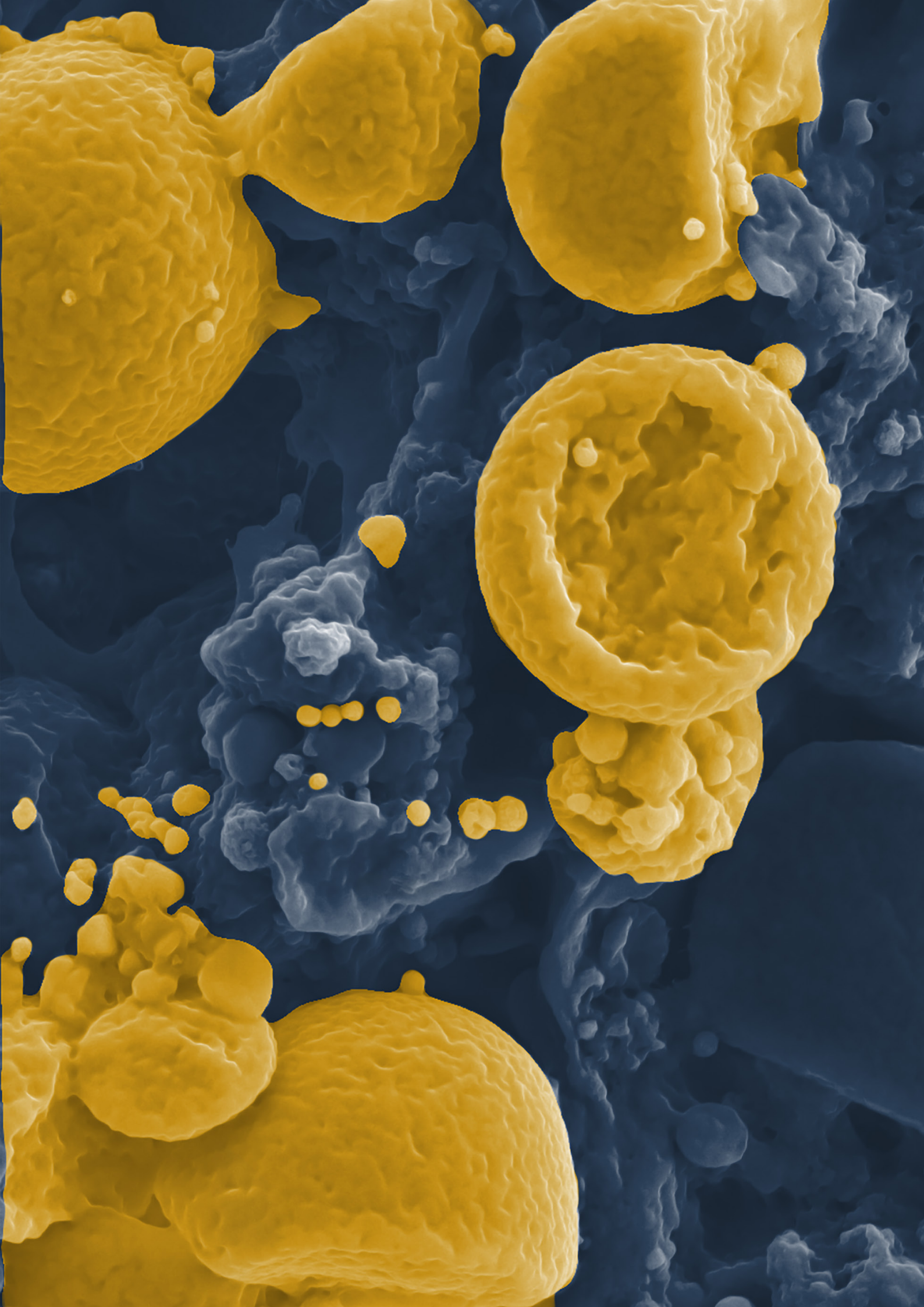


07

DISCUSSION

To date, 4 studies in *Arabidopsis thaliana*, *Oryza sativa* and *Populus trichocarpa*, show evidence that GATA factors modulate starch accumulation (Hudson et al, 2011; Hudson et al, 2013; Zubo et al, 2018; An et al, 2020). These studies focus on chloroplast development and photosynthesis, thus their observations that the GATA overexpression lines accumulate more starch are solely based in starch quantification assays and TEM images, obtained from chloroplasts located in photosynthetic cells. The authors state that increased chlorophyll biosynthesis leads to increased carbon fixation and, subsequently increased accumulation of transitory starch in leaves (Hudson et al, 2011; Hudson et al, 2013; Zubo et al, 2018; An et al, 2020).

In this dissertation, the combination of several -omics revealed a previously uncharacterized role of *GNC* and *GNL* in starch metabolism, ranging from starch granule growth in non-photosynthetic endodermal cells, to transitory starch catabolism at the whole-plant level. The multifaceted regulation of starch metabolism by the GATA factors, together with the contribution of *GNC* and *GNL* in chlorophyll accumulation, chloroplast development and stomata formation, illustrates their importance in primary plant metabolism.



GNC AND GNL PLAY A MULTIFACETED ROLE IN THE REGULATION OF STARCH METABOLISM

Regardless the observations that GATA factors impact starch accumulation in leaves (Hudson et al, 2011; Hudson et al, 2013; Zubo et al, 2018; An et al, 2020), there was no available transcriptomic data in *Arabidopsis thaliana* that described a direct implication of *GNC* and *GNL* on starch metabolism. In light-grown rice leaves, data obtained through Real-time Quantitative PCR analyses revealed that starch synthesis genes such as *SS1*, *SS2*, *ISA1* and *BE1* were upregulated in the *GNL* overexpression line (Hudson et al, 2013). The authors concluded that enhanced carbon acquisition resulted in upregulation of these genes (Hudson et al, 2013).

In an effort to uncover the role of *GNC* and *GNL* in starch metabolism, I performed an RNA sequencing experiment with seedlings grown in the dark. This allowed me to uncouple starch metabolism from impaired chlorophyll accumulation, and to avoid interreference from transitory starch synthesis and degradation during day-night cycles (Zeeman et al, 2002). The transcriptomic analysis revealed that the term category Starch metabolism was the most enriched GO categories among genes antagonistically regulated between *gnc gnl* and *GNL*ox, and one of the most enriched category among genes upregulated in *gnc gnl* (**Figure 4 and**

5). In contrast to light-grown rice plants, the expression of *SS1*, *SS2* and *BE1* was clearly downregulated in *GNL*ox seedlings grown in the dark, suggesting that *GNC* and *GNL* regulate starch synthesis in a light-dependent manner. In addition, genes involved in a wide range of functions such as starch anabolism, starch catabolism, starch granule development and even sugar transport, were also differentially regulated in *gnc gnl* and *GNL*ox (**Figure 5**) (**Appendix 1**). These results indicate that GATA factors play a multifaceted role in the regulation of starch metabolism.

I also observed a clear antagonistic regulation of starch metabolism genes between *gnc gnl* and *GNL*ox in the transcriptome of *Marchantia polymorpha* (**Figure 8**). In plants and fungi, GATA factors modulate starch metabolism (Hudson et al, 2011; Hudson et al, 2013; He et al, 2018; Zubo et al, 2018; An et al, 2020). The transcriptomic analyses in *Arabidopsis thaliana* and *Marchantia polymorpha* determined that the regulation of LLM-domain B-GATA factors on starch metabolism is specific, and conserved through evolution.

Starch granule initiation, and consequently, starch granule number and size, are regulated by *GNC* and *GNL*

Amyloplasts that function as statoliths are located in the hypocotyl endodermis and root columella cells (Kiss et al, 1989; Christie & Murphy, 2013). To

image starch granules located in endodermal cells, I stained seedlings with modified pseudo-Schiff Propidium iodide (mPS-PI) (Truernit et al, 2008). The size of starch granules was increased in *gnc gnl* endodermal and root columella cells, but decreased in GNLox (**Figure 9A, C, E and F**). In line with these observations, at the whole-seedling level the size of starch granules increased in *gnc gnl*, *sex1 gnc gnl* and *ss4 gnc gnl*, but decreased in GNLox, and *sex1* GNLox (**Figure 14**). Interestingly, starch granules in *ss4* GNLox reached 10 times the size detected in wild type (**Figure 14F and I**).

Several proteins have been reported to be involved with starch granule initiation (Mahlow et al, 2014; Malinova et al, 2014; Malinova et al, 2017; Lu et al, 2018; Seung et al, 2018). From these, SS4, PTST2, PHS1 and DPE2 are known to impact starch granule size and morphology (Liu et al, 2021a). Mutants lacking SS4 contain one big round starch granule per chloroplast due to fewer initiation events, in contrast to 4 smaller flattened starch granules in wild type mesophyll chloroplasts (Lu et al, 2018). On the other hand, overexpression of SS4 does not alter the number of granules per chloroplast, whereas plants overexpressing PTST2 contain more but smaller starch granules than the wild type (Seung et al, 2017). In addition, the content of starch in 35S:PTST2-YFP is similar to wild type (Seung et al, 2017). In my disser-

tation, I observed that the double *gnc gnl* mutant accumulated fewer, but bigger starch granules than wild type (**Figure 9A - B and 14 A and D**). On the other hand, GNLox contained more starch granules, but smaller in size (**Figure 9A - B and 14 A and D**). Taken together, these results suggest that *GNC* and *GNL* act upstream or in parallel of the protein complex involved in starch granule initiation, including proteins such as SS4 and PTST2. Thus, the differences observed in starch granule size and number in the GATA genotypes analyzed, could be explained by differences in starch granule initiation events.

The loss of *GNC* and *GNL* lead to bigger starch granules compared to the wild type (**Figure 9A - B and 14 A and D**). Addition of sucrose to the medium enhanced the growth of granules, leading to big round granules, rarely observed in wild type preparations (**Figure 14D**). These characteristics were conserved in different mutant combinations, such as *sex1 gnc gnl*, but specially enhanced in *ss4 gnc gnl* (**Figure 14F**). In GNLox, the marked reduction in size was also observed in *sex1* GNLox, but not in *ss4* GNLox, which lead to near-perfectly spherical granules aberrant in size (**Figure 14F**) similar to those described in *dpe2 ss4* and *dpe2 phs1 ss4* (Malinova et al, 2017). Lack of proteins involved in starch degradation, such as *GWD1* and *DPE2*, lead to larger starch granules than in wild type chloroplasts, indicating that starch synthesis and degradation are not separate processes (Mahlow et al,

2014; Malinova et al, 2014). Whereas the transcriptomic analysis of GNLox seedlings grown in the dark revealed that the expression of GWD1 was upregulated (**Figure 5**), I observed that the expression of several starch degradation proteins, such as DPE2, was downregulated (FDR > 0.05). Thus, it remains to be explored whether GNC and GNL interact with GWD1 and DPE2. In that hypothetical case, the combination of fewer initiation events, as described in the paragraph above, and additional downregulation of DPE2, would result in increased starch granule growth. Further research needs to be conducted to better understand the transcriptional regulation of the GATA factors on starch granule initiation, for instance, by performing a Chromatin Immunoprecipitation assay with dark grown seedlings.

In my analyses, I also detected compound granules in the double *gnc gnl* mutant (**Figure 15B**). To my knowledge, it is the first time that compound starch granules have been described in *Arabidopsis thaliana*. The quantity of compound granules intensified in *sex1 gnc gnl*, where granules contained up to 5 individually fused granules (**Figure 15E**), but completely disappeared in *ss4 gnc gnl* (**Figure 15H**). GNC and GNL repress starch granule initiation, a process which is tightly controlled by SS4. The observation that no compound granules were observed in the *ss4* background is well in line with a recent study suggesting that in the *ss4* mutant, starch is deposited almost

uniformly due to no simultaneous initiations (Burgy et al, 2021). In wild type chloroplasts, the authors indicate that starch granules originate from multiple coalescent initiations. In this case, starch expands in an anisotropic manner from each initial, fusing together into a final starch granule (Burgy et al, 2021). Nonetheless, in my work, the compound granules observed in *gnc gnl* and *sex1 gnc gnl* seedlings did not completely fuse together (**Figure 15**). Instead, the shape of individual granules forming a compound granule resemble initiation models described in the endosperm of cereals (Hawkins et al, 2021).

Besides the characteristic morphology of starch granules described in the different GATA genotypes analysed, the morphology of wild type starch granules also differed from the flattened-discoid morphology of starch granules located in chloroplasts (Burgy et al, 2021; Liu et al, 2021b; Lim et al, 2022). In all genotypes studied, starch granules from seedlings grown in the dark acquired a spherical morphology (**Figure 10, 14 and 15**). To my knowledge there is also no available data about the morphology of starch granules in non-photosynthetic tissues of *Arabidopsis thaliana* plants. However, it is known that in chloroplasts, starch granule growth occurs in the pockets that lie parallel to the thylakoids (Burgy et al, 2021). In the dark, the absence of differentiated thylakoids might not limit the growth of starch granules, allowing granules to adopt a spherical structure.

In the genotypes studied, alterations in starch granule initiation impact the size, number and morphology of starch granules (**Figure 9 and 14**), which in turn, seem to have an effect on the initiation events itself, and the degradation of starch. Thus, increasing the complexity in understanding the mechanisms behind starch granule initiation and morphology.

GNC and GNL repress transitory starch degradation

Aiming to understand whether the differences observed in starch granule size, morphology and number had an effect on the content of starch, I analysed starch distribution and accumulation in dark-grown seedlings. At the whole-seedling level, wild type, *gnc gnl* and GNLox seedlings accumulated similar amounts of starch (**Figure 16A and D**). In line with previous reports, the *sex1* single mutant and its respective genetic crosses accumulated more starch than wild type (Zeeman et al, 1998), whereas *ss4* accumulated less starch (**Figure 16**) (Crompton-Taylor et al, 2013). When I analysed transitory starch in dark-grown seedlings it became apparent that starch degradation was enhanced in *gnc gnl*, but attenuated in GNLox, compared to wild type (**Figure 17**).

In day-night growth, it is known that plants regulate the consumption of transitory starch in order to avoid starvation during night periods (Scialdone et al, 2013). For instance, 5% of starch remains at dawn (Scial-

done et al, 2013). Sucrose and Tre6P play a role in inhibiting starch consumption during the day, such that in light grown periods the increased levels of Tr6P from photosynthesis act as a feedback regulatory mechanism, buffering starch accumulation (Figueroa et al, 2016). In dark-grown wild type, *gnc gnl* and GNLox seedlings, the content of starch before sucrose treatment and 8 hrs after sucrose treatment was comparable (**Figure 17A**). Moreover, after 24 hrs without sucrose (**Figure 17B**), the content of starch was not lower than the basal content of starch before sucrose treatment (**Figure 17A**). Therefore, a regulatory mechanism similar to that occurring in day-night cycles might prevent overconsumption of starch in seedlings that do not have a functional circadian clock. GNLox plants accumulated higher content of sugars, specially S6P, but also TR6P, compared to the wild type (**Figure 32**). On the other hand, these sugars were reduced in *gnc gnl* (**Figure 32**). These results suggest that *GNC* and *GNL* can modulate transitory starch degradation indirectly, through differential sugar accumulation.

Along these lines, GATA factors could also regulate transitory starch accumulation in the light, through a differential accumulation of Tre6P. Therefore, reduced starch degradation and increased chlorophyll accumulation would result in increased starch accumulation during light growth periods, as seen in GNLox plants (**Figure 18**) (Hudson et al, 2011; Hudson et al, 2013; Zubo et al, 2018;

An et al, 2020). However, further research needs to be conducted to better understand the accumulation of sugars like Tre6P in dark-grown seedlings upon sucrose treatment, and in light-grown plants during day-night cycles.

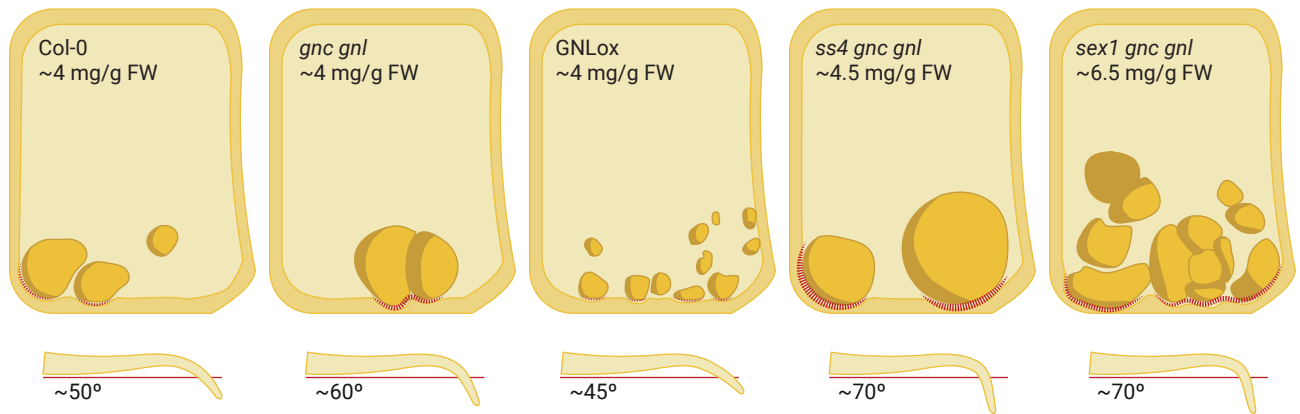
OVEREXPRESSION OF GNL INDUCES PLASTID DIFFERENTIATION, POTENTIALLY DOWNSTREAM OF PIF FACTORS AND CYTOKININ

GATA factors are known to regulate chloroplast differentiation and development (Chiang et al, 2012; Zubo et al, 2018). In this dissertation, the combination of different microscopy techniques exposed a role for GNC and GNL in repressing amyloplast differentiation. In hypocotyl endodermal cells, wild type and *gnc gnl* amyloplasts contained starch granules that covered most of the stroma (**Figure 22C, E and F**). On the contrary, amyloplasts in GNLox were characterized by the presence of etioplasmic structures, such as PLB and PT, and rather small starch granules (**Figure 22C, E and F**). These features are well in line with previous studies showing that ectopic expression of GNC induced the differentiation of proplastids to etioplasts.

The overexpression of GNC counteracts the repressive activity of PIF3, and possibly COP1, on chloroplast differentiation (Chiang et al, 2012;

Zubo et al, 2018). Moreover, GNC and GNL mediate the regulation of chloroplast division downstream of CK (Chiang et al, 2012; Zubo et al, 2018). Although the knowledge on amyloplast differentiation is still fragmentary, my observations point out that GNC and GNL induce the differentiation of amyloplasts to chloroplasts downstream of PIFs and CK.

Increased CK induces the expression of PLASTID DIVISION2 (PDV2), accelerating chloroplast division (Okazaki et al, 2009). However, the expression of PDV1 and PDV2 is not differentially regulated in GNCox (Chiang et al, 2012). The introduction of the *arc5* mutant into *gnc gnl* and GNLox resulted in increased plastid size, compared to the wild type (**Figure 22D and E**), however did not clarify the regulation of GNC and GNL on plastid division. Nevertheless, it allowed me to exclude the possibility that defects in amyloplast development result in smaller starch granules. In particular, the size of amyloplasts in *arc5* GNLox increased compared to wild type and GNLox, but the size of starch granules remained comparably low (**Figure 22D, E and F**). GNC and GNL do not interact with ARC3, ARC5, ARC6, PDV1 and PDV2 (Hudson et al, 2011). Taken together, these results indicate that the GATA factors regulate chloroplast division in parallel, or through other regulatory pathways.



THE PERCEPTION OF GRAVITY IS MODULATED BY THE REPRESSION OF *GNC* AND *GNL* ON STARCH GRANULE INITIATION

Plants require starch granules to sediment in the direction of gravity for full gravitropism (Nakamura et al, 2019). The strength of the gravitropic responses is dependent on the content of starch. For instance, *pgm1* and *pifq* accumulate fewer starch granules, compared to wild type, thus resulting in reduced gravitropism (Kiss et al, 1998; Weise & Kiss, 1999; Kim et al, 2011; Kim et al, 2016). On the other hand, increased starch content in *sex1* lead to stronger gravitropic responses (Vitha et al, 2007).

In this dissertation, I performed a series of gravitropism assays in shoots of plants grown in the light, and hypocotyls and roots of seedlings grown in the dark (**Figure 1**) aiming to understand whether the defects observed in the emergence angles of lateral shoots in the GATA genotypes (Ranftl et al, 2016) were related to defects in shoot negative gravitropism. Whereas *gnc gnl* inflorescences reor-

Illustration 6. Proposed model in which *GNC* and *GNL* modulate gravity perception. Sedimentation kinetics of starch granules (above), and root gravitropism response (below). The content of starch and the size, number and morphology of starch granules affect the sedimentation dynamics of statoliths. Larger starch granules compress the peripheral ER earlier and/or stronger, as indicated in red, which in turn modulates the perception of gravity.

iented faster than wild type, GNLox inflorescences fairly responded to gravity (**Figure 1A and B**). In the same way, the hypocotyl bending angle of 2-days-old seedlings was increased in *gnc gnl*, but decreased in GNLox (**Figure 1C, D, E and F**), thus concluding that *GNC* and *GNL* repress gravitropism.

Although the perception of gravity was impaired in *gnc gnl* and GNLox seedlings, I could not observe differences in the total content of starch, compared to the wild type (**Figure 16A and D**). Likewise, the roots from *ss4*, *ss4 gnc gnl* and *ss4* GNLox seedlings grown in the dark with 1% sucrose, bent faster towards the gravity vector despite no significant differences in the total content of starch compared to wild type, *gnc gnl* and GNLox (**Figure 12 and 24**). Nevertheless, the gravitropic response of hypocotyls strongly correlated with the size of starch granules in *gnc gnl* and GNLox endodermal cells (**Figure 22**). It is known that the force of

gravity acting on starch granules is sufficient to compress the cytoskeleton and peripheral ER, triggering a Ca^{2+} signalling response (Leitz et al, 2009). Therefore, it is sensible to hypothesize that the gravitational force acting on larger starch granules is greater, which in turn compresses the peripheral ER earlier and/or stronger. For instance, the larger starch granules observed in *gnc gnl* compared to wild type, can explain the increased bending angle of hypocotyls and roots (**Figure 1C - F and 9A - E**) (**Illustration 5**). Moreover, the aberrant granules in *ss4*, *ss4 gnc gnl* and *ss4 GNLox* seedlings can also explain the increased bending in roots, compared to wild type, *gnc gnl* and *GNLox* (**Figure 12 and 24**) (**Illustration 5**). This model suggests that large starch granules sediment faster towards the base of the cell (Leitz et al, 2009). The combination of increased sedimentation speed and larger contact surface allows the starch granule to compress the peripheral ER stronger and over a large surface area (**Illustration 6**). On the other hand, seedlings accumulated clearly more starch in the *sex1* background, which lead to stronger gravitropic responses independently of differences in starch granule size (**Figure 12 and 24**). These results indicate that gravity perception is not only dependent on the content of available starch, but to the combined effects of at least four factors: starch content, starch granule size, number and morphology.

The data obtained in dark-grown

seedlings is suitable to explain qualitative changes during gravitropism in shoots (**Figure 1**). The emergence angle of lateral shoots was modulated according to mutants defective in starch granule initiation and accumulation (**Figure 25**), thus supporting the hypothesis that differences in the angle of primary inflorescences, is a result of impaired starch granule growth in the GATA backgrounds.

Unfortunately, in this dissertation I cannot fully exclude the possibility that the modulation of auxin and gibberellin on *GNC* and *GNL* impact later stages of plant gravitropism (Richter et al, 2010; Richter et al, 2013b). For example, mutants deficient in the accumulation of gibberellin target the degradation of *PIN2* (Willige et al, 2011), which is involved in the directional transport of auxin required for root gravitropism (Luschnig et al, 1998). For this reason, additional research needs to be conducted in order to better understand the sedimentation dynamics in the genotypes analysed, as well as in mutants defective in the polar transport of auxin.

GNC AND GNL BALANCE BETWEEN GRAVITROPISM AND PHOTOTROPISM

This dissertation uncovers a complex role of *GNC* and *GNL* in the regulation of starch metabolism, starch granule initiation and growth, transitory starch degradation, sugar allocation and plastid differentiation. My work

integrates novel knowledge about the GATA factors, together with previous studies focusing on chlorophyll accumulation, chloroplast development and stomata formation (Hudson et al, 2011; Chiang et al, 2012; Hudson et al, 2013; Behringer et al, 2014; Klermund et al, 2016; Ranftl et al, 2016; Bastakis et al, 2018; Zubo et al, 2018; An et al, 2020), that positions the GATA factors as regulators of carbon assimilation, transport and storage (**Illustration 7**).

Skotomorphogenic growth is characterized by etioplasts located in cotyledons, and starch-filled amyloplasts in the hypocotyl elongation zone and the root columella, which contribute to the perception of gravity. After the transition to photomorphogenesis, plants mainly respond to the phototropic stimulus, whereas gravitropism becomes secondary (Vitha et al, 2000). In the dark, loss of *GNC* and *GNL* led to stronger gravitropic responses (**Figure 1**). However, upon illumination, seedlings overexpressing *GNL* bended faster towards the light stimulus (**Figure 27**), thus indicating that the GATA factors balance between gravitropism and phototropism.

Ectopic expression of *GNC* and *GNL* in seedlings grown in the dark induces the formation of etioplasts in cell types where their production is usually absent (**Figure 22**) (Chiang et al, 2012; Zubo et al, 2018) and represses starch granule initiation in hypocotyl endodermal and root columella cells (**Figure 9**) (**Illustration 7**). At the same

time, *GNC* inhibits the expression of several *PIF* factors (Zubo et al, 2018), which promote skotomorphogenesis and negatively regulate the expression of GATA factors (Richter et al, 2010).

Upon illumination, and to the detriment of gravity perception, *GNC* and *GNL* induce the bending of hypocotyls towards the source of light (**Figure 1 and 27**). GATA factors are transcriptionally regulated by light, hence exposure to light strengthens the repressive effects of *GNC* and *GNL* on starch metabolism, contributing to photomorphogenic growth. In this scenario, seedlings are in a photomorphogenic-ready-state in which the de-etiolation occurs rapidly due to the conversion of amyloplasts and etioplasts to active chloroplasts (**Figure 22**) (Chiang et al, 2012). The PLB disperses, releasing lipids that aid in formation of thylakoid membranes, and protochlorophyllide that converts into chlorophyll (Pyke, 2013). Furthermore the light-induced transcription of GATA factors (Richter et al, 2010) promote chloroplast growth, chlorophyll biosynthesis and stomata development (Klermund et al, 2016; Ranftl et al, 2016; Bastakis et al, 2018).

Enhanced greening and stomata formation result in increased photosynthesis rate, which in turn produces more sugars. In one hand, sucrose is known to play a role during chloroplast biogenesis and chlorophyll accumulation (Wolff & Price, 1960), and an increase in sucrose content

leads to an increased expression of chlorophyll biosynthesis genes, such as *GUN5*, *MAGNESIUM CHELATASE I2 (CHLI2)* and *3,8-DIVINYL PROTO-CHLOROPHYLLIDE A 8-VINYL REDUCTASE (DVR)* (McCarthy et al, 2016). These genes are, once more, known to be downstream targets of GATA factors (Bastakis et al, 2018), suggesting that *GNC* and *GNL* might take part in additional regulatory mechanisms, involving greening and sugars. Second, sucrose induces the formation of transitory starch in chloroplasts, thus plants overexpressing *GNC* and *GNL* also accumulate more starch (**Illustration 7**) (Hudson et al, 2011; Hudson et al, 2013; Zubo et al, 2018; An et al, 2020).

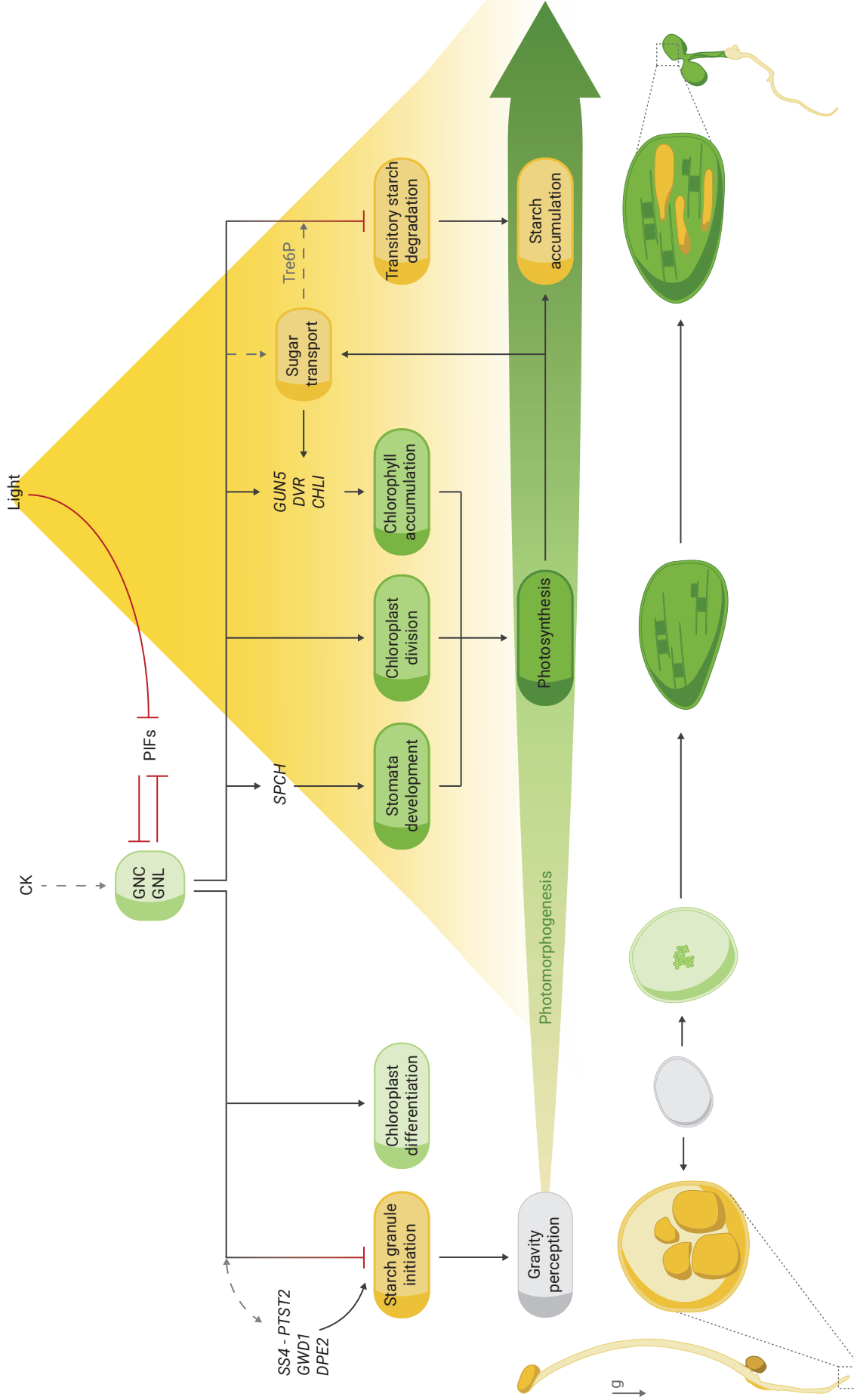


Illustration 7. Proposed model of the mechanism in which GNC and GNL contribute to photomorphogenic growth. Abbreviations: cytokinin (CK), GATA, NITRATE-INDUCIBLE CARBON METABOLISM INVOLVED (GNC), GNC-LIKE (GNL), PHYTOCHROME INTERACTING FACTOR (PIF), GENOMES UNCOUPLED 5 (GUN5), DIVINYL CHLOROPHYLLIDE 8-VINYL-REDUCTASE (DVR), MAGNESIUM CHELATASE 1 (CHLI), SPEECHLESS (SPCH).

REFERENCES

- Abt**, M. R. & Zeeman, S. C. (2020) Evolutionary innovations in starch metabolism. *Curr Opin Plant Biol*, 55, 109-117.
- An**, Y., Zhou, Y., Han, X., Shen, C., Wang, S., Liu, C., Yin, W. & Xia, X. (2020) The GATA transcription factor GNC plays an important role in photosynthesis and growth in poplar. *J Exp Bot*, 71(6), 1969-1984.
- Apriyanto**, A., Compart, J. & Fettke, J. (2022) A review of starch, a unique biopolymer - Structure, metabolism and in planta modifications. *Plant Sci*, 318, 111223.
- Arguello-Astorga**, G. & Herrera-Estrella, L. (1998) Evolution of Light-Regulated Plant Promoters. *Annu Rev Plant Physiol Plant Mol Biol*, 49, 525-555.
- Arst**, H. N., Jr. & Cove, D. J. (1973) Nitrogen metabolite repression in *Aspergillus nidulans*. *Mol Gen Genet*, 126(2), 111-41.
- Ballouz**, S., Pavlidis, P. & Gillis, J. (2017) Using predictive specificity to determine when gene set analysis is biologically meaningful. *Nucleic Acids Res*, 45(4), e20.
- Bastakis**, E., Hedtke, B., Klermund, C., Grimm, B. & Schwechheimer, C. (2018) LLM-Domain B-GATA Transcription Factors Play Multifaceted Roles in Controlling Greening in Arabidopsis. *Plant Cell*, 30(3), 582-599.
- Behringer**, C., Bastakis, E., Ranftl, Q. L., Mayer, K. F. & Schwechheimer, C. (2014) Functional diversification within the family of B-GATA transcription factors through the leucine-leucine-methionine domain. *Plant Physiol*, 166(1), 293-305.
- Behringer**, C. & Schwechheimer, C. (2015) B-GATA transcription factors - insights into their structure, regulation, and role in plant development. *Front Plant Sci*, 6, 90.
- Bi**, Y. M., Zhang, Y., Signorelli, T., Zhao, R., Zhu, T. & Rothstein, S. (2005) Genetic analysis of Arabidopsis GATA transcription factor gene family reveals a nitrate-inducible member important for chlorophyll synthesis and glucose sensitivity. *Plant J*, 44(4), 680-92.
- Blancaflor**, E. B. & Masson, P. H. (2003) Plant gravitropism. Unraveling the ups and downs of a complex process. *Plant Physiol*, 133(4), 1677-90.
- Blennow**, A., Hansen, M., Schulz, A., Jorgensen, K., Donald, A. M. & Sanderson, J. (2003) The molecular deposition of transgenically modified starch in the starch granule as imaged by functional microscopy. *J Struct Biol*, 143(3), 229-41.
- Bresnick**, E. H., Katsumura, K. R., Lee, H. Y., Johnson, K. D. & Perkins, A. S. (2012) Master regulatory GATA transcription factors: mechanistic principles and emerging links to hematologic malignancies. *Nucleic Acids Res*, 40(13), 5819-31.
- Briggs**, W. R. & Christie, J. M. (2002) Phototropins 1 and 2: versatile plant blue-light receptors. *Trends Plant Sci*, 7(5), 204-10.
- Burgy**, L., Eicke, S., Kopp, C., Jenny, C., Lu, K. J., Escrig, S., Meibom, A. & Zeeman, S. C. (2021) Coalescence and directed anisotropic growth of starch granule initials in subdomains of Arabidopsis thaliana chloroplasts. *Nat Commun*, 12(1), 6944.
- Cai**, C., Zhao, L., Huang, J., Chen, Y. & Wei, C. (2014) Morphology, structure and gelatinization properties of heterogeneous starch granules from high-amylose maize. *Carbohydr Polym*, 102, 606-14.
- Caspar**, T., Huber, S. C. & Somerville, C. (1985) Alterations in Growth, Photosynthesis, and Respiration in a Starchless Mutant of Arabidopsis thaliana (L.) Deficient in Chloroplast Phosphoglucomutase Activity. *Plant Physiol*, 79(1), 11-7.

- Cerqueira, F. M., Photenhauer, A. L., Pollet, R. M., Brown, H. A. & Koropatkin, N. M. (2020)** Starch Digestion by Gut Bacteria: Crowdsourcing for Carbs. *Trends Microbiol*, 28(2), 95-108.
- Cesbron-Lavau, G., Goux, A., Atkinson, F., Meynier, A. & Vinoy, S. (2021)** Deep Dive Into the Effects of Food Processing on Limiting Starch Digestibility and Lowering the Glycemic Response. *Nutrients*, 13(2).
- Chiang, Y. H., Zubo, Y. O., Tapken, W., Kim, H. J., Lavanway, A. M., Howard, L., Pilon, M., Kieber, J. J. & Schaller, G. E. (2012)** Functional characterization of the GATA transcription factors GNC and CGA1 reveals their key role in chloroplast development, growth, and division in Arabidopsis. *Plant Physiol*, 160(1), 332-48.
- Choi, H., Yi, T. & Ha, S. H. (2021)** Diversity of Plastid Types and Their Interconversions. *Front Plant Sci*, 12, 692024.
- Choi, I. S., Cardoso, D., de Queiroz, L. P., de Lima, H. C., Lee, C., Ruhlman, T. A., Jansen, R. K. & Wojciechowski, M. F. (2022)** Highly Resolved Papilionoid Legume Phylogeny Based on Plastid Phylogenomics. *Front Plant Sci*, 13, 823190.
- Chowdhury, M. R., Ahamed, M. S., Mas-Ud, M. A., Islam, H., Fatamatuzzohora, M., Hossain, M. F., Billah, M., Hossain, M. S. & Matin, M. N. (2021)** Stomatal development and genetic expression in Arabidopsis thaliana L. *Heliyon*, 7(8), e07889.
- Christie, J. M. & Murphy, A. S. (2013)** Shoot phototropism in higher plants: new light through old concepts. *Am J Bot*, 100(1), 35-46.
- Chudzicka-Ormaniec, P., Macios, M., Koper, M., Weedall, G. D., Caddick, M. X., Weglenski, P. & Dzikowska, A. (2019)** The role of the GATA transcription factor AreB in regulation of nitrogen and carbon metabolism in Aspergillus nidulans. *FEMS Microbiol Lett*, 366(6).
- Cordain, L., Eaton, S. B., Sebastian, A., Mann, N., Lindeberg, S., Watkins, B. A., O'Keefe, J. H. & Brand-Miller, J. (2005)** Origins and evolution of the Western diet: health implications for the 21st century. *Am J Clin Nutr*, 81(2), 341-54.
- Cottage, A., Mott, E. K., Kempster, J. A. & Gray, J. C. (2010)** The Arabidopsis plastid-signalling mutant gun1 (genomes uncoupled1) shows altered sensitivity to sucrose and abscisic acid and alterations in early seedling development. *J Exp Bot*, 61(13), 3773-86.
- Crumpton-Taylor, M., Pike, M., Lu, K. J., Hylton, C. M., Feil, R., Eicke, S., Lunn, J. E., Zeeman, S. C. & Smith, A. M. (2013)** Starch synthase 4 is essential for coordination of starch granule formation with chloroplast division during Arabidopsis leaf expansion. *New Phytol*, 200(4), 1064-75.
- de Silva, N. D. G., Murmu, J., Chabot, D., Hubbard, K., Ryser, P., Molina, I. & Rowland, O. (2021)** Root Suberin Plays Important Roles in Reducing Water Loss and Sodium Uptake in Arabidopsis thaliana. *Metabolites*, 11(11).
- Delvalle, D., Dumez, S., Wattebled, F., Roldan, I., Planchot, V., Berbezy, P., Colonna, P., Vyas, D., Chatterjee, M., Ball, S., Merida, A. & D'Hulst, C. (2005)** Soluble starch synthase I: a major determinant for the synthesis of amylopectin in Arabidopsis thaliana leaves. *Plant J*, 43(3), 398-412.
- DeMartino, P. & Cockburn, D. W. (2020)** Resistant starch: impact on the gut microbiome and health. *Curr Opin Biotechnol*, 61, 66-71.
- Domergue, F., Vishwanath, S. J., Joubes, J., Ono, J., Lee, J. A., Bourdon, M., Alhattab, R., Lowe, C., Pascal, S., Lessire, R. & Rowland, O. (2010)** Three Arabidopsis fatty acyl-coenzyme A reductases, FAR1, FAR4, and FAR5, generate primary fatty alcohols associated with suberin deposition. *Plant Physiol*, 153(4), 1539-54.
- Edner, C., Li, J., Albrecht, T., Mahlow, S., Hejazi, M., Hussain, H., Kaplan, F., Guy, C., Smith, S. M., Steup, M. & Ritte, G. (2007)** Glucan, water dikinase activity stimulates breakdown of starch granules

by plastidial beta-amylases. *Plant Physiol*, 145(1), 17-28.

Eom, J. S., Chen, L. Q., Sosso, D., Julius, B. T., Lin, I. W., Qu, X. Q., Braun, D. M. & Frommer, W. B. (2015) SWEETs, transporters for intracellular and intercellular sugar translocation. *Curr Opin Plant Biol*, 25, 53-62.

Feike, D., Pike, M., Gurrieri, L., Graf, A. & Smith, A. M. (2022) A dominant mutation in beta-AMYLASE1 disrupts nighttime control of starch degradation in Arabidopsis leaves. *Plant Physiol*, 188(4), 1979-1992.

Fernie, A. R., Willmitzer, L. & Trethewey, R. N. (2002) Sucrose to starch: a transition in molecular plant physiology. *Trends Plant Sci*, 7(1), 35-41.

Figuerola, C. M., Feil, R., Ishihara, H., Watanabe, M., Kolling, K., Krause, U., Hohne, M., Encke, B., Plaxton, W. C., Zeeman, S. C., Li, Z., Schulze, W. X., Hoefgen, R., Stitt, M. & Lunn, J. E. (2016) Trehalose 6-phosphate coordinates organic and amino acid metabolism with carbon availability. *Plant J*, 85(3), 410-23.

Flutsch, S., Wang, Y., Takemiya, A., Violet-Chabrand, S. R. M., Klejchova, M., Nigro, A., Hills, A., Lawson, T., Blatt, M. R. & Santelia, D. (2020) Guard Cell Starch Degradation Yields Glucose for Rapid Stomatal Opening in Arabidopsis. *Plant Cell*, 32(7), 2325-2344.

Fujiwara, M. T., Yasuzawa, M., Kojo, K. H., Niwa, Y., Abe, T., Yoshida, S., Nakano, T. & Itoh, R. D. (2018) The Arabidopsis *arc5* and *arc6* mutations differentially affect plastid morphology in pavement and guard cells in the leaf epidermis. *PLoS One*, 13(2), e0192380.

Fukaki, H., Wysocka-Diller, J., Kato, T., Fujisawa, H., Benfey, P. N. & Tasaka, M. (1998) Genetic evidence that the endodermis is essential for shoot gravitropism in Arabidopsis thaliana. *Plant J*, 14(4), 425-30.

Fulcher, B. D., Arnatkeviciute, A. & Fornito, A. (2021) Overcoming false-positive gene-category enrichment in the analysis of spatially resolved transcriptomic brain atlas data. *Nat Commun*, 12(1), 2669.

Funfgeld, M., Wang, W., Ishihara, H., Arrivault, S., Feil, R., Smith, A. M., Stitt, M., Lunn, J. E. & Niittyla, T. (2022) Sucrose synthases are not involved in starch synthesis in Arabidopsis leaves. *Nat Plants*, 8(5), 574-582.

Gamez-Arjona, F. M. & Merida, A. (2021) Interplay between the N-terminal domains of Arabidopsis Starch Synthase 3 determines the interaction of the enzyme with the starch granule. *Front Plant Sci*, 12, 704161.

Garcia-Vallve, S., Romeu, A. & Palau, J. (2000) Horizontal gene transfer in bacterial and archaeal complete genomes. *Genome Res*, 10(11), 1719-25.

Gonzali, S., Loreti, E., Solfanelli, C., Novi, G., Alpi, A. & Perata, P. (2006) Identification of sugar-modulated genes and evidence for in vivo sugar sensing in Arabidopsis. *J Plant Res*, 119(2), 115-23.

Hangarter, R. P. (1997) Gravity, light and plant form. *Plant Cell Environ*, 20(6), 796-800.

Hara, K., Yokoo, T., Kajita, R., Onishi, T., Yahata, S., Peterson, K. M., Torii, K. U. & Kakimoto, T. (2009) Epidermal cell density is autoregulated via a secretory peptide, EPIDERMAL PATTERNING FACTOR 2 in Arabidopsis leaves. *Plant Cell Physiol*, 50(6), 1019-31.

Hawkins, E., Chen, J., Watson-Lazowski, A., Ahn-Jarvis, J., Barclay, J. E., Fahy, B., Hartley, M., Warren, F. J. & Seung, D. (2021) STARCH SYNTHASE 4 is required for normal starch granule initiation in amyloplasts of wheat endosperm. *New Phytol*, 230(6), 2371-2386.

He, Q. P., Zhao, S., Wang, J. X., Li, C. X., Yan, Y. S., Wang, L., Liao, L. S. & Feng, J. X. (2018) Transcription Factor NsdD Regulates the Expression of Genes Involved in Plant Biomass-Degrading Enzymes,

Conidiation, and Pigment Biosynthesis in *Penicillium oxalicum*. *Appl Environ Microbiol*, 84(18).

He, W., Liu, X., Lin, L., Xu, A., Hao, D. & Wei, C. (2020) The defective effect of starch branching enzyme IIb from weak to strong induces the formation of biphasic starch granules in amylose-extender maize endosperm. *Plant Mol Biol*, 103(3), 355-371.

Hudson, D., Guevara, D., Yaish, M. W., Hannam, C., Long, N., Clarke, J. D., Bi, Y. M. & Rothstein, S. J. (2011) GNC and CGA1 modulate chlorophyll biosynthesis and glutamate synthase (GLU1/Fd-GOGAT) expression in *Arabidopsis*. *PLoS One*, 6(11), e26765.

Hudson, D., Guevara, D. R., Hand, A. J., Xu, Z., Hao, L., Chen, X., Zhu, T., Bi, Y. M. & Rothstein, S. J. (2013) Rice cytokinin GATA transcription Factor1 regulates chloroplast development and plant architecture. *Plant Physiol*, 162(1), 132-44.

Ichino, T. & Yazaki, K. (2022) Modes of secretion of plant lipophilic metabolites via ABCG transporter-dependent transport and vesicle-mediated trafficking. *Curr Opin Plant Biol*, 66, 102184.

Inoue, S., Takemiya, A. & Shimazaki, K. (2010) Phototropin signaling and stomatal opening as a model case. *Curr Opin Plant Biol*, 13(5), 587-93.

Jarvis, P. & Lopez-Juez, E. (2013) Biogenesis and homeostasis of chloroplasts and other plastids. *Nat Rev Mol Cell Biol*, 14(12), 787-802.

Kawamoto, N., Kanbe, Y., Nakamura, M., Mori, A. & Terao Morita, M. (2020) Gravity-Sensing Tissues for Gravitropism Are Required for „Anti-Gravitropic“ Phenotypes of *Lzy* Multiple Mutants in *Arabidopsis*. *Plants (Basel)*, 9(5).

Khurana, J. P., Best, T. R. & Poff, K. L. (1989) Influence of hook position on phototropic and gravitropic curvature by etiolated hypocotyls of *Arabidopsis thaliana*. *Plant Physiol*, 90, 376-9.

Kim, K., Jeong, J., Kim, J., Lee, N., Kim, M. E., Lee, S., Chang Kim, S. & Choi, G. (2016) PIF1 Regulates Plastid Development by Repressing Photosynthetic Genes in the Endodermis. *Mol Plant*, 9(10), 1415-1427.

Kim, K., Shin, J., Lee, S. H., Kweon, H. S., Maloof, J. N. & Choi, G. (2011) Phytochromes inhibit hypocotyl negative gravitropism by regulating the development of endodermal amyloplasts through phytochrome-interacting factors. *Proc Natl Acad Sci U S A*, 108(4), 1729-34.

Kiss, J. Z. (2000) Mechanisms of the early phases of plant gravitropism. *CRC Crit Rev Plant Sci*, 19(6), 551-73.

Kiss, J. Z., Guisinger, M. M. & Miller, A. J. (1998) What is the threshold amount of starch necessary for full gravitropic sensitivity? *Adv Space Res*, 21(8-9), 1197-202.

Kiss, J. Z., Hertel, R. & Sack, F. D. (1989) Amyloplasts are necessary for full gravitropic sensitivity in roots of *Arabidopsis thaliana*. *Planta*, 177(2), 198-206.

Klrmund, C., Ranftl, Q. L., Diener, J., Bastakis, E., Richter, R. & Schwechheimer, C. (2016) LLM-Domain B-GATA Transcription Factors Promote Stomatal Development Downstream of Light Signaling Pathways in *Arabidopsis thaliana* Hypocotyls. *Plant Cell*, 28(3), 646-60.

Klose, C., Viczian, A., Kircher, S., Schafer, E. & Nagy, F. (2015) Molecular mechanisms for mediating light-dependent nucleo/cytoplasmic partitioning of phytochrome photoreceptors. *New Phytol*, 206(3), 965-71.

Koide, E., Suetsugu, N., Iwano, M., Gotoh, E., Nomura, Y., Stolze, S. C., Nakagami, H., Kohchi, T. & Nishihama, R. (2020) Regulation of Photosynthetic Carbohydrate Metabolism by a Raf-Like Kinase in the Liverwort *Marchantia polymorpha*. *Plant Cell Physiol*, 61(3), 631-643.

Labuz, J., Sztatelman, O. & Hermanowicz, P. (2022) Molecular insights into the phototropin control of chloroplast movements. *J Exp Bot*, 73(18), 6034-6051.

- Lamesch, P., Berardini, T. Z., Li, D., Swarbreck, D., Wilks, C., Sasidharan, R., Muller, R., Dreher, K., Alexander, D. L., Garcia-Hernandez, M., Karthikeyan, A. S., Lee, C. H., Nelson, W. D., Ploetz, L., Singh, S., Wensel, A. & Huala, E. (2012) The Arabidopsis Information Resource (TAIR): improved gene annotation and new tools. *Nucleic Acids Res*, 40(Database issue), D1202-10.
- Lariguet, P., Boccalandro, H. E., Alonso, J. M., Ecker, J. R., Chory, J., Casal, J. J. & Fankhauser, C. (2003) A growth regulatory loop that provides homeostasis to phytochrome a signaling. *Plant Cell*, 15(12), 2966-78.
- Lau, O. S., Davies, K. A., Chang, J., Adrian, J., Rowe, M. H., Ballenger, C. E. & Bergmann, D. C. (2014) Direct roles of SPEECHLESS in the specification of stomatal self-renewing cells. *Science*, 345(6204), 1605-9.
- Lau, O. S., Song, Z., Zhou, Z., Davies, K. A., Chang, J., Yang, X., Wang, S., Lucyshyn, D., Tay, I. H. Z., Wigge, P. A. & Bergmann, D. C. (2018) Direct Control of SPEECHLESS by PIF4 in the High-Temperature Response of Stomatal Development. *Curr Biol*, 28(8), 1273-1280 e3.
- Legris, M. & Boccaccini, A. (2020) Stem phototropism toward blue and ultraviolet light. *Physiol Plant*, 169(3), 357-368.
- Legris, M., Szarzynska-Erden, B. M., Trevisan, M., Allenbach Petrolati, L. & Fankhauser, C. (2021) Phototropin-mediated perception of light direction in leaves regulates blade flattening. *Plant Physiol*, 187(3), 1235-1249.
- Leitz, G., Kang, B. H., Schoenwaelder, M. E. & Staehelin, L. A. (2009) Statolith sedimentation kinetics and force transduction to the cortical endoplasmic reticulum in gravity-sensing Arabidopsis columella cells. *Plant Cell*, 21(3), 843-60.
- Leivar, P. & Monte, E. (2014) PIFs: systems integrators in plant development. *Plant Cell*, 26(1), 56-78.
- Leivar, P. & Quail, P. H. (2011) PIFs: pivotal components in a cellular signaling hub. *Trends Plant Sci*, 16(1), 19-28.
- Lentjes, M. H., Niessen, H. E., Akiyama, Y., de Bruine, A. P., Melotte, V. & van Engeland, M. (2016) The emerging role of GATA transcription factors in development and disease. *Expert Rev Mol Med*, 18, e3.
- Li, K., Yu, R., Fan, L. M., Wei, N., Chen, H. & Deng, X. W. (2016) DELLA-mediated PIF degradation contributes to coordination of light and gibberellin signalling in Arabidopsis. *Nat Commun*, 7, 11868.
- Li, S., Wei, X., Ren, Y., Qiu, J., Jiao, G., Guo, X., Tang, S., Wan, J. & Hu, P. (2017) OsBT1 encodes an ADP-glucose transporter involved in starch synthesis and compound granule formation in rice endosperm. *Sci Rep*, 7, 40124.
- Lim, S. L., Flutsch, S., Liu, J., Distefano, L., Santelia, D. & Lim, B. L. (2022) Arabidopsis guard cell chloroplasts import cytosolic ATP for starch turnover and stomatal opening. *Nat Commun*, 13(1), 652.
- Liu, Q., Li, X. & Fettke, J. (2021a) Starch Granules in Arabidopsis thaliana Mesophyll and Guard Cells Show Similar Morphology but Differences in Size and Number. *Int J Mol Sci*, 22(11).
- Liu, Q., Zhou, Y. & Fettke, J. (2021b) Starch Granule Size and Morphology of Arabidopsis thaliana Starch-Related Mutants Analyzed during Diurnal Rhythm and Development. *Molecules*, 26(19).
- Lowry, J. A. & Atchley, W. R. (2000) Molecular evolution of the GATA family of transcription factors: conservation within the DNA-binding domain. *J Mol Evol*, 50(2), 103-15.
- Lu, K. J., Pfister, B., Jenny, C., Eicke, S. & Zeeman, S. C. (2018) Distinct Functions of STARCH SYNTHASE 4 Domains in Starch Granule Formation. *Plant Physiol*, 176(1), 566-581.
- Lu, K. J., Streb, S., Meier, F., Pfister, B. & Zeeman, S. C. (2015) Molecular Genetic Analysis of Glucan Branching Enzymes from Plants and Bacteria in Arabidopsis Reveals Marked Differences in Their Functions and Capacity to Mediate Starch Granule Formation. *Plant Physiol*, 169(3), 1638-55.

- Lunn, J. E., Feil, R., Hendriks, J. H., Gibon, Y., Morcuende, R., Osuna, D., Scheible, W. R., Carillo, P., Hajirezaei, M. R. & Stitt, M. (2006)** Sugar-induced increases in trehalose 6-phosphate are correlated with redox activation of ADPglucose pyrophosphorylase and higher rates of starch synthesis in *Arabidopsis thaliana*. *Biochem J*, 397(1), 139-48.
- Luschnig, C., Gaxiola, R. A., Grisafi, P. & Fink, G. R. (1998)** EIR1, a root-specific protein involved in auxin transport, is required for gravitropism in *Arabidopsis thaliana*. *Genes Dev*, 12(14), 2175-87.
- Mahlow, S., Hejazi, M., Kuhnert, F., Garz, A., Brust, H., Baumann, O. & Fettke, J. (2014)** Phosphorylation of transitory starch by alpha-glucan, water dikinase during starch turnover affects the surface properties and morphology of starch granules. *New Phytol*, 203(2), 495-507.
- Mak, C. A., Weis, K., Henao, T., Kuchtova, A., Chen, T., Sharma, S., Meekins, D. A., Thalmann, M., Vander Kooi, C. W. & Raththagala, M. (2021)** Cooperative Kinetics of the Glucan Phosphatase Starch Excess4. *Biochemistry*, 60(31), 2425-2435.
- Malinova, I., Alseekh, S., Feil, R., Fernie, A. R., Baumann, O., Schottler, M. A., Lunn, J. E. & Fettke, J. (2017)** Starch Synthase 4 and Plastidal Phosphorylase Differentially Affect Starch Granule Number and Morphology. *Plant Physiol*, 174(1), 73-85.
- Malinova, I. & Fettke, J. (2017)** Reduced starch granule number per chloroplast in the *dpe2/phs1* mutant is dependent on initiation of starch degradation. *PLoS One*, 12(11), e0187985.
- Malinova, I., Mahlow, S., Alseekh, S., Orawetz, T., Fernie, A. R., Baumann, O., Steup, M. & Fettke, J. (2014)** Double knockout mutants of *Arabidopsis* grown under normal conditions reveal that the plastidial phosphorylase isozyme participates in transitory starch metabolism. *Plant Physiol*, 164(2), 907-21.
- McCarthy, A., Chung, M., Ivanov, A. G., Krol, M., Inman, M., Maxwell, D. P. & Huner, N. P. A. (2016)** An established *Arabidopsis thaliana* var. *Landsberg erecta* cell suspension culture accumulates chlorophyll and exhibits a stay-green phenotype in response to high external sucrose concentrations. *J Plant Physiol*, 199, 40-51.
- Merida, A. & Fettke, J. (2021)** Starch granule initiation in *Arabidopsis thaliana* chloroplasts. *Plant J*, 107(3), 688-697.
- Montane, M. H. & Kloppstech, K. (2000)** The family of light-harvesting-related proteins (LHCs, ELIPs, HLIPs): was the harvesting of light their primary function? *Gene*, 258(1-2), 1-8.
- Morita, M. T. & Tasaka, M. (2004)** Gravity sensing and signaling. *Curr Opin Plant Biol*, 7(6), 712-8.
- Naito, T., Kiba, T., Koizumi, N., Yamashino, T. & Mizuno, T. (2007)** Characterization of a unique GATA family gene that responds to both light and cytokinin in *Arabidopsis thaliana*. *Biosci Biotechnol Biochem*, 71(6), 1557-60.
- Nakamura, M., Nishimura, T. & Morita, M. T. (2019)** Gravity sensing and signal conversion in plant gravitropism. *J Exp Bot*, 70(14), 3495-3506.
- Nakamura, Y., Steup, M., Colleoni, C., Iglesias, A. A., Bao, J., Fujita, N. & Tetlow, I. (2022)** Molecular regulation of starch metabolism. *Plant Mol Biol*, 108(4-5), 289-290.
- Nick, P. & Schafer, E. (1988)** Interaction of gravi- and phototropic stimulation in the response of maize (*Zea mays* L.) coleoptiles. *Planta*, 173(2), 213-20.
- Niwa, Y., Hirano, T., Yoshimoto, K., Shimizu, M. & Kobayashi, H. (1999)** Non-invasive quantitative detection and applications of non-toxic, S65T-type green fluorescent protein in living plants. *Plant J*, 18(4), 455-63.
- Okazaki, K., Kabeya, Y., Suzuki, K., Mori, T., Ichikawa, T., Matsui, M., Nakanishi, H. & Miyagishima, S. Y. (2009)** The PLASTID DIVISION1 and 2 components of the chloroplast division machinery deter-

mine the rate of chloroplast division in land plant cell differentiation. *Plant Cell*, 21(6), 1769-80.

Oliva, M. & Dunand, C. (2007) Waving and skewing: how gravity and the surface of growth media affect root development in Arabidopsis. *New Phytol*, 176(1), 37-43.

Palmieri, M. & Kiss, J. Z. (2005) Disruption of the F-actin cytoskeleton limits statolith movement in Arabidopsis hypocotyls. *J Exp Bot*, 56(419), 2539-50.

Periappuram, C., Steinhauer, L., Barton, D. L., Taylor, D. C., Chatson, B. & Zou, J. (2000) The plastidic phosphoglucomutase from Arabidopsis. A reversible enzyme reaction with an important role in metabolic control. *Plant Physiol*, 122(4), 1193-9.

Pietrzykowska, M., Suorsa, M., Semchonok, D. A., Tikkanen, M., Boekema, E. J., Aro, E. M. & Jansson, S. (2014) The light-harvesting chlorophyll a/b binding proteins Lhcb1 and Lhcb2 play complementary roles during state transitions in Arabidopsis. *Plant Cell*, 26(9), 3646-60.

Pinot, F. & Beisson, F. (2011) Cytochrome P450 metabolizing fatty acids in plants: characterization and physiological roles. *FEBS J*, 278(2), 195-205.

Price, J., Laxmi, A., St Martin, S. K. & Jang, J. C. (2004) Global transcription profiling reveals multiple sugar signal transduction mechanisms in Arabidopsis. *Plant Cell*, 16(8), 2128-50.

Pyke, K. (2011) Analysis of plastid number, size, and distribution in Arabidopsis plants by light and fluorescence microscopy. *Methods Mol Biol*, 774, 19-32.

Pyke, K. A. (2010) Plastid division. *AoB Plants*, 2010, plq016.

Pyke, K. A. (2013) Divide and shape: an endosymbiont in action. *Planta*, 237(2), 381-7.

Qian, J., Sun, T., Yan, J., Hsu, Y. F. & Zheng, M. (2020) Arabidopsis glucose-sensitive mutant 3 affects ABA biosynthesis and sensitivity during early seedling development. *Plant Physiol Biochem*, 156, 20-29.

Ranftl, Q. L., Bastakis, E., Klermund, C. & Schwechheimer, C. (2016) LLM-Domain Containing B-GATA Factors Control Different Aspects of Cytokinin-Regulated Development in Arabidopsis thaliana. *Plant Physiol*, 170(4), 2295-311.

Reyes, J. C., Muro-Pastor, M. I. & Florencio, F. J. (2004) The GATA family of transcription factors in Arabidopsis and rice. *Plant Physiol*, 134(4), 1718-32.

Reyniers, S., Ooms, N., Gomand, S. V. & Delcour, J. A. (2020) What makes starch from potato (*Solanum tuberosum* L.) tubers unique: A review. *Compr Rev Food Sci Food Saf*, 19(5), 2588-2612.

Richter, R., Bastakis, E. & Schwechheimer, C. (2013a) Cross-repressive interactions between SOC1 and the GATAs GNC and GNL/CGA1 in the control of greening, cold tolerance, and flowering time in Arabidopsis. *Plant Physiol*, 162(4), 1992-2004.

Richter, R., Behringer, C., Muller, I. K. & Schwechheimer, C. (2010) The GATA-type transcription factors GNC and GNL/CGA1 repress gibberellin signaling downstream from DELLA proteins and PHYTOCHROME-INTERACTING FACTORS. *Genes Dev*, 24(18), 2093-104.

Richter, R., Behringer, C., Zourelidou, M. & Schwechheimer, C. (2013b) Convergence of auxin and gibberellin signaling on the regulation of the GATA transcription factors GNC and GNL in Arabidopsis thaliana. *Proc Natl Acad Sci U S A*, 110(32), 13192-7.

Roldan, I., Wattedled, F., Mercedes Lucas, M., Delvalle, D., Planchot, V., Jimenez, S., Perez, R., Ball, S., D'Hulst, C. & Merida, A. (2007) The phenotype of soluble starch synthase IV defective mutants of Arabidopsis thaliana suggests a novel function of elongation enzymes in the control of starch granule formation. *Plant J*, 49(3), 492-504.

Saez-Aguayo, S., Parra-Rojas, J. P., Sepulveda-Orellana, P., Celiz-Balboa, J., Arenas-Morales, V., Salle, C., Salinas-Grenet, H., Largo-Gosens, A., North, H. M., Ralet, M. C. & Orellana, A. (2021) Transport of

- UDP-rhamnose by URG2, URG4, and URG6 modulates rhamnogalacturonan-I length. *Plant Physiol*, 185(3), 914-933.
- Saldanha, A. J.** (2004) Java Treeview--extensible visualization of microarray data. *Bioinformatics*, 20(17), 3246-8.
- Sato, E. M., Hijazi, H., Bennett, M. J., Vissenberg, K. & Swarup, R.** (2015) New insights into root gravitropic signalling. *J Exp Bot*, 66(8), 2155-65.
- Schindelin, J., Arganda-Carreras, I., Frise, E., Kaynig, V., Longair, M., Pietzsch, T., Preibisch, S., Rueden, C., Saalfeld, S., Schmid, B., Tinevez, J. Y., White, D. J., Hartenstein, V., Eliceiri, K., Tomancak, P. & Cardona, A.** (2012) Fiji: an open-source platform for biological-image analysis. *Nat Methods*, 9(7), 676-82.
- Schmid, B., Tripal, P., Fraass, T., Kersten, C., Ruder, B., Gruneboom, A., Huisken, J. & Palmisano, R.** (2019) 3Dscript: animating 3D/4D microscopy data using a natural-language-based syntax. *Nat Methods*, 16(4), 278-280.
- Schwechheimer, C., Schroder, P. M. & Blaby-Haas, C. E.** (2022) Plant GATA Factors: Their Biology, Phylogeny, and Phylogenomics. *Annu Rev Plant Biol*, 73, 123-148.
- Scialdone, A., Mugford, S. T., Feike, D., Skeffington, A., Borrill, P., Graf, A., Smith, A. M. & Howard, M.** (2013) Arabidopsis plants perform arithmetic division to prevent starvation at night. *Elife*, 2, e00669.
- Seung, D.** (2020) Amylose in starch: towards an understanding of biosynthesis, structure and function. *New Phytol*, 228(5), 1490-1504.
- Seung, D., Boudet, J., Monroe, J., Schreier, T. B., David, L. C., Abt, M., Lu, K. J., Zanella, M. & Zeeman, S. C.** (2017) Homologs of PROTEIN TARGETING TO STARCH Control Starch Granule Initiation in Arabidopsis Leaves. *Plant Cell*, 29(7), 1657-1677.
- Seung, D., Echevarria-Poza, A., Steuernagel, B. & Smith, A. M.** (2020) Natural Polymorphisms in Arabidopsis Result in Wide Variation or Loss of the Amylose Component of Starch. *Plant Physiol*, 182(2), 870-881.
- Seung, D., Schreier, T. B., Burgy, L., Eicke, S. & Zeeman, S. C.** (2018) Two Plastidial Coiled-Coil Proteins Are Essential for Normal Starch Granule Initiation in Arabidopsis. *Plant Cell*, 30(7), 1523-1542.
- Shannon, P., Markiel, A., Ozier, O., Baliga, N. S., Wang, J. T., Ramage, D., Amin, N., Schwikowski, B. & Ideker, T.** (2003) Cytoscape: a software environment for integrated models of biomolecular interaction networks. *Genome Res*, 13(11), 2498-504.
- Song, Y., Li, G., Nowak, J., Zhang, X., Xu, D., Yang, X., Huang, G., Liang, W., Yang, L., Wang, C., Bulone, V., Nikoloski, Z., Hu, J., Persson, S. & Zhang, D.** (2019) The Rice Actin-Binding Protein RMD Regulates Light-Dependent Shoot Gravitropism. *Plant Physiol*, 181(2), 630-644.
- Starch Europe** (2022) *Starch Europe Plant-based solutions*, 2022. Available online: [Accessed].
- Stettler, M., Eicke, S., Mettler, T., Messerli, G., Hortensteiner, S. & Zeeman, S. C.** (2009) Blocking the metabolism of starch breakdown products in Arabidopsis leaves triggers chloroplast degradation. *Mol Plant*, 2(6), 1233-46.
- Streb, S., Egli, B., Eicke, S. & Zeeman, S. C.** (2009) The debate on the pathway of starch synthesis: a closer look at low-starch mutants lacking plastidial phosphoglucomutase supports the chloroplast-localized pathway. *Plant Physiol*, 151(4), 1769-72.
- Streb, S., Eicke, S. & Zeeman, S. C.** (2012) The simultaneous abolition of three starch hydrolases blocks transient starch breakdown in Arabidopsis. *J Biol Chem*, 287(50), 41745-56.
- Streb, S. & Zeeman, S. C.** (2012) Starch metabolism in Arabidopsis. *Arabidopsis Book*, 10, e0160.
- Südstärke GmbH** (2021) *Sustainability Report 2021*.

- Sun, B., Zhang, Q. Y., Yuan, H., Gao, W., Han, B. & Zhang, M. (2020)** PDV1 and PDV2 Differentially Affect Remodeling and Assembly of the Chloroplast DRP5B Ring. *Plant Physiol*, 182(4), 1966-1978.
- Supek, F., Bosnjak, M., Skunca, N. & Smuc, T. (2011)** REVIGO summarizes and visualizes long lists of gene ontology terms. *PLoS One*, 6(7), e21800.
- Szklarczyk, D., Morris, J. H., Cook, H., Kuhn, M., Wyder, S., Simonovic, M., Santos, A., Doncheva, N. T., Roth, A., Bork, P., Jensen, L. J. & von Mering, C. (2017)** The STRING database in 2017: quality-controlled protein-protein association networks, made broadly accessible. *Nucleic Acids Res*, 45(D1), D362-D368.
- Szydlowski, N., Ragel, P., Raynaud, S., Lucas, M. M., Roldan, I., Montero, M., Munoz, F. J., Ovecka, M., Bahaji, A., Planchot, V., Pozueta-Romero, J., D'Hulst, C. & Merida, A. (2009)** Starch granule initiation in Arabidopsis requires the presence of either class IV or class III starch synthases. *Plant Cell*, 21(8), 2443-57.
- Tanaka, R., Kobayashi, K. & Masuda, T. (2011)** Tetrapyrrole Metabolism in Arabidopsis thaliana. *Arabidopsis Book*, 9, e0145.
- Tasaka, M., Kato, T. & Fukaki, H. (1999)** The endodermis and shoot gravitropism. *Trends Plant Sci*, 4(3), 103-7.
- Tetlow, I. J. & Bertoft, E. (2020)** A Review of Starch Biosynthesis in Relation to the Building Block-Backbone Model. *Int J Mol Sci*, 21(19).
- Thum, K. E., Shin, M. J., Palenchar, P. M., Kouranov, A. & Coruzzi, G. M. (2004)** Genome-wide investigation of light and carbon signaling interactions in Arabidopsis. *Genome Biol*, 5(2), R10.
- Toyosawa, Y., Kawagoe, Y., Matsushima, R., Crofts, N., Ogawa, M., Fukuda, M., Kumamaru, T., Okazaki, Y., Kusano, M., Saito, K., Toyooka, K., Sato, M., Ai, Y., Jane, J. L., Nakamura, Y. & Fujita, N. (2016)** Deficiency of Starch Synthase IIIa and IVb Alters Starch Granule Morphology from Polyhedral to Spherical in Rice Endosperm. *Plant Physiol*, 170(3), 1255-70.
- Truernit, E., Bauby, H., Dubreucq, B., Grandjean, O., Runions, J., Barthelemy, J. & Palauqui, J. C. (2008)** High-resolution whole-mount imaging of three-dimensional tissue organization and gene expression enables the study of Phloem development and structure in Arabidopsis. *Plant Cell*, 20(6), 1494-503.
- Vernoux, T., Brunoud, G., Farcot, E., Morin, V., Van den Daele, H., Legrand, J., Oliva, M., Das, P., Larrieu, A., Wells, D., Guedon, Y., Armitage, L., Picard, F., Guyomarc'h, S., Cellier, C., Parry, G., Koumproglou, R., Doonan, J. H., Estelle, M., Godin, C., Kepinski, S., Bennett, M., De Veylder, L. & Traas, J. (2011)** The auxin signalling network translates dynamic input into robust patterning at the shoot apex. *Mol Syst Biol*, 7, 508.
- Vitha, S., Yang, M., Sack, F. D. & Kiss, J. Z. (2007)** Gravitropism in the starch excess mutant of Arabidopsis thaliana. *Am J Bot*, 94(4), 590-8.
- Vitha, S., Zhao, L. & Sack, F. D. (2000)** Interaction of root gravitropism and phototropism in Arabidopsis wild-type and starchless mutants. *Plant Physiol*, 122(2), 453-62.
- Voisard, C., Wang, J., McEvoy, J. L., Xu, P. & Leong, S. A. (1993)** urbs1, a gene regulating siderophore biosynthesis in Ustilago maydis, encodes a protein similar to the erythroid transcription factor GATA-1. *Mol Cell Biol*, 13(11), 7091-100.
- Wang, R., Okamoto, M., Xing, X. & Crawford, N. M. (2003)** Microarray analysis of the nitrate response in Arabidopsis roots and shoots reveals over 1,000 rapidly responding genes and new linkages to glucose, trehalose-6-phosphate, iron, and sulfate metabolism. *Plant Physiol*, 132(2), 556-67.
- Weise, S. E. & Kiss, J. Z. (1999)** Gravitropism of inflorescence stems in starch-deficient mutants of Arabidopsis. *Int J Plant Sci*, 160(3), 521-7.

- Willige, B. C., Isono, E., Richter, R., Zourelidou, M. & Schwechheimer, C. (2011)** Gibberellin regulates PIN-FORMED abundance and is required for auxin transport-dependent growth and development in *Arabidopsis thaliana*. *Plant Cell*, 23(6), 2184-95.
- Wolff, J. B. & Price, L. (1960)** The effect of sugars on chlorophyll biosynthesis in higher plants. *J Biol Chem*, 235, 1603-8.
- Xia, X., Mi, X., Jin, L., Guo, R., Zhu, J., Xie, H., Liu, L., An, Y., Zhang, C., Wei, C. & Liu, S. (2021)** CsLAZY1 mediates shoot gravitropism and branch angle in tea plants (*Camellia sinensis*). *BMC Plant Biol*, 21(1), 243.
- Xu, D. (2020)** COP1 and BBXs-HY5-mediated light signal transduction in plants. *New Phytol*, 228(6), 1748-1753.
- Yang, M. & Sack, F. D. (1995)** The too many mouths and four lips mutations affect stomatal production in *Arabidopsis*. *Plant Cell*, 7(12), 2227-39.
- Yang, P., Wen, Q., Yu, R., Han, X., Deng, X. W. & Chen, H. (2020)** Light modulates the gravitropic responses through organ-specific PIFs and HY5 regulation of LAZY4 expression in *Arabidopsis*. *Proc Natl Acad Sci U S A*, 117(31), 18840-18848.
- Yu, T. S., Kofler, H., Hausler, R. E., Hille, D., Flugge, U. I., Zeeman, S. C., Smith, A. M., Kossmann, J., Lloyd, J., Ritte, G., Steup, M., Lue, W. L., Chen, J. & Weber, A. (2001)** The *Arabidopsis* *sex1* mutant is defective in the R1 protein, a general regulator of starch degradation in plants, and not in the chloroplast hexose transporter. *Plant Cell*, 13(8), 1907-18.
- Zeeman, S. C., Northrop, F., Smith, A. M. & Rees, T. (1998)** A starch-accumulating mutant of *Arabidopsis thaliana* deficient in a chloroplastic starch-hydrolysing enzyme. *Plant J*, 15(3), 357-65.
- Zeeman, S. C., Tiessen, A., Pilling, E., Kato, K. L., Donald, A. M. & Smith, A. M. (2002)** Starch synthesis in *Arabidopsis*. Granule synthesis, composition, and structure. *Plant Physiol*, 129(2), 516-29.
- Zhang, X., Szydlowski, N., Delvalle, D., D'Hulst, C., James, M. G. & Myers, A. M. (2008)** Overlapping functions of the starch synthases SSII and SSIII in amylopectin biosynthesis in *Arabidopsis*. *BMC Plant Biol*, 8, 96.
- Zhao, Y., Medrano, L., Ohashi, K., Fletcher, J. C., Yu, H., Sakai, H. & Meyerowitz, E. M. (2004)** HANABATA-RANU is a GATA transcription factor that regulates shoot apical meristem and flower development in *Arabidopsis*. *Plant Cell*, 16(10), 2586-600.
- Zhong, Y., Xie, J., Wen, S., Wu, W., Tan, L., Lei, M., Shi, H. & Zhu, J. K. (2020)** TPST is involved in fructose regulation of primary root growth in *Arabidopsis thaliana*. *Plant Mol Biol*, 103(4-5), 511-525.
- Zubo, Y. O., Blakley, I. C., Franco-Zorrilla, J. M., Yamburenko, M. V., Solano, R., Kieber, J. J., Loraine, A. E. & Schaller, G. E. (2018)** Coordination of Chloroplast Development through the Action of the GNC and GLK Transcription Factor Families. *Plant Physiol*, 178(1), 130-147.

APPENDIX

GO term	ID	Symbol	Log2	FDR
Pho. light harvesting	AT3G27690	LHCB2.4	3.106	1.6E-12
Pho. light harvesting	AT1G29920	LHCB1.1	2.972	1.8E-7
Pho. light harvesting	AT1G29920	LHCB1.2	2.972	1.8E-7
Pho. light harvesting	AT5G54270	LHCB3	2.668	1.2E-9
Pho. light harvesting	AT2G34430	Lhb1B1	2.116	8.3E-6
Pho. light harvesting	AT3G54890	LHCA1	2.068	1.0E-6
Pho. light harvesting	AT2G05070	LHCB2.2	1.786	4.2E-6
Pho. light harvesting	AT1G15820	CP24	1.537	2.8E-6
Pho. light harvesting	AT3G47470	LHCA4	1.292	4.0E-4
Pho. light harvesting	AT1G29930	LHCB1.3	1.269	6.9E-5
Pho. light harvesting	AT1G19150	LHCA6	1.012	9.1E-4
Pho. light harvesting	AT2G34420	Lhb1B2	0.994	2.3E-2
Pho. light harvesting	AT1G08380	PSAO	0.893	5.1E-4
Pho. light harvesting	AT2G05100	LHCB2.1	0.814	1.6E-2
Pho. light harvesting	AT4G10340	LHCB5	0.694	3.4E-2
Starch metabolism	AT5G48300	APS1	1.476	8.3E-13
Starch metabolism	AT3G59480	FRK4	1.376	2.7E-5
Starch metabolism	AT3G52180	DSP4	1.242	1.2E-4
Starch metabolism	AT1G32900	GBSS1	1.124	4.8E-3
Starch metabolism	AT4G28706	AT4G28706	1.043	2.5E-5
Starch metabolism	AT1G03310	ISA2	0.970	2.5E-6
Starch metabolism	AT3G20440	SBE3	0.714	3.8E-3
Starch metabolism	AT3G55800	SBPASE	0.689	2.6E-3
Starch metabolism	AT5G64860	DPE1	0.627	5.7E-4
Starch metabolism	AT3G55760	LESV	0.579	3.2E-2
Starch metabolism	AT5G51820	PGMP	0.576	1.4E-3
Starch metabolism	AT1G66430	FRK3	0.559	6.6E-4
Starch metabolism	AT5G17520	MEX1	0.522	3.1E-2
Starch metabolism	AT4G39210	APL3	0.497	1.7E-2
Starch metabolism	AT1G27680	APL2	0.494	2.3E-2
Starch metabolism	AT2G39930	ISA1	0.477	4.0E-3
Starch metabolism	AT2G40840	DPE2	0.476	2.8E-3
Starch metabolism	AT5G24300	SS1	0.395	1.6E-2
Stomata development	AT1G04110	SBT1.2	3.499	5.8E-7
Stomata development	AT1G34245	EPF2	2.523	2.4E-5

Stomata development	AT1G15570	CYCA2-3	1.438	6.6E-7
Stomata development	AT3G20940	CYP705A30	1.414	5.3E-4
Stomata development	AT5G60880	BASL	1.382	1.6E-2
Stomata development	AT1G09470	NEAP3	1.377	4.7E-3
Stomata development	AT5G53210	SPCH	1.137	2.2E-4
Stomata development	AT1G80370	CYCA2-4	1.007	5.1E-4
Stomata development	AT3G22760	TCX3	0.930	5.8E-4
Stomata development	AT5G07180	ERL2	0.787	2.8E-4
Stomata development	AT1G80080	TMM	0.738	1.6E-4
Stomata development	AT5G62230	ERL1	0.713	1.7E-2
Stomata development	AT4G14770	TCX2	0.696	6.3E-5
Stomata development	AT3G02120	AT3G02120	0.690	1.6E-2
Stomata development	AT4G34160	CYCD3-1	0.589	5.4E-3
Stomata development	AT3G07320	F21O3.3	0.567	4.7E-3
Stomata development	AT1G67040	TRM22	0.558	8.5E-3
Stomata development	AT1G12860	SCRM2	0.535	4.4E-3
Stomata development	AT3G50070	CYCD3-3	0.507	8.9E-3
Stomata development	AT3G22780	TSO1	0.438	7.1E-3
Stomata development	AT4G36180	MUL	0.360	4.6E-2
DNA replication	AT2G27120	POL2B	2.087	4.5E-3
DNA replication	AT4G14700	ORC1A	1.664	6.6E-3
DNA replication	AT1G15570	CYCA2-3	1.438	6.6E-7
DNA replication	AT3G54710	CDT1B	1.087	4.2E-2
DNA replication	AT2G16440	MCM4	0.936	4.0E-6
DNA replication	AT1G44900	MCM2	0.879	1.1E-5
DNA replication	AT2G40550	ETG1	0.865	3.9E-4
DNA replication	AT2G31270	CDT1A	0.855	1.1E-3
DNA replication	AT3G20260	AT3G20260	0.848	5.4E-3
DNA replication	AT4G37630	CYCD5-1	0.847	2.4E-3
DNA replication	AT1G34380	AT1G34380	0.819	1.3E-2
DNA replication	AT3G48160	E2FE	0.787	1.3E-2
DNA replication	AT5G44635	MCM6	0.783	3.7E-3
DNA replication	AT4G02060	MCM7	0.776	1.7E-4
DNA replication	AT1G07370	PCNA	0.773	8.0E-3
DNA replication	AT5G13060	ABAP1	0.751	3.5E-2
DNA replication	AT5G61000	RPA1D	0.652	3.3E-2
DNA replication	AT2G07690	MCM5	0.647	1.9E-3
DNA replication	AT5G46280	MCM3	0.590	1.6E-2

DNA replication	AT3G42660	EOL1	0.562	2.8E-3
DNA replication	AT1G10930	RECQL4A	0.543	4.3E-3
DNA replication	AT1G67630	POLA2	0.531	2.5E-2
DNA replication	AT1G08840	JHS1	0.464	1.3E-2
DNA replication	AT4G14310	AT4G14310	0.435	3.4E-2
DNA replication	AT1G63160	RFC2	0.375	4.4E-2
DNA replication	AT5G67100	POLA	0.346	5.0E-2
Alpha-amino aci. bio.	AT1G50110	BCAT6	0.930	1.4E-3
Alpha-amino aci. bio.	AT3G59890	DAPB2	0.919	2.3E-3
Alpha-amino aci. bio.	AT5G21060	AT5G21060	0.799	1.4E-3
Alpha-amino aci. bio.	AT5G05590	PAI2	0.746	2.6E-2
Alpha-amino aci. bio.	AT5G35630	GLN2	0.643	2.0E-3
Alpha-amino aci. bio.	AT5G60890	MYB34	0.639	1.6E-3
Alpha-amino aci. bio.	AT3G62030	CYP20-3	0.638	3.4E-4
Alpha-amino aci. bio.	AT2G17630	PSAT2	0.617	1.5E-2
Alpha-amino aci. bio.	AT4G13930	SHM4	0.598	2.5E-5
Alpha-amino aci. bio.	AT5G14060	AK2	0.579	1.3E-3
Alpha-amino aci. bio.	AT1G25220	ASB1	0.546	6.2E-3
Alpha-amino aci. bio.	AT4G34200	PGDH1	0.532	5.9E-4
Alpha-amino aci. bio.	AT5G05730	ASA1	0.516	3.1E-3
Alpha-amino aci. bio.	AT1G11790	ADT1	0.512	2.7E-2
Alpha-amino aci. bio.	AT3G10050	OMR1	0.501	4.5E-3
Alpha-amino aci. bio.	AT3G23940	DHAD	0.490	1.6E-3
Alpha-amino aci. bio.	AT1G17745	PGDH2	0.479	4.5E-3
Alpha-amino aci. bio.	AT3G54640	TSA1	0.463	8.0E-3
Alpha-amino aci. bio.	AT1G18640	PSP	0.423	1.3E-2
Alpha-amino aci. bio.	AT3G03780	MS2	0.410	3.6E-2
Alpha-amino aci. bio.	AT1G72810	TS2	0.407	2.2E-2
Alpha-amino aci. bio.	AT4G24830	AT4G24830	0.405	1.9E-2
Alpha-amino aci. bio.	AT3G59970	MTHFR1	0.390	6.5E-3
Alpha-amino aci. bio.	AT4G19710	AKHSDH2	0.375	1.3E-2
Alpha-amino aci. bio.	AT1G29900	CARB	0.368	2.9E-2
Alpha-amino aci. bio.	AT1G80560	IMDH2	0.367	1.9E-2
Alpha-amino aci. bio.	AT5G26780	SHM2	0.352	3.6E-2
Alpha-amino aci. bio.	AT4G33680	DAP	0.350	2.3E-2
Alpha-amino aci. bio.	AT4G31500	CYP83B1	0.337	3.2E-2
Alpha-amino aci. bio.	AT5G38530	TSBtype2	0.292	3.5E-2

Appendix 1. Differentially expressed genes from *gnc gnl* belonging to the five most prominent GO terms categories. List of 110 upregulated genes, after filtering by a FDR corrected p-value < 0.05. Log2 fold changes and FDR corrected p-values are presented.

